The Pennsylvania State University

The Graduate School

Department of Architectural Engineering

IMPROVING PHOTOCONTROL SYSTEM PERFORMANCE UNDER DIFFERENT SHADING AND SUNLIGHT CONDITIONS

A Thesis in
Architectural Engineering

by

Abdulrahman Aljuhani

Submitted in Partial Fulfillment
of the Requirements
for the Degree of

Master of Science

December 2018

The thesis of Abdulrahman Aljuhani was reviewed and approved* by the following:

Richard G. Mistrick
Associate Professor of Architectural Engineering
Thesis Advisor

Kevin W. Houser
Professor of Architectural Engineering

Gregory Pavlak
Assistant Professor of Architectural Engineering

William Bahnfleth
Professor of Architectural Engineering
Chair of Graduate Program of Architectural Engineering

*Signatures are on file in the Graduate School

ABSTRACT

A number of previous research studies were dedicated to providing guidelines to optimize locating a photosensor under different space configurations. Other researchers focused on improving photocontrol performance by reducing the effect of direct sunlight reflections on photosensors by integrating automated shades in their study models. This study aimed to verify the previous studies regarding a single closed-loop photocontrol sensor and improve the performance of the photocontrol systems. Advanced photocontrol systems, including more than one photosensor, were studied in an effort to reduce the sunlight factor that causes disagreement between sensor signals and illuminance on the workplane of the study model or to rectify the photocontrol signals and provide a more consistent photosenosr signal to workplane illuminance ratio.

All photocontrol systems were investigated based on the two most critical points on the workplane of the office space by applying automated shades (shades up, halfway and down). All comparisons were performed based on two evaluation measures: root mean square error and energy savings. A higher performing system is one that delivers less root mean square error and higher energy savings.

The advanced multisensor photocontrol systems were compared to a referenced single-sensor system in the proposed space (a model office). To optimize the configuration of the referenced photosensor system, several locations on the ceiling that were centered on the window were investigated for both narrow and wideband sensors according to recommendations from previous research studies. Then, the best photosensor configuration from these was compared to a photosensor location that was centered on the exterior wall. The location with better performance was selected as the single photosensor system reference condition.

A symmetrical two-photosensor system was applied as a possible improvement to the single photosensor system, to accommodate conditions where one side of the room receives less daylight than the other. Since certain daylight conditions still produced higher photosensor signal to workplane illuminance ratios (S/E) than others, tests were performed to determine if the application of a third photosensor could be used to identify and correct when S/E ratios were high, and adjust these readings to better align them with the workplane illuminance. A narrow band sensor positioned to view the windows and adjacent floor area showed good correlation to the S/E ratio and was used to correct the readings from the other two photosensors. Each of the three photocontrol configurations (utilizing one, two, and three-sensors) was

subject to four different windows orientations at two very different climate locations to study their performance and to address the system calibration process.

This work achieved two main points: increasing the agreement between workplane illuminance and photosensor signals and boosting the energy savings by implementing a two-sensor and a corrected two-sensor system, which requires three sensors. Investigating the four main orientations (South, North, East, and West) confirmed these achievements and developed two different options (a fixed correction equation, and a correction equation derived from preferred shade and sky condition readings) to commission the corrected two-sensor system for the study space.

Table of Contents

List of Figures vii
List of Tables xii
Acknowledgments xiii
1. Introduction 1
2. Literature review 2
2.1 Critical point 2
2.2 RMSE 3
2.3 Photosensor performance analysis 4
2.3.1 Sky condition influence 4
2.3.2 Space properties and orientation influence 5
2.3.3 Photosensor position 7
2.3.4 Photosensor spatial sensitivity 8
2.3.5 Shade setting and impact 8
3. Research Objectives 9
4. Research Hypotheses 9
5. Methodology 10
5.1 Fixed space and system variables 10
5.1.1 Space model 10
5.1.2 Photosensor models 13
5.1.3 Electric light models 13
5.1.4 Critical point 14
5.1.5 Shade settings 14
5.2 Simulations 17
5.2.1 Simulation tool 17
5.2.2 Simulation inputs and setups 18
5.2.3 Configuration simulation runs 19
5.3 Statistical analysis 20
5.3.1 Statistical analysis tool 20
5.3.2 Control system options 20
5.3.2.1 Single sensor control system 20
5.3.2.2 Two sensor control system 21
5.3.2.3 Two sensor control system with correction 21

5.4 Study variables 23
6. Results and analysis 24
6.1 Critical points 24
6.2 Shade setting 25
6.3 Single sensor approach 26
6.3.1 Optimizing FOV for a single sensor centered on the window 26
6.3.2 Single window-centered sensor analysis 30
6.3.3 Window-centered and room-center photosensor comparison 31
6.4 Two-sensor approach 32
6.5 Two-sensor corrected approach 33
6.6 Tables of results 37
6.7 Discussion on Table 3 and Table 4 40
6.8 Correction line setup over several months for the both sites 42
6.9 Discussion on Table 5, Table 6 and Table 7 45
7. Conclusion 47
8. Recommendations and contributions 49
8.1 Photosensor system 49
8.2 Two-sensor corrected system calibration 50
8.2.1 Correction equation option 50
8.2.2 Shade and sky conditions option 51
8.3 Study contributions 51
Appendix A. Optimum energy savings based on critical points 53
Appendix B. Representing different shade implementations through a year 54
South orientation 54
North orientation 59
East orientation 64
West orientation 69
References 74

List of Figures

Figure 1. The highlighted grid points represent the four critical point locations in Subramaniam's model (the window is along the bottom of this figure)..... 2
Figure 2. Correlation grid and the three highlighted candidates having the same correlation values..... 3
Figure 3. RMSE values for the three location candidates 4
Figure 4. The complete view of the AutoCAD model 12
Figure 5. The office space view of the AutoCAD model 12
Figure 6. Spatial sensitivity of a wideband sensor (cosine sensor) (Chen, 2013).....13
Figure 7. Spatial sensitivity of a narrow band sensor (cosine 30 sensor).....13
Figure 8. The candela distribution of the 2GTL4_4400LM_LP835 troffer. 14
Figure 9. 0.305-meter (1-foot) shade setup 15
Figure 10. 0.609-meter (2-feet) shade setup.....15
Figure 11. 0.914-meter (3-feet) shade setup.....16
Figure 12. 1.219-meter (4-feet) shade setup.....16
Figure 13. Photosensor grid showing numbered analysis points in the space and the shade trigger location (point 46) for North orientation halfway shades application 17
Figure 14. The isometric view of the luminaire layout 18
Figure 15. The illuminance contours of the luminaire layout 19
Figure 16. Configuration of a cosine 30 sensor 22
Figure 17. The configuration of a cosine 30 tilted toward the window 22
Figure 18. The critical point locations in the simulation model 24
Figure 19. 0.305-meter versus 1.22-meter shade setup performance plot in South facing State College office 25
Figure 20. Cosine 30 sensor locations for centered-on-window sensor investigation.....26
Figure 21. Scatter plot of dimming level (DL) and final signal (S) for a cosine 30 sensor located at (2.68, 3.96, 3.05) and vertically aimed to the workplane in South facing State College office.....27
Figure 22. Scatter plot of dimming level (DL) and final signal (S) for a cosine 30 sensor located at (2.68, 1.83, 3.05) and tilted 45 degrees toward the window in South facing State College office.....27
Figure 23. Scatter plot of dimming level (DL) and final signal (S) for a cosine 30 sensor located at (2.68, 1.83, 3.05) and tilted 45 degrees inward in a South facing State College office.....28
Figure 24. Locations of cosine and 35-degree-tilted cosine 30 sensors for centered-on-window sensor investigation 29
Figure 25. Scatter plot of dimming level (DL) and final signal (S) for a cosine sensor located at (2.68, 3.96, 3.05) and vertically aimed to the workplane in a South facing State College office 29
Figure 26. Scatter plot of dimming level (DL) and final signal (S) for a cosine sensor located at (2.68, 2.44, 3.05) and vertically aimed to the workplane in South facing State College office.....30
Figure 27. Scatter plot of dimming level (DL) and final signal (S) for a cosine sensor located at (5.11, 2.44, 3.05) and vertically aimed to the workplane in South facing State College office.....32
Figure 28. Scatter plot of dimming level (DL) and final signal (S) for two cosine sensor configuration in South facing State College office.....33

Figure 29. Scatter plot of a coupling between the daylight signal to daylight illuminance ratio ($S_d/E_dS_d/E_d$) of the two sensor system and the third sensor signal (S) which is set as Fig. 16 in South facing State College office 34
Figure 30. Scatter plot of a coupling between the daylight signal to daylight illuminance ratio (S_d/E_d) of the two sensor system and the third sensor signal (S) which is set as Fig. 17 in South facing State College office 34
Figure 31. Plot (a) represents the performance of the two sensor system in State College-South orientation; plot (b) is the coupling between the two-sensor S_d/E_d and the correcting signals 35
Figure 32. Scatter plot of dimming level (DL) and final signal (S) for the corrected signals of the two photosensor configuration in South facing State College office 35
Figure 33. Scatter plot of a coupling between the daylight signal to daylight illuminance ratio (S_d/E_d) of the two sensor system and the correcting sensor signal (S) which is set as Fig. 17 in East facing State College office (the correcting line is in middle of the whole coupling pattern).....36
Figure 34. Scatter plot of a coupling between the daylight signal to daylight illuminance ratio (S_d/E_d) of the two sensor system and the correcting sensor signal (S) which is set as Fig. 17 in East facing State College office (the correcting line is in middle of the upper coupling pattern) 37
Figure 35. The distribution of scattered data points for a South orientation in State College in both December and February with an automated shades setting showing the correction line from the equation derived from whole year data. 45
Figure 36. The distribution of scattered data points for a South orientation in State College in March with an automated shades setting showing the correction line from the equation derived from whole year data. 46
Figure 37. The distribution of scattered data points for a South orientation in State College in March with an automated shades setting showing the main correction line shifted up and crossing the halfway shades condition data points. 46
Figure 38. Space dimensions and photosensor locations 49
Figure 39. Daylight signal to daylight illuminance ratios of the two-sensor system and the correcting signals for the South orientation in the month of February in State College. (Blue points are shades up, yellow points are halfway shades and gray points are shades down).....54
Figure 40. Daylight signal to daylight illuminance ratios of the two-sensor system and the correcting signals for the South orientation in the month of February in Phoenix. (Blue points are shades up, yellow points are halfway shades and gray points are shades down) 54
Figure 41. Daylight signal to daylight illuminance ratios of the two-sensor system and the correcting signals for the South orientation in the month of March in State College. (Blue points are shades up, yellow points are halfway shades and gray points are shades down).....55
Figure 42. Daylight signal to daylight illuminance ratios of the two-sensor system and the correcting signals for the South orientation in the month of March in Phoenix. (Blue points are shades up, yellow points are halfway shades and gray points are shades down) 55
Figure 43. Daylight signal to daylight illuminance ratios of the two-sensor system and the correcting signals for the South orientation in the month of April in State College. (Blue points are shades up, yellow points are halfway shades and gray points are shades down) 56
Figure 44. Daylight signal to daylight illuminance ratios of the two-sensor system and the correcting signals for the South orientation in the month of April in Phoenix. (Blue points are shades up, yellow points are halfway shades and gray points are shades down) 56

Figure 45. Daylight signal to daylight illuminance ratios of the two-sensor system and the correcting signals for the South orientation in the month of May in State College. (Blue points are shades up, yellow points are halfway shades and gray points are shades down) 57
Figure 46. Daylight signal to daylight illuminance ratios of the two-sensor system and the correcting signals for the South orientation in the month of May in Phoenix. (Blue points are shades up, yellow points are halfway shades and gray points are shades down) 57
Figure 47. Daylight signal to daylight illuminance ratios of the two-sensor system and the correcting signals for the South orientation in the month of July in State College. (Blue points are shades up, yellow points are halfway shades and gray points are shades down) 58
Figure 48. Daylight signal to daylight illuminance ratios of the two-sensor system and the correcting signals for the South orientation in the month of July in Phoenix. (Blue points are shades up, yellow points are halfway shades and gray points are shades down) 58
Figure 49. Daylight signal to daylight illuminance ratios of the two-sensor system and the correcting signals for the North orientation in the month of February in State College. (Blue points are shades up, yellow points are halfway shades and gray points are shades down).....59
Figure 50. Daylight signal to daylight illuminance ratios of the two-sensor system and the correcting signals for the North orientation in the month of February in Phoenix. (Blue points are shades up, yellow points are halfway shades and gray points are shades down) 59
Figure 51. Daylight signal to daylight illuminance ratios of the two-sensor system and the correcting signals for the North orientation in the month of March in State College. (Blue points are shades up, yellow points are halfway shades and gray points are shades down).....60
Figure 52. Daylight signal to daylight illuminance ratios of the two-sensor system and the correcting signals for the North orientation in the month of March in Phoenix. (Blue points are shades up, yellow points are halfway shades and gray points are shades down) 60
Figure 53. Daylight signal to daylight illuminance ratios of the two-sensor system and the correcting signals for the North orientation in the month of April in State College. (Blue points are shades up, yellow points are halfway shades and gray points are shades down) 61
Figure 54. Daylight signal to daylight illuminance ratios of the two-sensor system and the correcting signals for the North orientation in the month of April in Phoenix. (Blue points are shades up, yellow points are halfway shades and gray points are shades down) 61
Figure 55. Daylight signal to daylight illuminance ratios of the two-sensor system and the correcting signals for the North orientation in the month of May in State College. (Blue points are shades up, yellow points are halfway shades and gray points are shades down) 62
Figure 56. Daylight signal to daylight illuminance ratios of the two-sensor system and the correcting signals for the North orientation in the month of May in Phoenix. (Blue points are shades up, yellow points are halfway shades and gray points are shades down) 62
Figure 57. Daylight signal to daylight illuminance ratios of the two-sensor system and the correcting signals for the North orientation in the month of July in State College. (Blue points are shades up, yellow points are halfway shades and gray points are shades down) 63
Figure 58. Daylight signal to daylight illuminance ratios of the two-sensor system and the correcting signals for the North orientation in the month of July in Phoenix. (Blue points are shades up, yellow points are halfway shades and gray points are shades down) 63

Figure 59. Daylight signal to daylight illuminance ratios of the two-sensor system and the correcting signals for the East orientation in the month of February in State College. (Blue points are shades up, yellow points are halfway shades and gray points are shades down).....64
Figure 60. Daylight signal to daylight illuminance ratios of the two-sensor system and the correcting signals for the East orientation in the month of February in Phoenix. (Blue points are shades up, yellow points are halfway shades and gray points are shades down) 64
Figure 61. Daylight signal to daylight illuminance ratios of the two-sensor system and the correcting signals for the East orientation in the month of March in State College. (Blue points are shades up, yellow points are halfway shades and gray points are shades down) 65
Figure 62. Daylight signal to daylight illuminance ratios of the two-sensor system and the correcting signals for the East orientation in the month of March in Phoenix(Blue points are shades up, yellow points are halfway shades and gray points are shades down).....65
Figure 63. Daylight signal to daylight illuminance ratios of the two-sensor system and the correcting signals for the East orientation in the month of April in State College. (Blue points are shades up, yellow points are halfway shades and gray points are shades down) 66
Figure 64. Daylight signal to daylight illuminance ratios of the two-sensor system and the correcting signals for the East orientation in the month of April in Phoenix. (Blue points are shades up, yellow points are halfway shades and gray points are shades down).....66
Figure 65. Daylight signal to daylight illuminance ratios of the two-sensor system and the correcting signals for the East orientation in the month of May in State College. (Blue points are shades up, yellow points are halfway shades and gray points are shades down) 67
Figure 66. Daylight signal to daylight illuminance ratios of the two-sensor system and the correcting signals for the East orientation in the month of May in Phoenix. (Blue points are shades up, yellow points are halfway shades and gray points are shades down).....67
Figure 67. Daylight signal to daylight illuminance ratios of the two-sensor system and the correcting signals for the East orientation in the month of July in State College. (Blue points are shades up, yellow points are halfway shades and gray points are shades down) 68
Figure 68. Daylight signal to daylight illuminance ratios of the two-sensor system and the correcting signals for the East orientation in the month of July in Phoenix. (Blue points are shades up, yellow points are halfway shades and gray points are shades down).....68
Figure 69. Daylight signal to daylight illuminance ratios of the two-sensor system and the correcting signals for the West orientation in the month of February in State College. (Blue points are shades up, yellow points are halfway shades and gray points are shades down).....69
Figure 70. Daylight signal to daylight illuminance ratios of the two-sensor system and the correcting signals for the West orientation in the month of February in Phoenix. (Blue points are shades up, yellow points are halfway shades and gray points are shades down) 69
Figure 71. Daylight signal to daylight illuminance ratios of the two-sensor system and the correcting signals for the West orientation in the month of March in State College. (Blue points are shades up, yellow points are halfway shades and gray points are shades down).....70
Figure 72. Daylight signal to daylight illuminance ratios of the two-sensor system and the correcting signals for the West orientation in the month of March in Phoenix. (Blue points are shades up, yellow points are halfway shades and gray points are shades down) 70

Figure 73. Daylight signal to daylight illuminance ratios of the two-sensor system and the correcting signals for the West orientation in the month of April in State College. (Blue points are shades up, yellow points are halfway shades and gray points are shades down) 71
Figure 74. Daylight signal to daylight illuminance ratios of the two-sensor system and the correcting signals for the West orientation in the month of April in Phoenix. (Blue points are shades up, yellow points are halfway shades and gray points are shades down) 71
Figure 75. Daylight signal to daylight illuminance ratios of the two-sensor system and the correcting signals for the West orientation in the month of May in State College. (Blue points are shades up, yellow points are halfway shades and gray points are shades down) 72
Figure 76. Daylight signal to daylight illuminance ratios of the two-sensor system and the correcting signals for the West orientation in the month of May in Phoenix. (Blue points are shades up, yellow points are halfway shades and gray points are shades down) 72
Figure 77. Daylight signal to daylight illuminance ratios of the two-sensor system and the correcting signals for the West orientation in the month of July in State College. (Blue points are shades up, yellow points are halfway shades and gray points are shades down) 73
Figure 78. Daylight signal to daylight illuminance ratios of the two-sensor system and the correcting signals for the West orientation in the month of July in Phoenix. (Blue points are shades up, yellow points are halfway shades and gray points are shades down).....73

List of Tables

Table 1. Fixed conditions applied in this study 10
Table 2. Simulation variables - locations, orientations, and shade conditions 24
Table 3. Performance summary for the three photosensor configurations, with details on correction equations 38
Table 4. Results of applying different intercepts to the photosensor correction equations 39
Table 5. Calibration appraisals for month and orientation combinations 43
Table 6. Preferred calibration conditions for different months and orientation under automated shades (all times are local stander time in correspond to the center of TMI hourly data window) 44
Table 7. Alternate calibration conditions for high and medium risk orientations and times from Tables 5 and 6. 45
Table 8. Photosensor system recommendations. Locations (i.e., the referenced circles) refer to locations shown in Fig. 38. 50
Table 9. Correction equation recommendations 51
Table 10. Optimum energy savings for different orientations 53

ACKNOWLEDGMENTS

I would like to express my heartful thanks to God (Allah) who supported me in my life and in this work.

I would like to express my sincere appreciation to Dr. Richard Mistrick for his invaluable guidance through this work and excellent academic advice through my master's period. He is a person who worked hard to best shape my ability to think critically and helped me to add precious value to my academic path.

I would like to acknowledge the support of my great father and mother. Their sacrifices, encouragement, and advice are driving forces for pursuing my advanced degrees and achievements.

I would like to thank my uncle Ayed and my aunt Malak. Their continuous encouragement and support kept me motivated while I was away from my home country.

I would like to thank Dr. Kevin Houser and Dr. Gregory Pavlak for their support as committee members. Their contributions to this work were truly appreciated.

1. Introduction

Architectural sustainability works to enhance the health inside the building, as this is one of its ultimate goals. To serve this direction, a series of conferences were held worldwide since 1988 in order to standardize the factors that affect indoor environmental quality. Safety, energy performance, comfort, and productivity are some important elements in the field of indoor environment quality and are maintained through several approaches, including daylighting strategies (Casares and others, 2014). Energy savings is also often a goal for electrical light energy. However, occupant satisfaction should be achieved through an effective daylight-adaptive lighting control system that results in the required illuminance level and an acceptable illuminance distribution. Consequently, this creates an indoor climate with better performance and production (Caicedo and others, 2014). Promoting electric light energy savings and providing the optimum illuminance level to the workplane are a primary focus of this study.

Previous studies have focused on developing techniques to optimize the electric energy consumed by artificial light through photosensors and lighting control algorithms such as open loop and closed loop algorithms. These algorithms are used and the photosensors are installed based on different recommendations coming from several daylighting research activities that applied distinct spaces with different configurations in order to maximize the benefit of the accessed daylight. One of the latest developments in this field is seeking the best photosensor location with a closed loop control algorithm based on specific daylight delivery systems and shade conditions as well as different space orientations. To improve the performance of a daylight responsive dimming system, considerable studies targeted different mathematical evaluation methods so the proposed control system could produce the required illuminance over the majority of the expected time. Daylight coefficient, correlation coefficient, root mean square error (RMSE) and energy savings are some methods to differentiate between particular design choices. For this purpose, Subramaniam and others (2013) attempted to evaluate locating a photosensor on specific spots in the ceiling with calibration based on the illuminance values of a critical illuminance point. They showed their findings based on a location comparison implementing correlation coefficient, RMSE, and energy savings. However, the resulting photosensor signal to workplane illuminance plots still requires an improvement to elevate the energy savings level and the relationship between the photosensor signal and workplane illuminance.

2. Literature review

2.1 Critical point

Mistrick and Sarkar (2005) had a definition of a critical point on a workplane that they integrated into their five classroom study. The critical point indicates the spot on the workplane that requires the highest setting of dimmed zone output throughout a year. The consideration of this setting should raise the illumination of all points on the workplane to the target illuminance in order to achieve proper dimming performance. Since the daylight conditions vary from one hour to another and from one day to another, the location of the critical point changes throughout the year. Therefore, it is required to evaluate the location of the critical point at all units of time across the year to specify the location that holds the "most frequent critical point" property.

According to Casey and Mistrick's study (2005), and Subramaniam and his partners' report (2013), the location of critical illuminance points fluctuates between a few spots on the workplane. Considering these locations in dimming systems leads to the optimum dimming level with high energy savings. As in Subramaniam's model, there are four critical locations result from the evaluation, achieving 93% energy savings throughout a year. These points are located around the two ends of the space between the two electrical zones (dimmed zone and non-dimmed zone). Fig. 1 illustrates the location of these critical points.

7.2m																
6.6m																
5.9m																
5.3m																
4.7m																
4.1m																
3.5m																
2.9m	11%															40%
2.3m	13%		4%											3%		29%
1.7m																
1.1m																
0.5m																
North ↑	0.6m	1.2m	1.8m	2.4m	3.m	3.7m	4.3m	4.9m	5.5m	6.1m	6.7m	7.3m	7.9m	8.5m	9.1m	9.8m	10.4m

Figure 1. The highlighted grid points represent the four critical point locations in Subramaniam's model (the window is along the bottom of this figure).

2.2 RMSE

The root mean square error (RMSE), or the standard deviation of residuals, is a mathematical technique used in some approaches in daylighting calculations. In terms of comparing different methods for daylight simulation, Reinhart and Herkel (2000) claim that the results that rely on the RMSE method show the weakness of some daylight calculation methods to evaluate different daylight systems, such as the daylight factor method. Likewise, Subramaniam and others (2013) draw a similar conclusion emphasizing the superiority of using the RMSE method in assessing the performance of an integrated daylighting control system. Fig. 2 shows three good candidates for a photosensor location where they present the same correlation coefficients between the photosensor signal and the critical point illuminance. The same three chosen locations, where examined using the RMSE method, clarifying the shortage that the correlation coefficient method has. Fig. 3 proves this claim with numbers where the three photosensor locations, holding the same correlation coefficient values, have different RMSE values giving the closest photosensor location to the South side the priority of localization. This location is the best choice since it has the lowest possible error among the three locations. They finalize that correlation analysis is not always accurate in terms of predicting the performance of a responsive daylight dimming system. The RMSE analysis method is a better evaluator for more accurate selection between specific control algorithms.

7.2m	96	96	96	97	97	97	**97**	**97**	**98**	**97**	97	97	96	96	96	96	96
6.6m	96	97	96	97	97	97	**97**	**97**	**97**	**98**	97	96	96	96	96	96	96
5.9m	96	96	96	96	96	97	97	96	**97**	**97**	96	96	95	95	96	96	96
5.3m	96	96	96	96	96	96	95	97	96	96	95	93	94	94	95	95	94
4.7m	95	95	96	96	95	95	95	95	95	95	96	95	94	93	94	95	93
4.1m	95	94	95	94	93	94	95	95	94	94	94	93	93	92	93	94	94
3.5m	94	95	94	94	95	94	94	94	93	93	93	93	92	92	91	93	92
2.9m	94	95	94	94	94	94	93	94	94	93	92	93	93	91	91	91	93
2.3m	93	94	94	94	93	93	93	95	94	93	93	92	93	91	90	92	91
1.7m	94	94	93	92	93	93	94	94	93	93	93	93	91	91	91	90	92
1.1m	93	91	86	85	84	85	87	91	92	89	87	86	82	82	86	89	91
0.5m	93	88	81	81	80	79	80	85	89	84	82	81	81	77	79	89	92
North↑	**0.6m**	**1.2m**	**1.8m**	**2.4m**	**3.m**	**3.7m**	**4.3m**	**4.9m**	**5.5m**	**6.1m**	**6.7m**	**7.3m**	**7.9m**	**8.5m**	**9.1m**	**9.8m**	**10.4m**

Figure 2. Correlation grid and the three highlighted candidates having the same correlation values

7.2m	6	6	5	5	4	**4**	**4**	**4**	**3**	**4**	4	4	5	6	8	8	8
6.6m	6	5	6	5	4	**4**	**4**	**4**	**4**	4	4	5	6	8	9	10	10
5.9m	6	7	6	5	5	4	4	4	**4**	4	4	5	7	8	9	11	13
5.3m	7	7	6	6	5	4	5	4	4	5	5	7	7	9	11	14	19
4.7m	8	7	6	6	7	5	5	5	5	5	5	6	7	9	11	13	18
4.1m	7	8	8	8	7	6	5	5	5	6	6	7	8	11	12	14	14
3.5m	8	8	8	7	6	6	5	6	7	7	7	7	8	9	13	14	14
2.9m	8	8	8	8	7	6	7	6	6	7	8	7	7	10	11	16	17
2.3m	9	8	8	8	7	7	7	6	6	7	7	8	7	9	11	16	24
1.7m	8	8	7	7	6	6	5	6	6	6	6	7	6	7	9	16	24
1.1m	7	8	9	9	8	8	7	6	6	7	8	8	8	8	8	12	20
0.5m	6	9	12	11	11	10	10	8	7	11	11	11	11	10	9	11	16
North	**0.6m**	**1.2m**	**1.8m**	**2.4m**	**3.m**	**3.7m**	**4.3m**	**4.9m**	**5.5m**	**6.1m**	**6.7m**	**7.3m**	**7.9m**	**8.5m**	**9.1m**	**9.8m**	**10.4m**

Figure 3. RMSE values for the three location candidates

2.3 Photosensor performance analysis

2.3.1 Sky condition influence

Since the main source of all daylight is the sun and its rays are scattered in the sky, interacting with the components of the sky and ground, the received daylight varies over time causing a problem in a daylight responsive control system. Directional variations result in a wide variation in the sensor signal to work plane illuminance ratio. Mistrick and Sarkar conducted research to show the impact of different sky conditions on the commissioning process. They conclude that a sunlight patch is a serious issue which causes illuminance below the illuminance target when the photosensor is calibrated for conditions with an overcast sky. The reason is that the received signal is higher than the expected level for the given daylight condition (Mistrick and Sarkar, 2005). In the IES handbook, DiLaura and others (2011) emphasize that the performance of a photosensor is affected by the daylight condition at calibration. It is preferable to avoid conditions when a weak signal is received or when sunlight penetrates the space. In another study, Choi and Mistrick report that Ed/Sd, the daylight illuminance to daylight signal ratio, for different sky conditions produces higher or lower workplane illuminance than the target illuminance (Choi and Mistrick, 1997).

Littlefair and Motin, in their research, studied a cosine sensor which is shielded by a tube having a very low reflectance in order to avoid direct sunlight on sunny days. The results of this setup are subject to different factors such as sun patch locations. Therefore, they conclude a partially shielded sensor, with care in installation, can reduce the responding signal to half on sunny days, which increases the agreement between the received signal and the workplane illuminance (Littlefair and Motin, 2001).

Seasonal changes cause high variations in the dimming results, so Choi and Sung highly recommend to have a calibration setup that considers these changes in daylight distribution (Choi and Sung, 2000). Park and his colleagues, also draw a similar conclusion. They note that continuous deviations in the relationship between the photosensor signal and the workplane illuminance are caused by highly changeable daylight conditions. To improve the relationship between the photosensor signal and the workplane illuminance and the resulting scatter plot, they conducted a field experiment using a dividing time approach and Id/IT ratio (diffuse solar irradiance (Id) to global solar irradiance (IT)). They use the Julian day as a dividing time and the Id/IT ratio to modify the proportional closed-loop control algorithm. Implementing a Julian day divider results in producing more than 98.64 percent of the workplane illuminance, where the control system provides the target illuminance through a six-month test period. Also, the Id/IT ratio improved the dimming algorithm where the level of illuminance at the workplane remains more than 90 percent through 98.4 percent of the test period (Park and others, 2011).

Due to this variation, Chen, in her master thesis (2013), applied an automated shade setting in order to minimize sunlight penetration. This strategy reduced the reflections from direct sun patches, resulting in a stronger relationship between the photosensor signal and the workplane illuminance level.

2.3.2 Space properties and orientation influence

Mistrick and Sarkar, in their study regarding the performance of daylight control in five different daylighted spaces, portray some guidelines for five different room configurations. The different configurations of rooms have less impact on wideband cosine than on narrowband photosensors. This is because the field of view (FOV) of the narrow band sensor is highly sensitive to any change in the features of the space (Mistrick and Sarkar, 2005). For better photosensor performance and a stronger relationship between the photosensor signal and workplane illuminance, the outputs of the daylight delivery system in any space should be directed away from photosensors. To illustrate this, when daylight is reflected from blinds toward a photosensor, the dimming system performs poorly since the sensor receives a higher signal than expected for the workplane illuminance. This causes the system to over-dim (Kim and Mistrick, 2001).

To investigate the performance of photosensors in different daylight delivery configurations, Littlefair and Motin conducted a study on several innovative delivery designs with photosensors mounted in the middle of a room. They found the daylight delivery mechanism affects the performance of a photosensor critically. Conducting this experiment with clear glazing was the first step to have a baseline of data. Applying Venetian blinds does not make obvious differences in the ratio of signal to illuminance even though the

slats reflect daylight up to the ceiling. This is because the photosensor in the center of the room receives a weak daylight signal. Exchanging the window material with a prismatic film causes direct light to be spread in all directions into space. In this delivery system, they tested shielded and unshielded photosensors. With the unshielded sensor, the ratio of photosensor signal to the illuminance on the workplane was almost similar to the clear glazing plot. However, the shielded photosensor has a narrower field of view that results in more sensitivity in the variation of illuminance at the workplane. As a result, this causes variation in the signal to illuminance ratio when sunlight hits the floor. Littlefair and Motin also examined adding a light shelf with both shielded and unshielded photosensors. The daylight dimming system responds linearly except when daylight is reflected to the sensor by the light shelves, causing over-dimming. Overall, the shielded photosensor produced a better scatter plot if the shelf design blocks the direct sunlight all the time (Littlefair and Motin, 2001).

The introduction of furniture to the space with higher reflectance than the standard floor reflectance is applied in Chen's master thesis. This implementation improves the relationship between the photosensor signal and the workplane illuminance because the workplane becomes a better diffuser with furniture. This causes the signal to illuminance ratio to be more stabilized (Chen, 2013).

In terms of the orientation of the space, Choi and Mistrick, based on their study on daylight responsive dimming system performance, conclude that the orientation of windows affects dimming performance (Choi and Mistrick, 1998). Mistrick and Thongtipaya, in their small office study, conclude that the North orientation gives excellent conditions for photosensor control. However, the South orientation provides several restrictions to be considered in order for photosensors to perform well. In this case, the photosensors are required to be located away from the South apertures and closer to the back of the space. Then, a higher correlation and a better relationship between the photosensor signal and the workplane illuminance is achieved. They recommend different blinds for different orientations in order to produce good photosensor performance. Horizontal blinds are a better choice for the South windows. While, the windows on the East side of the space require vertical blinds where they work better than the horizontal ones in blocking the sun's rays (Mistrick and Thongtipaya, 1997). On the same approach, Kim and Mistrick in 2001 conducted a study on a small room with two windows on one side of the room. They came up with some recommendations from orienting the room to the North and South. When the windows face north, the photosensor signal to workplane illuminance ratio remains fairly constant. This is because the North side is not exposed to direct sunlight, providing only a diffuse component of daylight into the apertures. On the other hand, facing the windows to the south side produces different ratio behavior with less correlation than the North orientation.

Even though photosensors with North-facing windows don't have obvious variation in the signal to illuminance ratio, Chen emphasizes that this orientation is not necessary to produce better performance than a South facing space. This is concluded because of the daylight conditions on a North-façade when sunlight hits the ground and enters the space toward the spatial sensitivity of the cosine sensor causing over-dimming (Chen, 2013).

2.3.3 Photosensor position

According to the five classroom comparison, photosensor accuracy in tracking the daylight is affected dramatically by its view field. It is recommended to mount the photosensor where there is no direct daylight received by the sensor. In other words, the field of view of the sensor should not see the vertical daylight opening. This results in an improvement in the correlation between the signals and the workplane illuminance. Otherwise, the presented data by the photosensors will be highly variable when they are mounted near the vertical daylight apertures. Since the position sensitivity of the sensors increases with narrower view fields, they are required to be moved away from the windows and sun patches to generate a high level of agreement between the photosensor signal and the workplane illuminance. In other words, the key point for providing better tracking of the critical point illuminance is to position the photosensors to limit their field of view from sunlight patches, daylight apertures, or luminaires (Mistrick and Sarkar, 2005).

Optimum performance of the control system should be the target when determining the mounting location of a photosensor. Considering the critical point illuminance as the reference to calculate the correlation between the signals and illuminance improves the control system. Using the RMSE (root mean square error) measure provides more accurate information to determine the best location for the sensors so they can produce closer outputs to the optimum (Subramaniam and others, 2013).

In Chen's thesis, there are three shading setups to prevent direct sunlight from penetrating into space. When the photosensor is located next to the windows, the resulting scatter plots are not desirable, reflecting a low relationship between the photosensor signals and the critical point illuminance on the workplane (Chen, 2013).

2.3.4 Photosensor spatial sensitivity

The location and field of view are critical determinants for the best-designed control system. A narrow band photosensor is very sensitive to any change under the sensor including sunlight patches that may cause it to receive higher signals compared to the workplane illuminance, resulting in over-dimming. Therefore, narrow band sensors should be placed at a significant distance from the vertical daylight opening in order to avoid being affected by the sun patches. Also, a wideband photosensor's performance is better than a narrow one when direct sunlight hits the exterior ground if both see the exterior sunlight patches (Mistrick and Sarkar, 2005). Another study indicates this same concept, that the capability to provide a particular dimming level is subject to some factors, including the spatial sensitivity of the sensor. Different spatial sensitivities produce better outputs in a small room since they receive the majority of light from the walls and horizontal surfaces in the room. However, large spaces don't have this property of a high level of reflected light from the walls, so sensors require other considerations including the location and the field of view (Mistrick and Ranasinghe, 2003).

Other studies apply physical restrictions to the FOV of cosine sensors. Littlefair and Motin compare shielded to unshielded photosensor performance in their innovative daylighting systems study. They emphasize that a fully shielded sensor is not recommended since it is highly affected by sun patches in its field of view. An unshielded sensor gives a better correlation on sunny days since it receives light from the walls. This type of sensor works better for those who subjectively judge the brightness of the space. Also, they partially shielded a photosensor to avoid seeing the windows and accept light from the other surfaces of the space. This step gives acceptable outputs, but it requires more careful installation so that the sensor does not see the window. If the shield does not fully block the view at the window, the results could be worse than the unshielded sensors (Littlefair and Motin, 2001).

2.3.5 Shade setting and impact

On a study of an integrated automatic roller shade and dimming control system, the shade height and the diffuse irradiance to solar irradiance ratio affected system performance (Park and others, 2011). Chen, in her thesis, has a daylight delivery configuration of three shading setups (no shade, halfway shade and full shade down) accompanying a light shelf. Each setting condition has an individual contribution to the total energy savings based on the dimming system. 43% savings of the total lighting energy is achieved from the no shade setup, but permitting sunlight to penetrate into space causes extremely scattered points in the resulting photosensor performance plot. When a halfway shade is set, 36% savings of the total lighting

energy is achieved. In the halfway condition, the signal to illuminance ratio drops dramatically when the photosensor is located close to the window compared to the no shade and full shade down settings. When the photosensor is located deep into space, the control system with a halfway setting performs better since the sensor sees the illumination of the lower portion of the walls and floor by the bottom half of the windows. In the case of full shade down only, 14% saving of the total lighting energy is achieved. This condition minimizes the glare probability and sunlight penetration, but it also reduces the energy savings significantly. Implementing all conditions in an automatic shading system is effective when the location of the sensor and the calibration condition reduce the over-dimming conditions and provide a signal to illuminance ratio close to the no shade case.

3. Research Objectives

This study focuses on promoting the performance of photocontrol systems under different shading and sunlight conditions. In particular, it aims to minimize the partial disagreement between the photosensor signal and the workplane illuminance, rectify any misleading signals, and produce the required electrical light level. This treatment will include at least three shade configurations to reflect the flexibility of a daylight delivery system that blocks direct sunlight and admits more daylight. For practical purposes, the modified results are compared to those generated by a single photosensor, which is calibrated based on the concept of critical points; this sensor is linked with a closed-loop algorithm and mounted on the ceiling according to recommendations from the latest studies in this field. The proposed control system configuration should present a lower RMSE value based on commissioning of a two percent over-dimming, which is allowed based on dimming levels producing illumination less than ninety percent of the illuminance target. The control system configuration must be examined for validation. To achieve this validation, the control system is applied in multiple climate zones and space orientations.

4. Research Hypotheses

- This study hypothesizes that the utilization of two photosensors will outperform a single photosensor in delivering an appropriate dimming level in a space that is subject to non-symmetrical daylight conditions.
- Photosensor system performance can be improved by modifying photosensor signals when the signal to workplane illuminance varies.

- Photosensor performance is orientation-dependent which affects both performance and system commissioning.
- Selection of proper daylighting and shade settings is required for proper photo-control system calibration.

5. Methodology

To generate realistic results, selected system variables for the architectural space model, a trustful simulation tool, statistical analysis methods, and changing variables are employed. The next sections present these four elements of the methodology applied in this study.

5.1 Fixed space and system variables

5.1.1 Space model

Table 1. Fixed conditions applied in this study

Variables	**Discerption**
Space type	Commercial office
Space dimensions	10.21 m x 9.14 m x 3.05 m (33.5 ft x 30 ft x 10 ft)
Internal and external reflectance of the space	80% for the ceiling, 60% for the walls, 30% for the floor, and 20% for the ground
Glass transparency	50% transmittance for windows' glasses
Daylight delivery system configuration	The two windows have symmetrical positions with one vertical centered mullion for each. The fabric shades (halfway and fully down shades) have 3% openness and 5% diffusion.
Type of sensors	Broad sensitivity with a cosine response and a narrow band with a cosine 30 response
Electric light type	2x4 LED recessed troffer at a 3.05 meter height.
Electric light layout	The dimmed zone has two rows of luminaires, each row consists of 4 luminaires (4 troffers), and this zone is next to the windows. The non-dimmed zone consists of one row of luminaires
Target illuminance on the workplane	400 Lux
Number of referenced critical points	Two critical points
Automated shade setting	Three shading conditions (shades up, halfway shades and shades down)

This study targets a relatively large size office with windows on one side and a flat ceiling. Mullions, wall thickness, extended facades, and ground are applied for realistic results (See Table 1) (IES handbook, 2011). AutoCAD is the Autodesk program that was used for creating the model space.

The initial investigation considered a standard large office located in State College, Pennsylvania and oriented to the South. This space is illustrated in Fig. 4 and Fig. 5. Fig. 4 shows the attached exterior elements starting with the extended façade having a 28.96 meter (95-foot) width and 4.27 meter (14-foot) height. The ground has a 28.96-meter x 15.24-meter (95-foot x 50-foot) area and the building has a sloped roof. The exterior side of the window has a vertical mullion attached to each window occupying 7.6×10^{-2}-meter x 1.83-meter (0.25-feet x 6-feet) of the gross area of the window. Also, the mullions have the same thickness as the façade wall, which is 0.2 meter (0.67 feet).

The interior surfaces of the space model have a rectangular shape for walls, ceiling, floor, shade and windows as shown in Fig. 5. The office space has a 10.21-meter (33.5-foot) width, 9.14-meter (30-foot) depth, and 3.05-meter (10-foot) height. Two windows are located in the front wall having a height of 1.83 meters (6 feet) and width of 3.05 meters (10 feet) for each. They have symmetrical positions in the exterior wall where they are mounted 0.914 meters (3 feet) from the floor and have a 1.14-meter (3.75-foot) offset from the end of the wall. There are two internal shade settings considered. One setting fully covers the two windows and the other setting covers the top half area of the windows.

The exterior and interior surfaces have distinct reflectance values emulating the average reflectance of real environments and constructions. The ground has a reflectance of 20 percent while the exterior surfaces have 30 percent reflectance except for the sloped roof which has a 60 percent reflectance. The ceiling has a reflectance of 80 percent, the interior walls have 60 percent reflectance, and the floor reflects 30 percent of the light. The daylight delivery system (side daylight apertures) has a glass with a 50 percent transmittance, whereas this 50 percent daylight admission is reduced by the 8 percent visual transmission of the fabric shades that includes 3 percent openness plus 5 percent diffuse daylight admission.

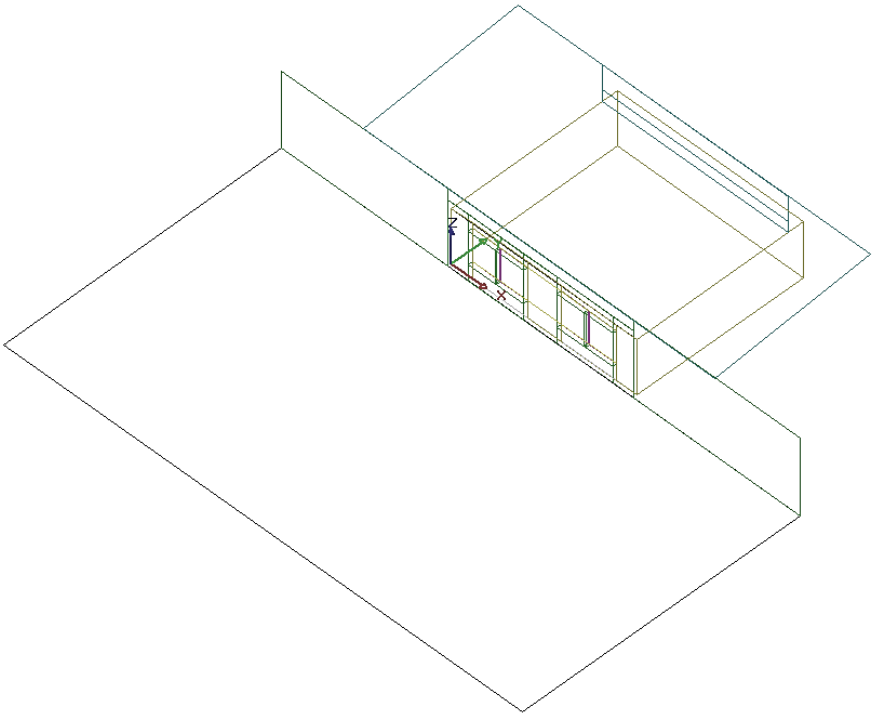

Figure 4. The complete view of the AutoCAD model

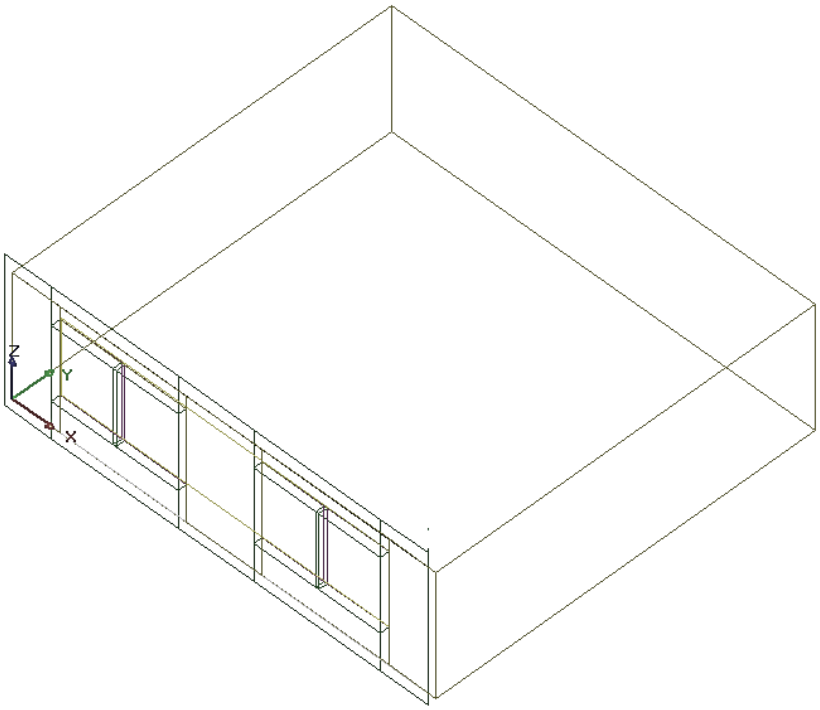

Figure 5. The office space view of the AutoCAD model

5.1.2 Photosensor models

Two photosensor files were used in the simulation, as illustrated in Fig. 6 and Fig. 7. A wideband cosine sensor was used to collect the main control signals. The other photosensor is a narrow band sensor that views a 60-degree cone.

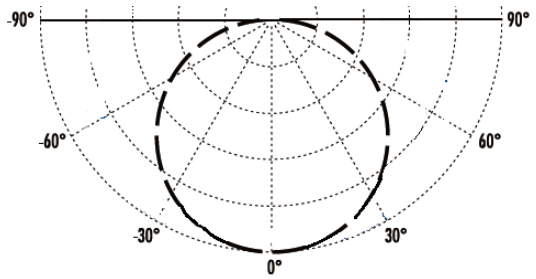

Figure 6. Spatial sensitivity of a wideband sensor (cosine sensor) (Chen, 2013)

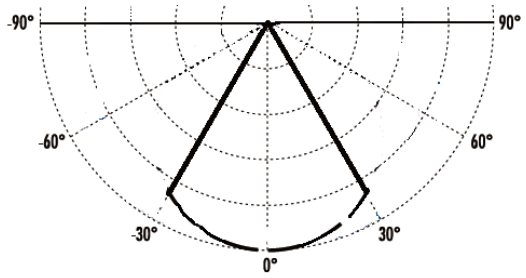

Figure 7. Spatial sensitivity of a narrow band sensor (cosine 30 sensor)

5.1.3 Electric light models

The electrical lighting system being studied is a recessed 2x4 LED troffer. The manufacturer is Lithonia Lighting and the catalog number is 2GTL4_4400LM_LP835. The candela distribution is shown in Fig. 8.

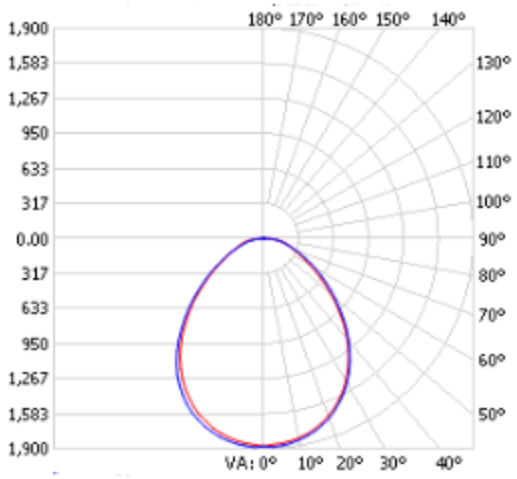

Figure 8. The candela distribution of the 2GTL4_4400LM_LP835 troffer.

5.1.4 Critical point

After extracting the data from the main simulation, the illumination from daylight and electric light across the grid of sensors at the workplane level is applied to locate the critical points. With a target illuminance of 400 lux, all grid points are calculated for the electric light they require from the dimmed zone at every hour in the year. Next, all points are checked to determine the point that has the highest need of electric light at every hour. Then, the points are characterized by the number of hours they served as the critical point for the space. Based on previous studies, more than one critical point works better than one critical point as explained in Chen's thesis (2013). Therefore, for the investigation of sensor signal correction, this work applies the two most frequent critical points throughout the year and implements the one that requires more electrical light from the dimmed zone to compute the desired dimming level at each hour of the year.

5.1.5 Shade settings

To approach this part, the profile angle of the sun and the direct sun's illumination (E_{dn}) are calculated for each hour of the year. Then, the operation of shades (shades up, shades down and halfway shades) is evaluated based on the depth of sunlight penetration and a direct sun illumination trigger, an E_{dn} threshold of 1000 lux. There are four shade control depths considered: 0.305-meter, 0.609-meter, 0.914-meter, and 1.219-meter (1-foot, 2-foot, 3-foot, and 4-foot) depths from the window wall. These depths are demonstrated in Fig. 9, Fig. 10, Fig. 11 and Fig. 12, and each depth categorizes the functionality of the shades based on the determined angles. The shade control depth that shows a high range of final sensor signals and higher agreement between the received signals and workplane illuminance is given the priority to be used for the rest of this work.

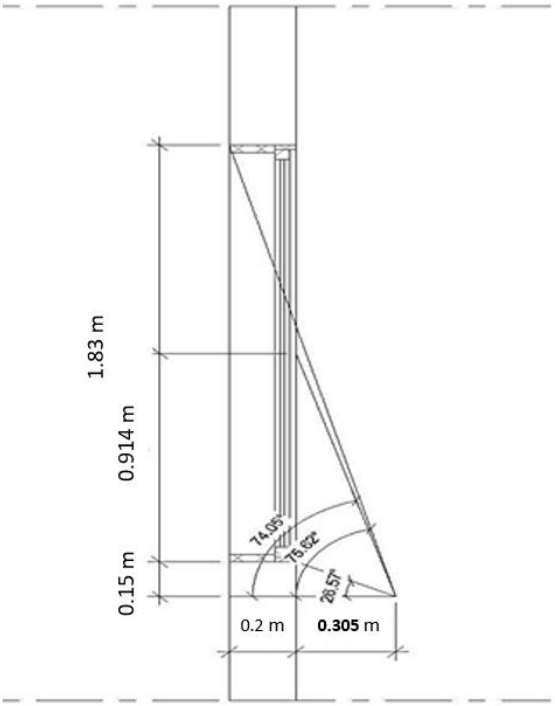

Figure 9. 0.305-meter (1-foot) shade setup

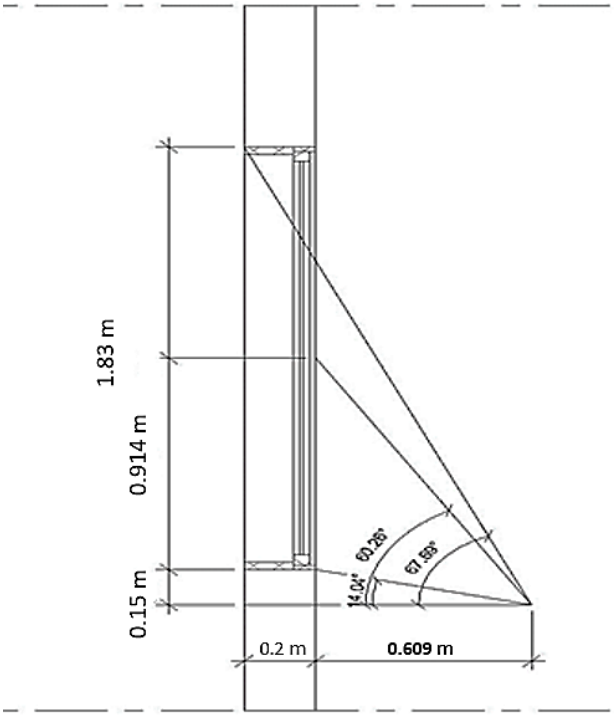

Figure 10. 0.609-meter (2-feet) shade setup

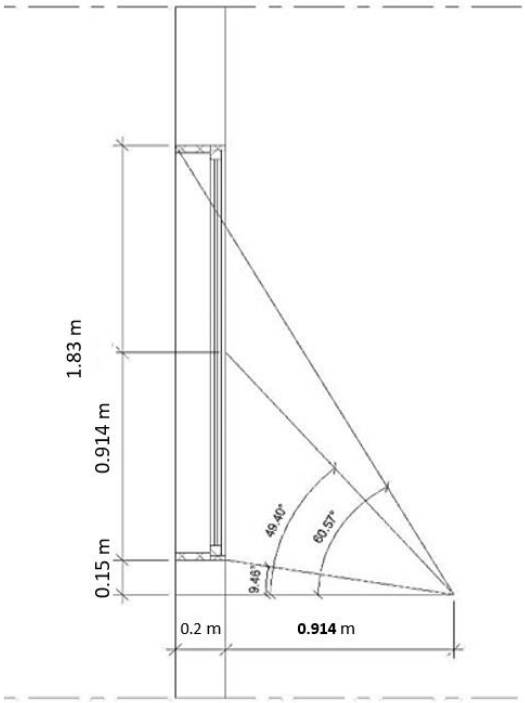

Figure 11. 0.914-meter (3-feet) shade setup

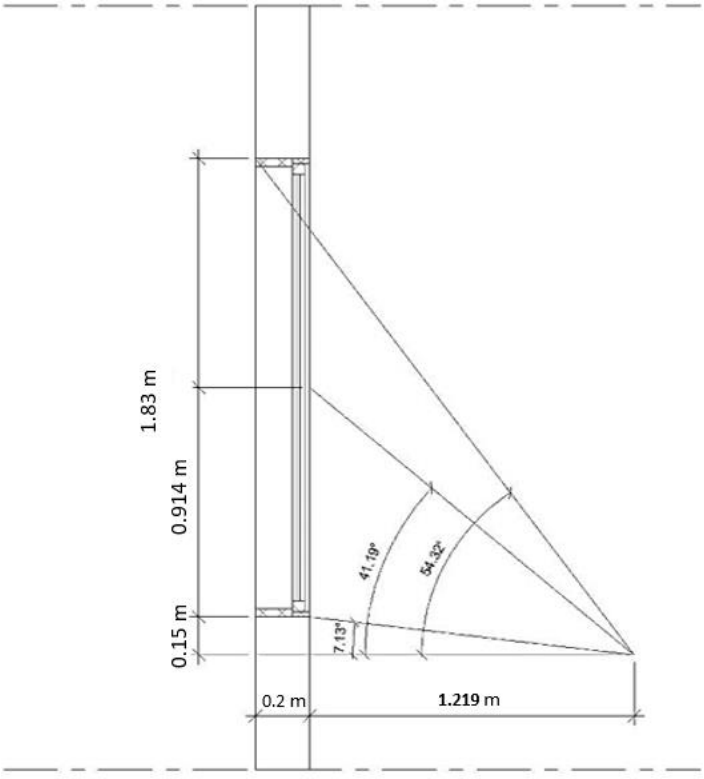

Figure 12. 1.219-meter (4-feet) shade setup

The examination of sunlight penetration depth works only for the South, East and West model orientations since sunlight hits these facades for a significant number of daylight hours. The north orientation has another measure to implement a halfway shades condition. This measure first requires identifying the sensor location from the workplane illuminance grid that receives the highest daylight level throughout the year. Fig. 13 illustrates the photosensor grid and shows a candidate spot at point 46 to activate the halfway shades condition in the North orientation in both sites. The second step is selecting a threshold daylight illuminance to activate the halfway shades conditions for the brightest 10 percent of the daylight hours in order to evaluate the control performance with this shade setting.

241	226	211	196	181	166	151	136	121	106	91	76	61	46	31	16	1
242	227	212	197	182	167	152	137	122	107	92	77	62	47	32	17	2
243	228	213	198	183	168	153	138	123	108	93	78	63	48	33	18	3
244	229	214	199	184	169	154	139	124	109	94	79	64	49	34	19	4
245	230	215	200	185	170	155	140	125	110	95	80	65	50	35	20	5
246	231	216	201	186	171	156	141	126	111	96	81	66	51	36	21	6
247	232	217	202	187	172	157	142	127	112	97	82	67	52	37	22	7
248	233	218	203	188	173	158	143	128	113	98	83	68	53	38	23	8
249	234	219	204	189	174	159	144	129	114	99	84	69	54	39	24	9
250	235	220	205	190	175	160	145	130	115	100	85	70	55	40	25	10
251	236	221	206	191	176	161	146	131	116	101	86	71	56	41	26	11
252	237	222	207	192	177	162	147	132	117	102	87	72	57	42	27	12
253	238	223	208	193	178	163	148	133	118	103	88	73	58	43	28	13
254	239	224	209	194	179	164	149	134	119	104	89	74	59	44	29	14
255	240	225	210	195	180	165	150	135	120	105	90	75	60	45	30	15

N

Figure 13. Photosensor grid showing numbered analysis points in the space and the shade trigger location (point 46) for North orientation halfway shades application

5.2 Simulations

5.2.1 Simulation tool

DAYSIMps is a Radiance-based advanced daylighting analysis tool. It is the main simulation tool used in this research since Radiance is considered as the most accurate daylighting software (Gibson and Krarti, 2015). After the model simulations are run by DAYSIMps, a set of results files is created with all daylight and electric light data, including illuminance, signals, and other accompanying details. These results are required for further statistical analysis. To obtain these simulation results, there are some required inputs to the DAYSIM program.

5.2.2 Simulation inputs and setups

Conducting a simulation on DAYSIMps requires the TMY weather file for a specific site. An occupancy file is also required, as well as the Radiance modeling geometry and material data. The number of sensor points on the workplane is 255, distributed evenly and directed toward the positive Z-axis. The grid distribution on the workplane has a 0.61-meter (2-foot) spacing between sensors and is offset 0.23 meter (0.75 foot) in the X-direction, 0.305 meter (1 foot) in the Y-direction, and 0.76 meter (2.5 feet) in the Z-direction. For the luminaire layout, Fig. 14 displays the four columns and three rows of 2x4 LED troffers on the ceiling. It also shows the luminaire placement on the ceiling where they are spaced 2.44 meters (8 feet) in the X-direction and 3.05 meters (10 feet) in the Y-direction. As shown in Fig. 15, this luminaire configuration produces acceptable illuminance contours. This means maintaining the uniformity of illumination on the workplane at the illumination level target, which is 400 lux. Fig. 15 also displays that there are two luminaire zones specified for control purposes. The two red rows, representing a dimmed zone, are placed next to the windows. The last row (the green luminaire row) is a non-dimmed zone.

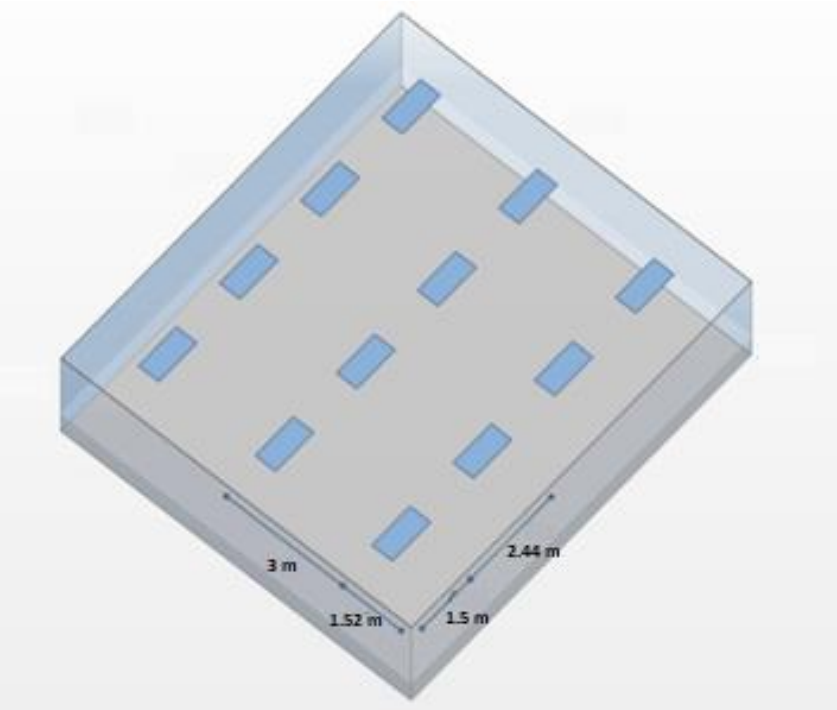

Figure 14. The isometric view of the luminaire layout

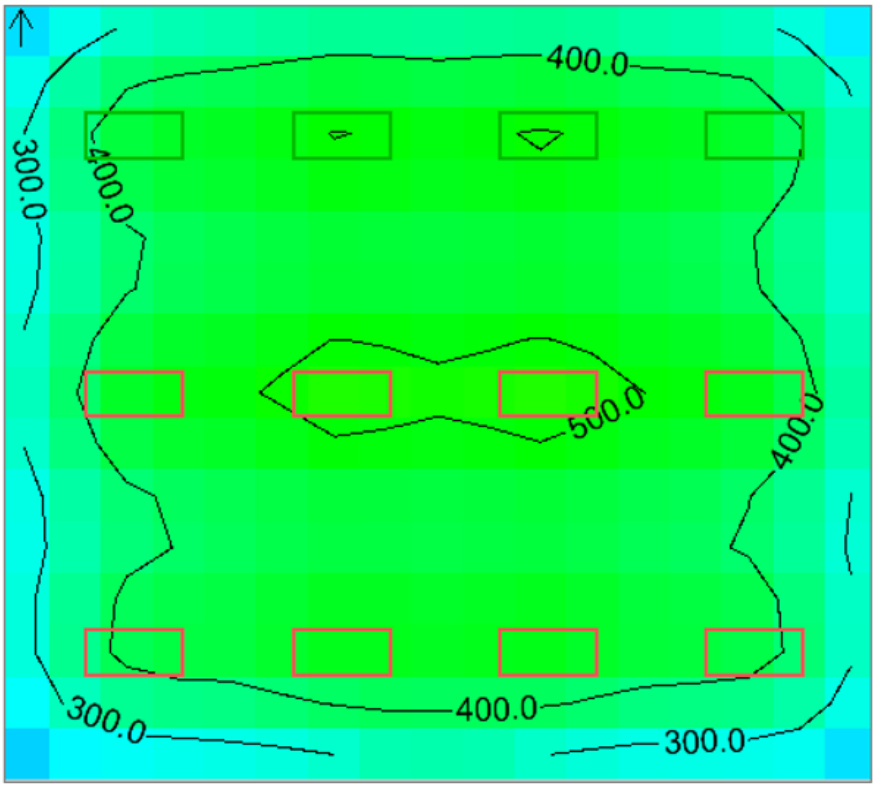

Figure 15. The illuminance contours of the luminaire layout

5.2.3 Configuration simulation runs

After all simulation preparation, the main DAYSIMps simulation is run to create the illumination files for the electric light and daylight throughout a year at the workplane grid points. Then, other minor DAYSIMps simulations are run for different sensor views, locations or aiming. Some minor simulation runs are done as the main responsive control sensors are varied based on their field of views and configurations.

Running these sensor configurations results in signal files for the non-dimmed zone and dimmed zone electric light and other files for shades up, shades down and halfway shade cases throughout the year. Based on the location and the configuration of a photosensor, the same configured sensor is symmetrically relocated on the other side of the space and simulations run to produce its signal files. The last minor run is related to a narrow band correction photosensor (cosine 30) aimed toward the window. Each one of these runs is needed for the analysis process and to build the final signal correction model.

5.3 Statistical analysis

5.3.1 Statistical analysis tool

An Excel spreadsheet was created to manipulate and process the extracted data from the simulation runs. It helps in sorting data, using formulas across a grid of cells, and then building suitable charts. Also, it has the capability of generating plots using colors for clearer differentiation. Its plot builder is a great help for predicting relation patterns, identifying trends and key points to the user. Furthermore, it provides a flexible data environment to consolidate information from different files and sheets.

5.3.2 Control system options

After selecting the critical points and the shade settings, different methods of control of the dimming zone electric light were investigated. The first approach uses one photosensor for control. This system required some investigation regarding the sensor field of view and its location to obtain satisfying results. The next approach adds another sensor symmetrically positioned on the other side of the space and selects the lower signal at each hour of the year. The results from this two-sensor control system are upgraded as a third approach. The control signal was adjusted by means of a correction factor equation to increase the agreement between the two-sensor system signals and the workplane illuminance.

5.3.2.1 Single sensor control system

This section describes the steps that were followed to evaluate the potential results from installing one photosensor in a space. According to previous studies regarding the best control system performance, the location of a photosensor should be carefully evaluated to strengthen the relationship between the sensor signal and the work plane illuminance. Also, the location that produces a minimum RMSE value and a wide range of signals is recommended (Chen, 2013). To begin the analysis, a photosensor is located and the simulation is run. Signal files from shades up, shades down, halfway shades, the non-dimmed zone, and the dimmed zone are created and entered into an Excel file with the four-foot sunlight penetration criteria applied to select a shade setting. Based on the selected critical point illuminance and the shade setup, the associated dimming levels are calculated along with the associated daylight signals. The final signal is calculated as a summation of the signal from the daylight, non-dimmed zone, and dimmed zone.

Final signal = daylight signal + non-dimmed light zone signal + DL * Dimmed light zone,

where DL is the computed optimum dimming level.

Next, a scatter plot of performance is generated showing the paired values of the final signals and their associated dimming levels.

The evaluation begins with finding the calibration line equation. This line is selected to limit performance to 2 percent over-dimming. Over-dimming refers to delivery of less than 90 percent of the target illuminance (400lux) at one of the two critical points. The dimming algorithm produced by this calibration line produces different resulting signals and linked dimming levels (DL_C). From these new dimming levels (DL_C), the root mean square error is calculated between the optimum dimming level (DL) and the calibrated algorithm dimming level (DL_C).

5.3.2.2 Two sensor control system

The first attempt at improving the results from the one photosensor control system applies a second symmetrical photosensor and selects the lower of the two signals at each hour for all shade setups. The purpose of selecting the lowest signal value is to address the darker side of the room, which is typically affected by sunlight patches on the floor or on a sidewall. This process causes the scattered points to be closer to each other throughout the early and late day hours providing a stronger relationship between the sensor signal and the workplane illuminance. Next, the resulting signal file is implemented as if it is a one-sensor system; the calibration line equation is applied to generate the signals and associated dimming levels (DL_C) for the two-sensor system. From this new dimming level (DL_C), the root mean square error is calculated between the optimum dimming level (the same as from the single sensor analysis) and the equation dimming level (DL_C). Furthermore, the potential energy savings from this two-sensor configuration is calculated and compared to the single sensor system.

5.3.2.3 Two sensor control system with correction

The concept of correcting the resulting signal comes from recognizing that different signal to illuminance ratios for daylight is the reason for disagreement seen in the scatter plots. A modification to the main photosensor signals is proposed to produce signals that better represent the workplane daylight levels in the space. To implement this concept, the mounting position and aiming of a third narrow-band (cosine 30) photosensor are used to assess the daylight signal to daylight illuminance ratio of a two-sensor system. Using a third sensor (a correcting sensor) to evaluate the nature of the photosensor signal to workplane

illuminance ratio from daylight alone, S_d/E_d, for the purpose of correcting it, will be investigated. Multiple configuration options of the correcting sensor were tested. These configuration options collect daylight signals on the ceiling that come either from the windows and the adjacent floor. The collected daylight signals from these correcting sensors were coupled with the resulting daylight signal to daylight illuminance ratio from a two-photosensor system in an attempt to predict when the S_d/E_d ratio was high. Indeed, location and field of view of the correcting sensor play the main role in determining whether this coupling process is acceptable or not.

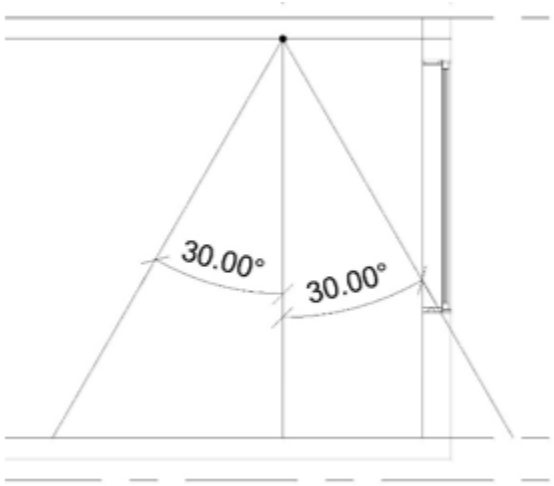

Figure 16. Configuration of a cosine 30 sensor

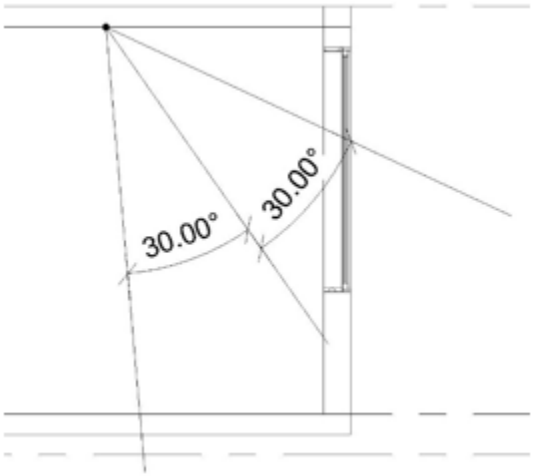

Figure 17. The configuration of a cosine 30 sensor tilted toward the window

To decide which configuration of the correcting sensor produces an acceptable coupling pattern, it was located on the ceiling close to the windows where it can receive high daylight signals. It was either directed vertically down toward the workplane or tilted toward the window as shown in Fig. 16 and Fig. 17. If the trend in the generated scatter plot is obvious, this correcting sensor data can be applied in a correction factor equation.

To find the correction factors, a correction line was applied through the middle of the pattern. The second step is to locate a daylight condition on the calibration line of the two-sensor control system and determine the daylight signal to daylight illuminance ratio (S'/E) of this condition. Then, the correction line is used to adjust the associated daylight signal based on its associated correcting photosensor signal and the correction line. For this adjustment, the daylight signal is divided by the ratio of the two corresponding S/E values on the correction line. This process generates a correction factor for every daylight signal at each hour throughout a year.

The daylight signal of the two-sensor system is multiplied by the synchronized correction factor at each hour, generating a more stable S/E distribution across all hours of the year. Finally, the RMSE and potential energy savings from this two-sensor system with correction are calculated and compared to the single sensor performance.

5.4 Study variables

This analytical process was applied in different office orientations and climate zones. The three control system configurations (single, two-sensor, and two-sensor-corrected) were applied in the office model in both State College, PA and Phoenix, AZ with the details listed in Table 2. Each orientation/shade combination at each location required three DAYSIMps runs (one simulation run for each sensor).

Table 2. Simulation variables - locations, orientations, and shade conditions

	Orientations				
	South	North		East	West
State College	3 shade settings (up / ½ / down)	Shades up All hours	Shades up, Halfway shades	3 shade settings (up / ½ / down)	3 shade settings (up / ½ / down)
Phoenix	3 shade settings (up / ½ / down)	Shades up all hours	Shades up, Halfway shades	3 shade settings (up / ½ / down)	3 shade settings (up / ½ / down)

6. Results and analysis

6.1 Critical points

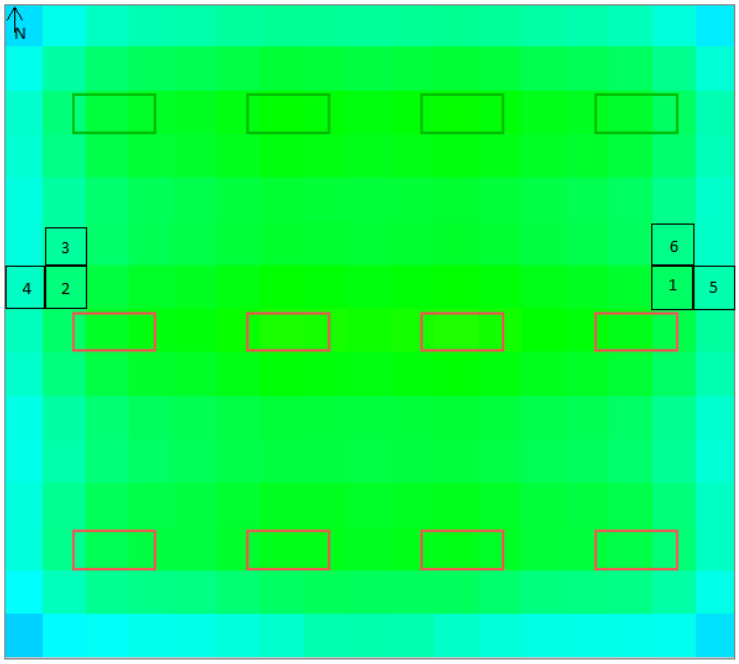

Figure 18. The critical point locations in the simulation model

To identify the critical points, all grid points were checked for the highest need of electric light for every hour in the State College simulation with a South orientation. The points that are served by the highest number of hours were the critical points of the office space. These points are represented in Fig. 18. Point

one indicates the most frequent critical point location throughout the year with 2759 hours, while point two is second with 430 hours. 59, 21, 12 and 9 are the hours of the third, fourth, fifth and sixth most critical locations respectively. The first and second points were applied to the calibration process in this study in the determination of the optimum dimming level at any hour.

6.2 Shade setting

The shade setup that shows more agreement between the illuminance and the total sensor signal was implemented for the rest of this study. The 1-foot sunlight penetration criteria closed the shades across a large range of angles and severely limited daylight levels within the space. Fig. 19 presents the relationship between the optimum dimming level and the photosensor signal based on the two critical points produced based on a cosine sensor located at (2.68, 1.83, 3.05) and aimed vertically down. It results in a 34% RMSE that displays a lack of agreement between the signals and illuminance with the 0.305-meter (1-foot) shade setup. This condition is still apparent at the 0.61-meter (2-foot) and 0.914-meter (3-foot) shade trigger distances. However, the shade setup with 1.22-meter (4-foot) sunlight penetration provides less shade down hours than the 1-foot setup by half and shows a higher agreement between the workplane illuminance and photosensor signals where it results in a 30% RMSE.

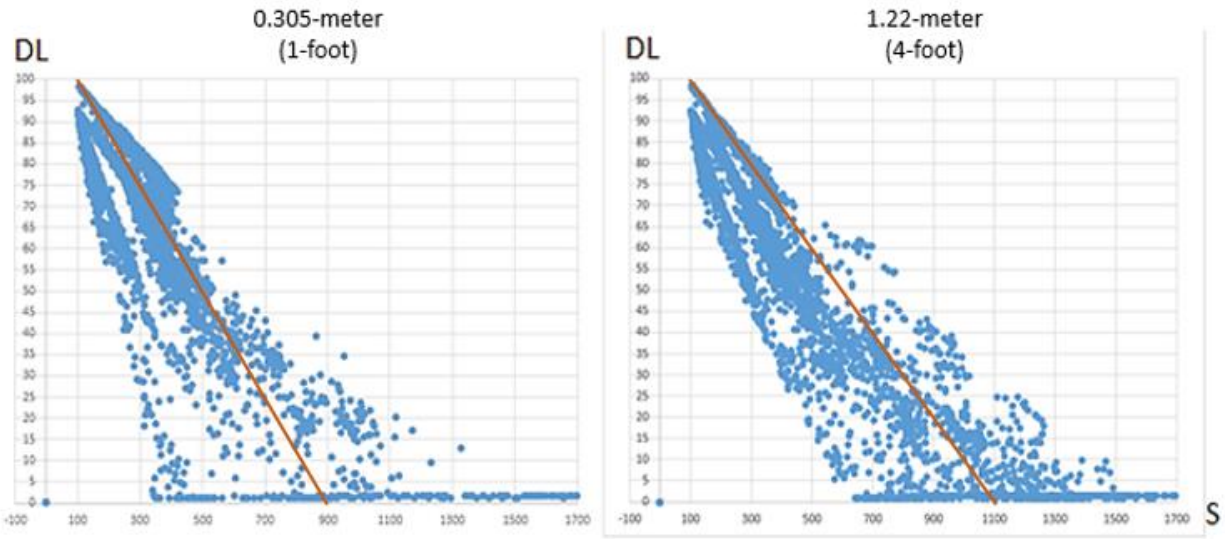

Figure 19. 0.305-meter versus 1.22-meter shade trigger performance plot in South facing State College office

6.3 Single sensor approach

6.3.1 Optimizing FOV for a single sensor centered on the window

For the application of a single photosensor, different photosensor configurations were examined to determine the optimum field of view and spatial sensitivity that provide the best control performance of a single photosensor centered on the window. Using the South-oriented model in State College, a cosine 30 sensor was located at (2.68, 3.96, 3.05), which is centered on the west window, with a vertical orientation direction to the floor. In Fig. 20, spot number 1 illustrates the location of this cosine 30 sensor. Processing the resulting signal data from the simulation of this sensor configuration generates the signal versus dimming level scatter plot (a performance plot) shown in Fig. 21. In this figure, the calibration line that allows 2 percent over-dimming is the line from (40.89, 100) to (160.9, 1) resulting in a 28.63 RMSE.

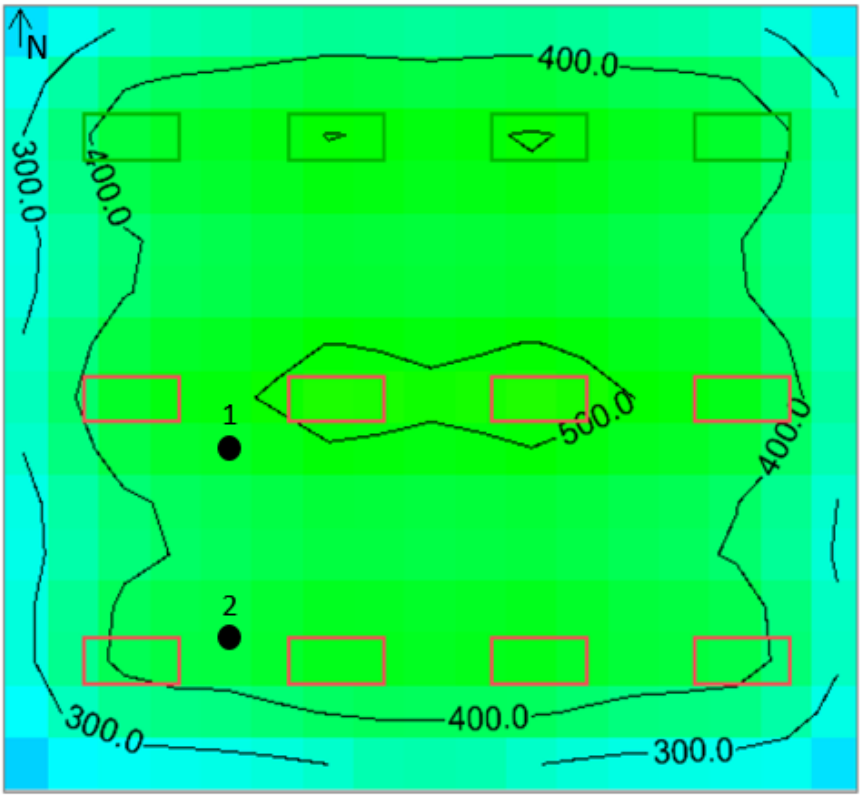

Figure 20. Cosine 30 sensor locations for centered-on-window sensor investigation

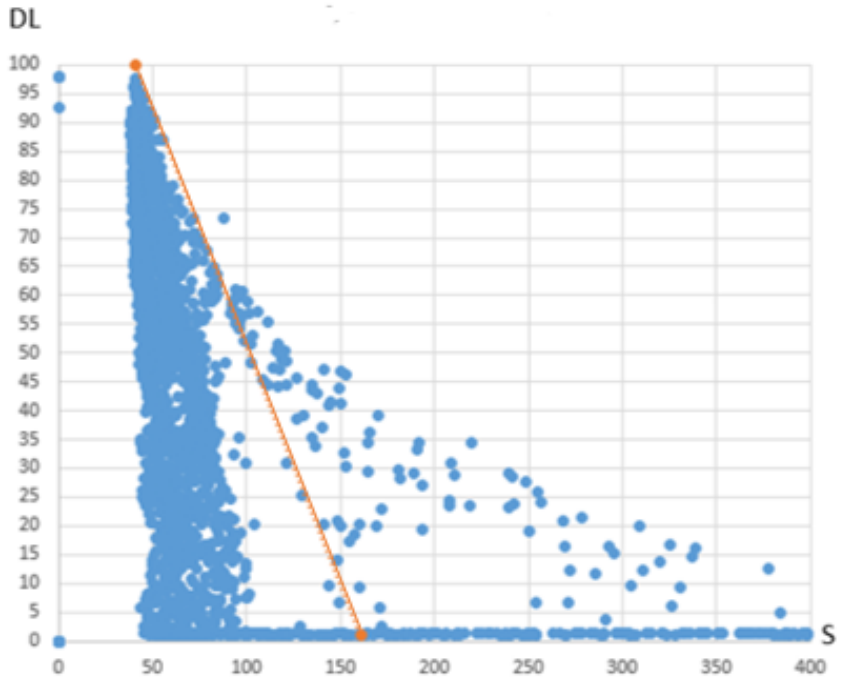

Figure 21. Scatter plot of dimming level (DL) and final signal (S) for a cosine 30 sensor located at (2.68, 3.96, 3.05) and vertically aimed to the workplane in South facing State College office

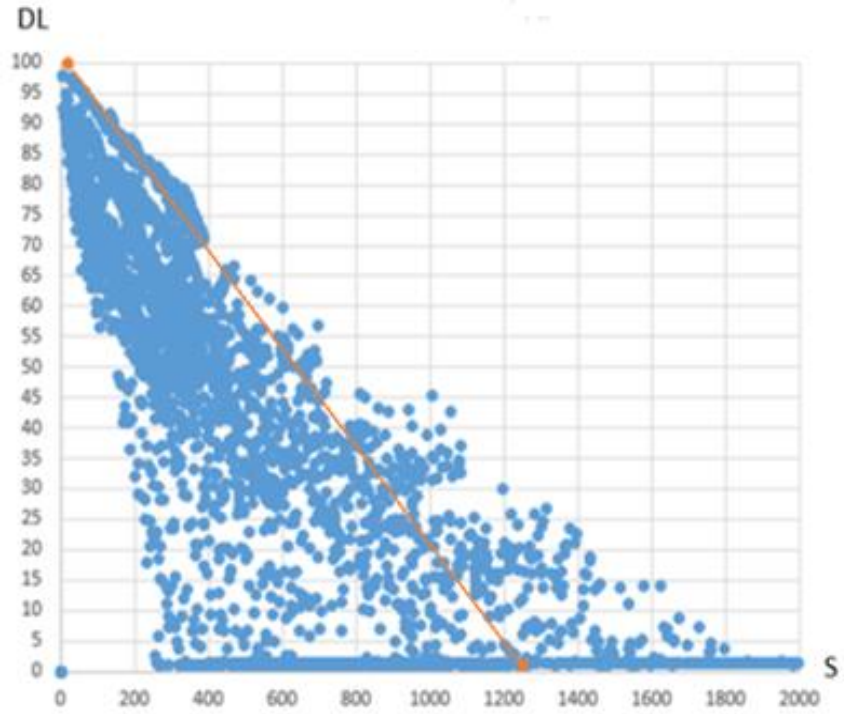

Figure 22. Scatter plot of dimming level (DL) and final signal (S) for a cosine 30 sensor located at (2.68, 1.83, 3.05) and tilted 45 degrees toward the window in South facing State College office

Relocating the cosine 30 photosensor to (2.68, 1.83, 3.05) with a new direction to (0, -1, -1) produced the performance plot shown in Fig.22. The location of this photosensor is illustrated as a spot number 2 which is closer to the South side of the South-oriented office as presented in Fig. 20. Under a 2 percent over-dimming criterion, the calibration line was placed between points (18.4, 100) and (1250, 1) resulting in a 22.23 RMSE.

When the cosine 30 photosensor was directed away from the window at 45 degrees from the same location (2.68, 1.83, 3.05), a different scatter plot was generated from its resulting signals. Its location is illustrated with the same spot number 2 which is closer to the South facing window in Fig. 20. Fig. 23 displays performance of this cosine 30 sensor configuration where the calibrating line lies between the points (41, 100) and (147.15, 1) and allows 2 percent over-dimming, resulting in a 28.99 RMSE.

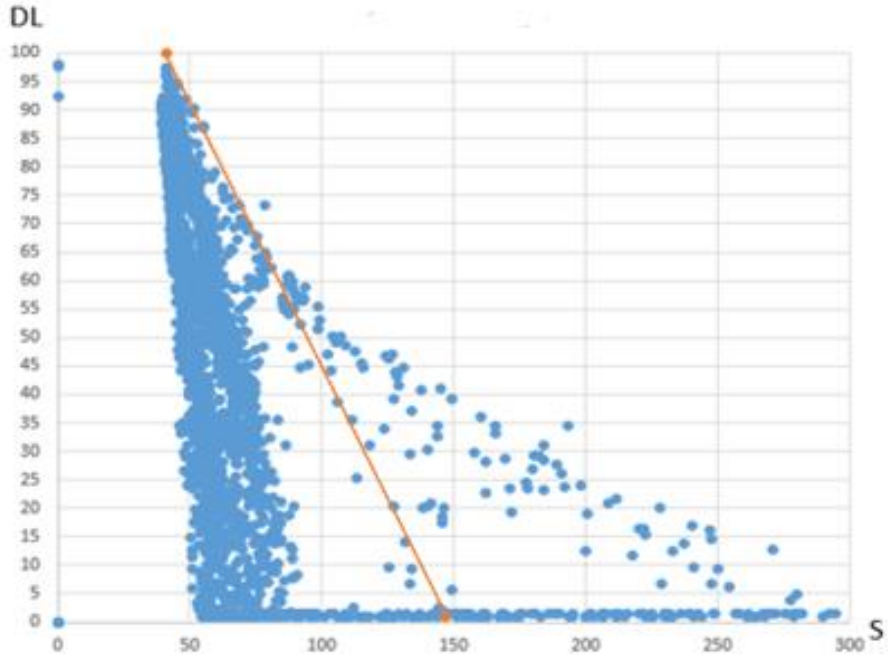

Figure 23. Scatter plot of dimming level (DL) and final signal (S) for a cosine 30 sensor located at (2.68, 1.83, 3.05) and tilted 45 degrees inward in a South facing State College office

Checking the performance of another sensor setup with a different spatial sensitivity, a wideband cosine sensor was located at (2.68, 3.96, 3.05) and directed vertically to the floor. This location is illustrated as a deep spot with number 1 in Fig. 24. The resulting dimming level versus final illuminance signal plot is shown in Fig. 25. For the 2 percent over-dimming criterion, the calibration line lies between the points (118.36, 100) and (601.9, 1) and produces a 19.82 RMSE.

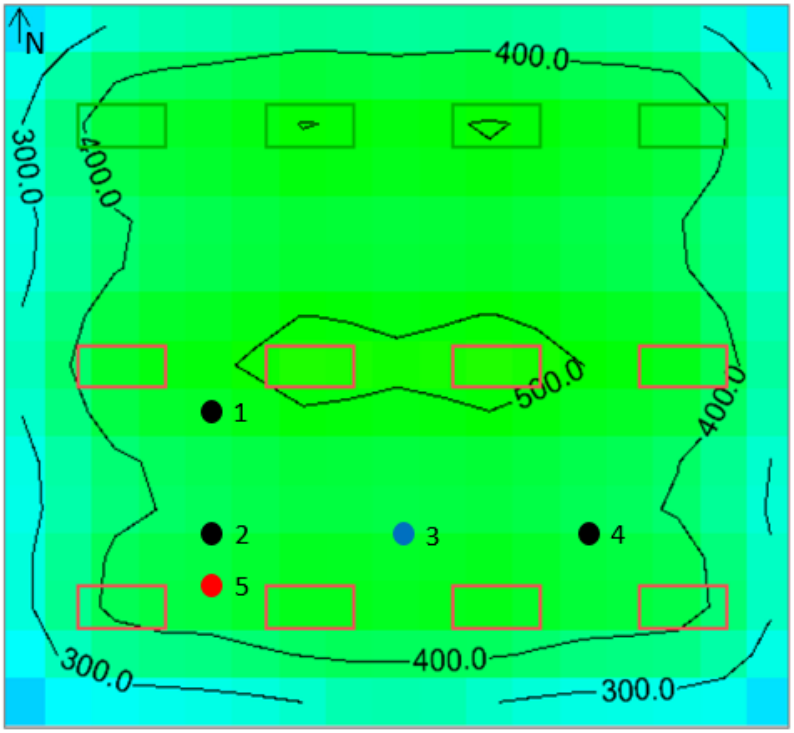

Figure 24. Locations of cosine and 35-degree-tilted cosine 30 sensors for centered-on-window sensor investigation

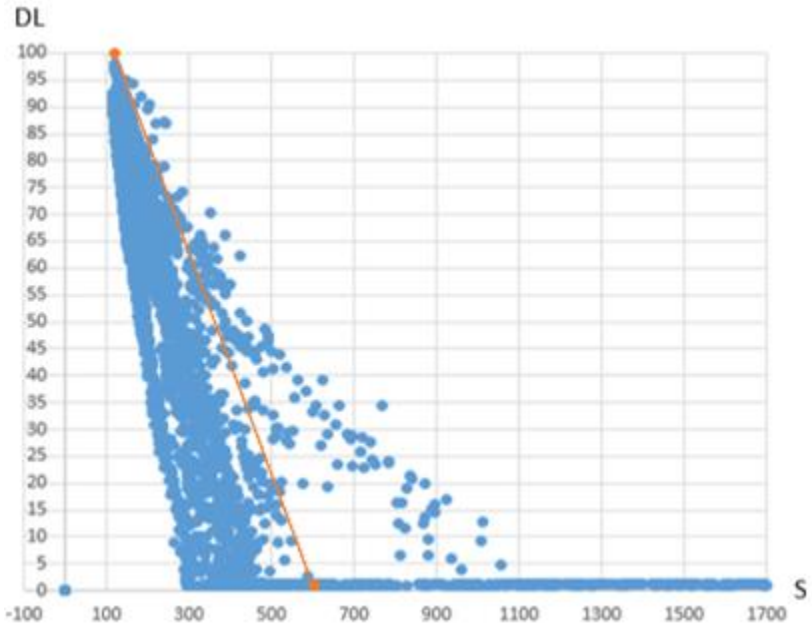

Figure 25. Scatter plot of dimming level (DL) and final signal (S) for a cosine sensor located at (2.68, 3.96, 3.05) and vertically aimed to the workplane in a South facing State College office

The same wideband cosine sensor was moved to (2.68, 2.44, 3.05), and its direction was still vertically down to the workplane. Its location is displayed as a spot number 2 in Fig. 24. This sensor configuration results in a calibration line that starts with a 118.4 signal and 100 percent dimming level and ends with 996.9 signal and 1 percent dimming level meeting the 2 percent over-dimming criterion (See Fig. 26). This calibration line resulted in a 17.07 RMSE.

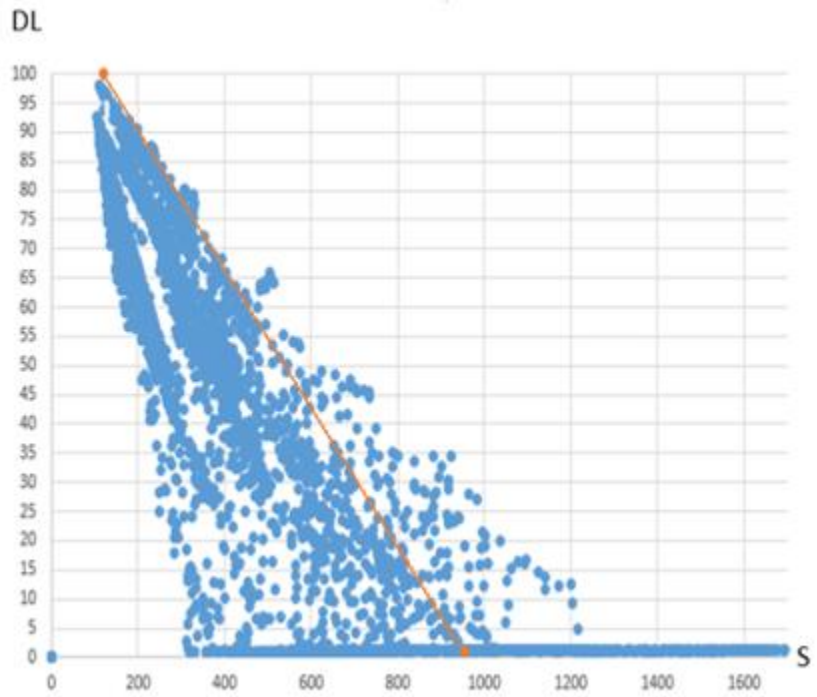

Figure 26. Scatter plot of dimming level (DL) and final signal (S) for a cosine sensor located at (2.68, 2.44, 3.05) and vertically aimed to the workplane in South facing State College office

6.3.2 Single window-centered sensor analysis

The locations of the window-centered photosensors in the single sensor control system were chosen based on previous studies with some added modifications such as tilting sensors in order to check their performance with different directions. Starting with the narrow cosine sensor, the vertical option at 3.96-meter (13-foot) depth developed a steep plot pattern where it did not provide a wide range of signal distribution. Also, it had many extreme scattered points, indicating that the sensor's FOV is highly affected by sunlight patches on the floor, resulting in a high RMSE. When this narrow sensor was moved to the depth of 1.82-meter (6-foot) and tilted toward the window, the RMSE value obviously decreased since the sensor was subject directly to the changes in daylight level. However, the scattered points were not close

to each other, and many points were under-dimmed producing more electric light than the illuminance target. This occurred because the sensor was on the West side of the office and affected by sunlight in the early morning. Redirecting this sensor toward space instead of the window did not help. It produced similar results to the cosine 30 sensor at a depth of 3.96 meters (13 feet). The other option was increasing the spatial sensitivity using a wide FOV sensor, the cosine sensor. The cosine sensor at a depth of 3.96 meters (13 feet) results in a steep algorithmic line, but it was less steep than both the 3.96-meter-depth cosine 30 sensor and the cosine 30 sensor tilted into the office space. Also, it produced less RMSE by far. Moving the wideband sensor to 2.44 meter (8 feet) depth improved control performance dramatically and reduced the RMSE value. Since the narrow cosine sensor configurations had higher RMSE values than the wide cosine sensor setups, the wide sensor was better in term of results.

Therefore, in this South-oriented office model, the cosine photosensor at (2.68, 2.44, 3.05) and vertically aimed to the workplane was the recommended choice for a window-centered photosensor in a single sensor control system that was evaluated based on two-workplane illuminance critical points. Indeed, placing the sensor at this location produced strong signals, a wide range of signals and a strong linear relationship between the sensor signal and the workplane illuminance. Moreover, the potential energy savings from this sensor configuration computed based on the generated dimming level from the calibration line (DL_E) was approximately 39.04 percent for the dimmed zone lighting energy in the South-oriented office in State College. In a final evaluation of the window-centered single sensor, the resulting performance was not very pleasing. This leads to the investigation of alternative approaches that strengthen the relationship between the signals and the workplane illuminance.

Furthermore, these window-centered sensors were centered on the west window in the south and north scenarios because these orientations have symmetry in the represented daylight values where left or right placements produce relatively similar data throughout a year. However, the window-centered sensors were applied when centered on the south window in the East and West orientations in order to minimize the influence of sunlight patches.

6.3.3 Window-centered and room-center photosensor comparison

This section provides data on which single photosensor location achieved better performance values in the South-oriented office in State College. For this comparison, a cosine sensor was located at the same depth of 2.44 meter along the center of the exterior wall and directed vertically to the workplane. Its location is displayed as a blue spot with number 3 in Fig. 24. Fig. 27 shows the performance of this photosensor

condition. For the 2 percent over-dimming criterion, the assigned calibration line was between the points (116.61, 100) and (901.9, 1). It resulted in 17.19 percent RMSE and 38.38 percent energy savings representing a very slight drop in the savings compared to the selected window-centered sensor. This comparison process was applied at both sites and at all orientations to determine the more optimum single photosensor position (See Table 3). The best performing single (centered-on-window or room-center) sensor was used to show the improvement of the next control approaches for each orientation (See Table 3).

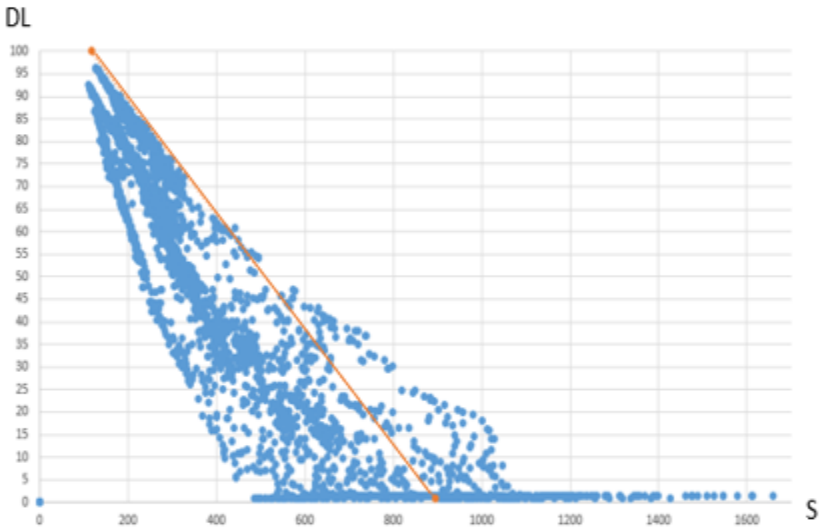

Figure 27. Scatter plot of dimming level (DL) and final signal (S) for a cosine sensor located at (5.11, 2.44, 3.05) and vertically aimed to the workplane in South facing State College office

6.4 Two-sensor approach

This approach works to select the lowest signal from two side photosensors. One sensor is the optimum window-centered sensor from the first approach and the second is a symmetrical sensor on the other side. Applying a two-sensor system in the South-oriented office in State College using the two critical points and shading setup resulted in a performance plot as shown in Fig. 28. A calibration line, allowing 2 percent over-dimming criterion, was set between (108.9, 100) and (901.9, 1) that produced a 14.04% RMSE and 41.9% energy savings. This approach was applied to all four orientations in both cities and the results are presented in Table 3.

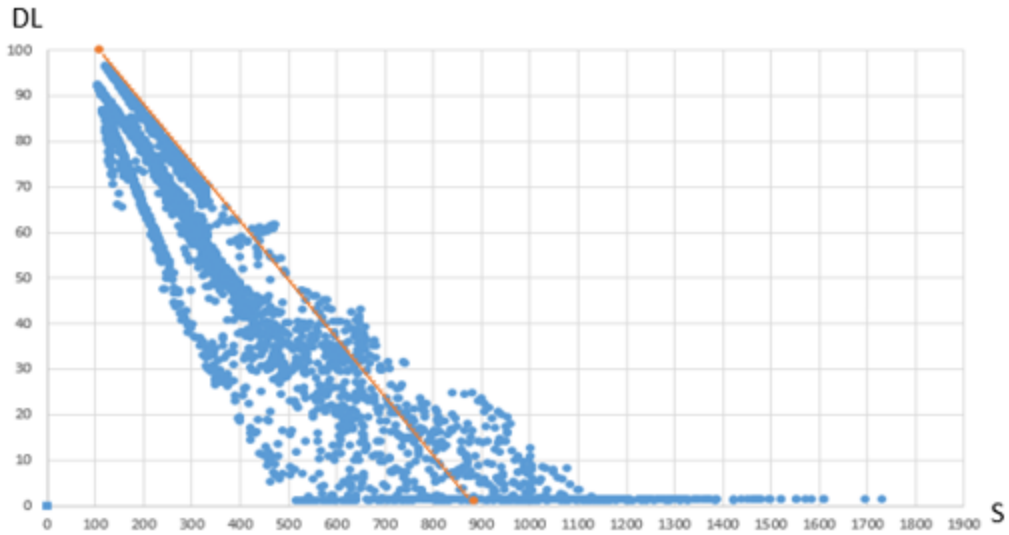

Figure 28. Scatter plot of dimming level (DL) and final signal (S) for two cosine sensor configuration in South facing State College office

6.5 Two-sensor corrected approach

Variable signal to illuminance ratios across different daylight and shading conditions cause scatter in the data represented in Fig. 28. Applying a correction factor to the might limit the S/E variability. This type of modification to the main control (two-sensor) signals was applied to produce signals are more correlated to the workplane illumination values. To implement this concept, a correcting (cosine 30) sensor was integrated. The received daylight signals from this correcting sensor were coupled with the resulting daylight signal to daylight illuminance ratios from a two photosensor system. Locating and aiming the correcting sensor played the main role in determining whether the coupling process was acceptable or not. From running the cosine 30 sensor in two different locations with different FOV in the South-oriented State College office, two distinct coupling plots were produced. Fig. 29 and Fig. 30 display the results from coupling the daylight signal to daylight illuminance ratio of the two-sensor control system with the daylight signal that resulted from both correcting sensor configurations. The correcting sensor was placed on the ceiling at (2.68, 1.22, 3.05) with a –z-direction to view light reflected from the floor. The coupling of its signal with the daylight signal to daylight illuminance ratio (S_d/E_d) of a two-sensor system data is shown in Fig. 29. Then, the correcting sensor was relocated to (2.68, 1.83, 3.05) on the ceiling viewing the window to receive a high level of daylight, and Fig. 30 presents the coupling of its signals with S_d/E_d ratios of a two-sensor system data.

The coupling plot in Fig. 29 does not show a strong trend line. However, Fig. 30 has a trend-line pattern showing where S_d/E_d is high and low, so correction was a possible solution with the correcting sensor tilted

toward the window. To improve a two-sensor control system, the resulting daylight signals of this system were modified by applying a correction factor equation from the coupling data in Fig. 30. This correction equation was generated by setting a trend line through the pattern of the coupling data (See the line in Fig. 30). The result is a more stable S/E ratio (See Fig. 31). The correction factors are multipliers for converting all points along the coupling line into a horizontal line at a selected S/E value. The produced signals from the two-sensor system are then multiplied by the corresponding correction factor based on the correcting sensor reading at that daylight condition. Fig. 32 shows the scatter plot from applying this correction process. Under the 2 percent dimming criterion, this new set of data and calibration line resulted in a 10.53 RMSE. This corrected system also achieved 45.09 percent energy savings for this South-oriented office in State College.

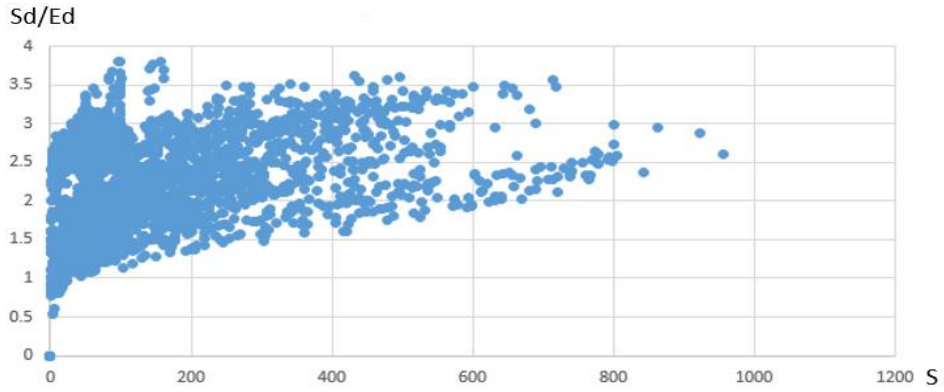

Figure 29. Scatter plot of a coupling between the daylight signal to daylight illuminance ratio (S_d/E_d) of the two sensor system and the third sensor signal (S) which is set as Fig. 16 in South facing State College office

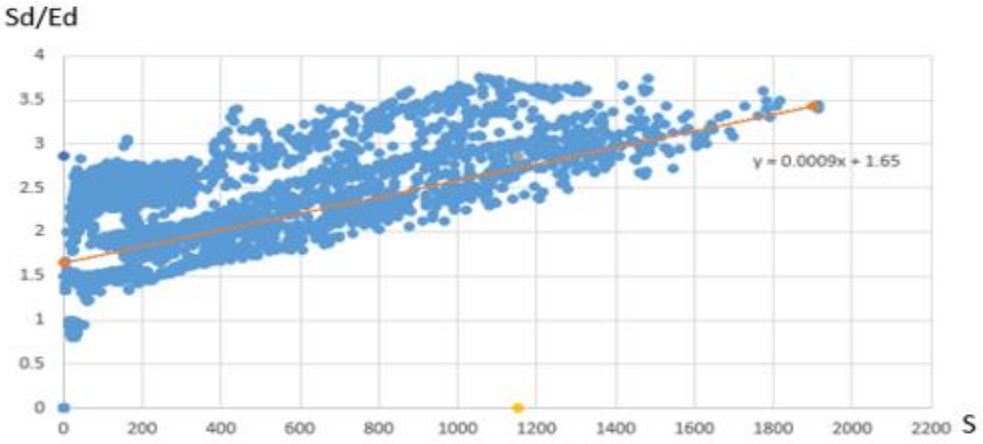

Figure 30. Scatter plot of a coupling between the daylight signal to daylight illuminance ratio (S_dS_d/E_d) of the two sensor system and the third sensor signal (S) which is set as Fig. 17 in South facing State College office

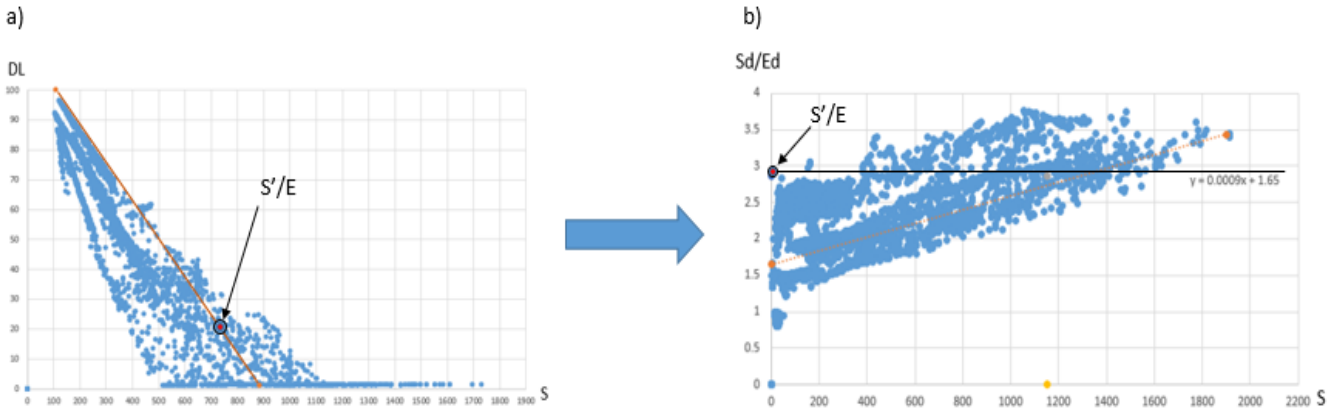

Figure 31. Plot (a) represents the performance of the two sensor system in State College-South orientation; plot (b) is the coupling between the two-sensor S_dS_d/E_d and the correcting signals

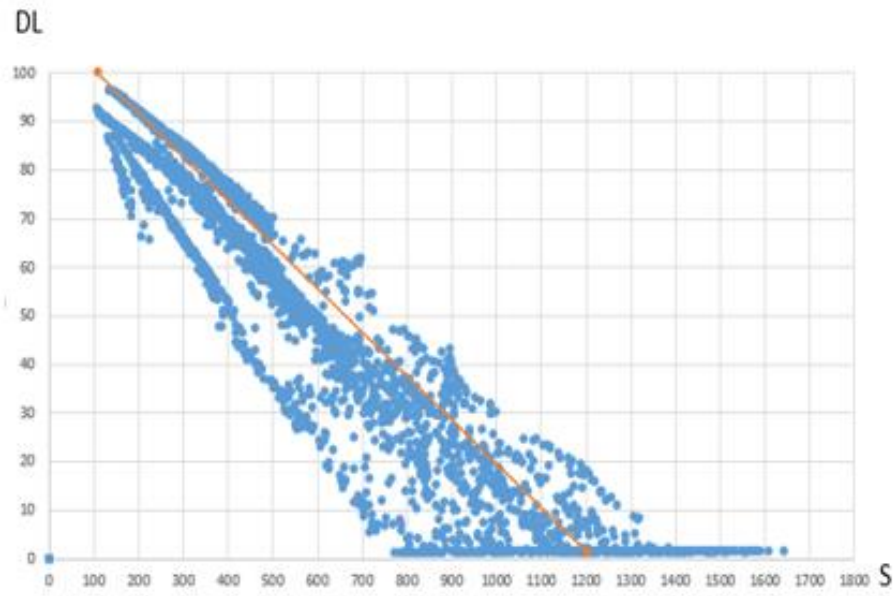

Figure 32. Scatter plot of dimming level (DL) and final signal (S) for the corrected signals of the two photosensor configuration in South facing State College office

The correction line for the North orientations had lower correction line intercept values than South orientations as shown in Table 3. A higher value of the intercept in the South orientation occurred because of the effect of sunlight patches that increase the value of daylight signals throughout the daylight hours.

However, the coupling of daylight signals from the correcting sensor with daylight signal to daylight illuminance ratios from a two-photosensor system generated a split pattern for the East and West orientations. Fig. 33 displays the resulting coupling when the office was faced to the East in State College.

This occurs because orienting the office to the East develops both North and South effects on the sensors at different hours of the day causing a coupling pattern with high and low groupings. The high set included shades down and halfway shade conditions as the automated shades reacted to the sunbeams in the morning as illustrated by gray and yellow dots, respectively, in Fig. 34. The low set of the pattern included the shades up conditions, showing the effect of either no direct sunlight hitting the façade as if it is a North orientation, or inadequate direct daylight illuminance to activate either halfway or fully down shades, as illustrated by blue dots in Fig. 34. For these orientations, correction factors were determined by setting a correction line through the whole coupling pattern and through the upper pattern part as presented in Fig. 33 and Fig. 34 respectively. The more preferred correction line equation was the one with lower RMSE and increased savings. In terms of correction line slope, the low slope (10×10^{-4}) of the correction line in Fig. 33 resulted in higher RMSE and lower energy savings than the higher slope (15.4×10^{-4}) of the correction line (Fig. 34) as shown in Table 3. Not only was slope a critical factor, but intercept value made a substantial difference. Setting the higher slope correction line in the upper pattern, which is closer to the algorithmic S'/E ratio (2.74), decreased the generated correction factors and meant less RMSE and more energy savings than the lower slope correction line. Applying both of the slopes in the upper patter part in East and West orientations in both cities resulted in a similar conclusion where the higher slope was more suitable for RMSE and energy savings in the office facing to the East and West.

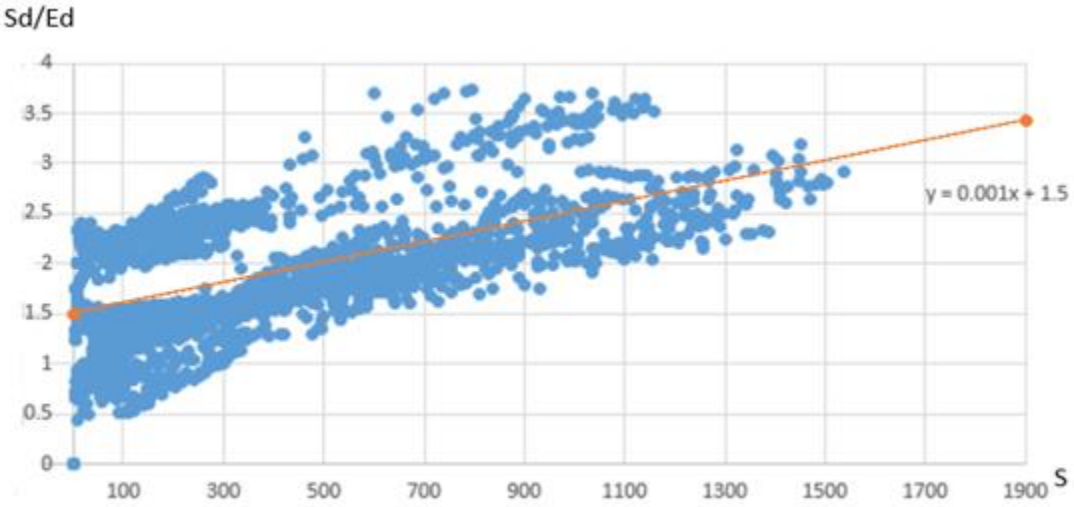

Figure 33. Scatter plot of a coupling between the daylight signal to daylight illuminance ratio (S_dS_d/E_d) of the two sensor system and the correcting sensor signal (S) which is set as Fig. 17 in East facing State College office (the correcting line is in middle of the whole coupling pattern)

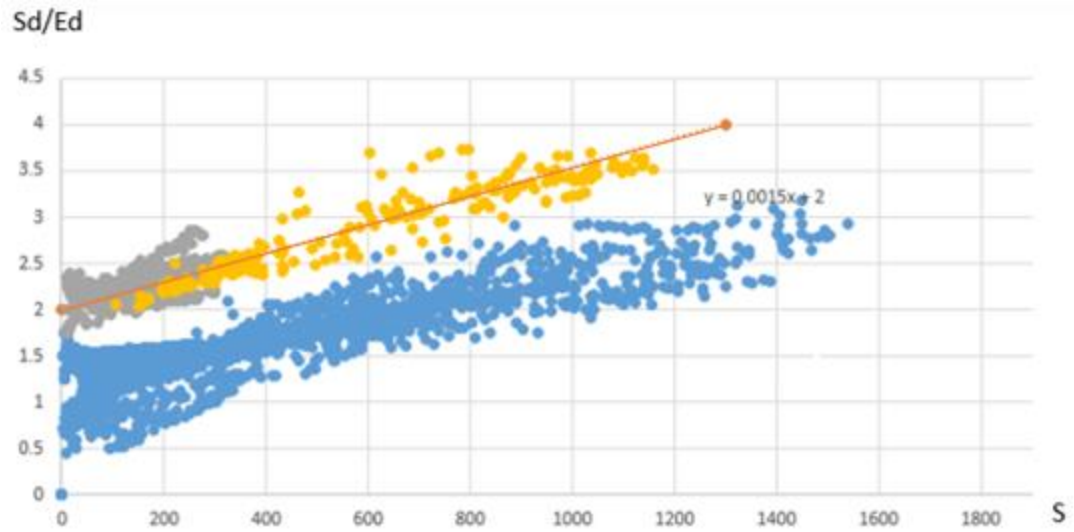

Figure 34. Scatter plot of a coupling between the daylight signal to daylight illuminance ratio ($S_d/E_dS_d/E_d$) of the two sensor system and the correcting sensor signal (S) which is set as Fig. 17 in East facing State College office (the correcting line is in middle of the upper coupling pattern)

6.6 Tables of results

The three photosensor system approaches were applied to the office model for the four main orientations at both sites, the results were generated, and placed in Table 3, Table 4 and Table 6. Table 3 displays the direct results (RMSE and energy savings) from applying the three approaches and the resulting RMSE and energy savings from applying different slopes in the correction process. On the other hand, changing the intercepts of the main correction equations resulted in producing different RMSE and energy savings as shown in Table 4. Examining different slopes and intercepts were proposed to provide a fixed conclusion for the proper correction equations for the main orientations in State College and Phoenix. The other option to set proper correction equations is to state the possible shade and sky conditions to set a correction line for each orientation in both cities. For this purpose, high and low points of the main correction lines were investigated and the resulting data are shown in Table 6.

Table 3. Performance summary for the three photosensor configurations, with details on correction equations

		Single sensor			Two-sensor		Two-sensor corrected		Correction line		m'_1 10×10^{-4}		m'_2 12×10^{-4}		m'_3 14×10^{-4}		m'_4 16×10^{-4}	
		location	R	S	R	S	R	S	b	m	R	S	R	S	R	S	R	S
State College	South	Left window	17.07	39.04	14.04	41.90	10.53	45.09	1.65	9.0×10^{-4}	10.12	45.45	9.91	45.98	11.00	45.43	15.02	43.05
		Centered	17.19	38.38														
	North-shades up	Left window	32.52	35.13	33.26	34.60	27.42	46.45	1.00	9.0×10^{-4}	26.92	46.99	28.68	43.93	39.10	38.05	53.27	29.89
		Centered	32.55	35.54														
	North-shades up & halfway	Left window	17.78	36.47	17.95	36.30	10.67	46.90	1.00	10.3×10^{-4}	10.76	46.69	11.54	45.55	12.01	46.04	15.63	39.51
		Centered	17.23	36.98														
	East	Left window	19.29	36.05	19.63	35.70	14.56	40.34	2.00	15.4×10^{-4}	16.46	38.43	15.66	39.2	14.85	40.00	14.34	40.55
		Centered	24.00	31.85														
	West	Right window	17.21	33.57	17.68	37.72	15.34	39.61	1.90	16.2×10^{-4}	16.56	38.49	16.03	38.95	15.68	39.27	15.40	39.55
		Centered	16.15	34.72														
Phoenix	South	Left window	13.82	53.49	10.35	57.12	8.22	58.24	1.70	10.3×10^{-4}	8.19	58.25	8.76	57.97	10.98	56.33	14.72	53.67
		Centered	13.56	53.18														
	North-shades up	Left window	35.28	37.45	36.76	36.73	30.37	49.57	1.15	17.1×10^{-4}	42.20	44.47	36.25	46.06	32.42	47.89	30.85	49.21
		Centered	35.12	38.59														
	North-shades up & halfway	Left window	15.55	40.08	15.54	40.10	5.79	52.55	1.15	17.1×10^{-4}	5.97	54.12	5.44	54.05	5.38	53.18	5.50	52.91
		Centered	13.78	41.12														
	East	Left window	19.45	42.96	18.02	48.50	17.10	49.42	2.10	12.2×10^{-4}	17.13	49.35	17.10	49.42	17.05	49.51	16.98	49.63
		Centered	23.82	36.54														
	West	Right window	20.24	43.60	19.35	47.70	18.06	48.99	2.20	9.4×10^{-4}	18.08	48.91	18.18	48.88	18.25	48.87	18.33	48.83
		Centered	19.03	44.12														

R = RMSE S = Savings in % b = Intercept m = Slope b' = Different examined intercepts

Table 4. Results of applying different intercepts to the photosensor correction equations

		Correction line		b'_1 (1.0)		b'_2 (1.1)		b'_3 (1.2)		b'_4 (1.3)		b'_5 (1.4)		b'_6 (1.5)		b'_7 (1.6)		b'_8 (1.7)		b'_9 (1.8)		b'_{10} (1.9)		b'_{11} (2.0)		b'_{12} (2.1)	
		m	b	R	S	R	S	R	S	R	S	R	s	R	S	R	S	R	S	R	S	R	S	R	S	R	S
State College	South	9.0×10^{-4}	1.65	9.8	45.96	9.79	45.96	9.84	45.86	10.0	45.66	10.18	45.55	10.3	45.46	10.47	45.13	10.65	44.86	10.74	44.76	10.9	44.56	11.1	44.36	11.23	44.16
	North-shades up	9.0×10^{-4}	1.0	27.42	46.45	27.6	46.4	27.8	45.9	28.0	45.4	28.2	44.8	28.3	44.5	28.5	44.0	28.6	43.6	28.8	43.2	28.9	42.9	29.0	42.6	29.13	42.4
	North-shades up & halfway	10.3×10^{-4}	1.0	10.67	46.9	10.77	46.5	10.9	46	11.04	45.7	11.2	45.3	11.4	44.8	11.6	44.5	11.8	44.2	11.9	43.8	12.1	43.4	12.2	43.2	12.5	42.7
	East	15.4×10^{-4}	2.0	14.03	41.2	14.33	41.3	14.23	41.27	14.08	41.2	15.83	39.4	13.93	41.1	14.03	41.0	14.13	40.8	14.23	40.7	14.38	40.5	14.56	40.34	14.67	40.2
	West	16.2×10^{-4}	1.9	15.23	40.1	15.25	40	15.35	39.7	15.37	39.68	15.32	39.69	15.28	39.7	15.25	39.72	15.26	39.7	15.28	39.7	15.34	39.61	15.45	39.5	15.55	39.4
Phoenix	South	10.3×10^{-4}	1.7	10.32	56.85	9.52	57.35	9.02	57.75	8.72	58.0	8.52	58.05	8.42	58.15	8.32	58.17	8.22	58.24	8.12	58.15	8.12	58.15	8.12	58.15	8.12	58.15
	North-	17.1×10^{-4}	1.15	30.26	49.7	30.3	49.6	30.4	49.53	30.5	49.4	30.7	49.0	30.9	48.6	31.0	48.2	31.14	47.9	31.27	47.5	31.41	47.13	31.53	46.8	31.65	46.4
	North-shades up & halfway	17.1×10^{-4}	1.15	5.87	52.68	5.83	52.7	5.77	52.4	5.8	52.1	5.87	51.7	5.99	51.4	6.14	51.1	6.3	50.8	6.5	50.4	6.64	50.1	6.8	49.8	7.00	49.5
	East	12.2×10^{-4}	2.1	30.42	37.87	28.82	39.27	27.37	40.47	25.92	41.57	24.52	42.67	23.22	43.77	22.22	44.67	21.22	45.57	20.02	46.67	19.02	47.57	18.02	48.57	17.1	49.42
	West	9.4×10^{-4}	2.2	33.12	34.89	31.62	36.29	30.22	37.69	28.72	38.99	27.32	40.19	25.92	41.29	24.62	42.49	23.42	43.59	22.42	44.69	21.32	45.79	20.12	46.79	19.12	47.79

R = RMSE S = Savings in % b = Intercept m = slope b‘ = Different examined intercepts

6.7 Discussion on Table 3 and Table 4

To discuss the results from locating the space model in State College and Phoenix, each orientation is analyzed and studied separately. For the photosensor, a 2.44-meter (8-foot) depth and cosine response function were determined as the best configuration in the office model. When this model is oriented to the South in both cities, the cosine photosensor is centered on the west window and on the exterior wall for the single photosensor approach. These two locations display a slight difference in terms of control performance. The similarity in performance occurs as a result of having a wide band cosine response that is affected by the sunlight patches throughout daytime hours. However, the resulting energy savings in Phoenix is higher than State College and the RMSE value is less since Phoenix has longer daylight hours and clearer skies. In the two-sensor configuration, State College's setup reduces the RMSE by 17.75% and raises the energy savings by 7.33 a%, while the RMSE decreased by 23.67% with a 7.4% increase in energy savings in Phoenix compared to a single sensor setup. A corrected two-sensor system achieves a 38.3% reduction in the RMSE and 15.5% increase in the savings in State College; whereas the RMSE decreases by 39.38% and the savings increases by 9.52% in Phoenix. Obtaining these evaluation values in the corrected setup comes from setting a correction line with a slope of 9×10^{-4} in State College and 10.3×10^{-4} in Phoenix. Testing other slopes for a South orientation shows that setting a correction line in both cities can provide reasonable RMSE and high energy savings with a range of slope between 10×10^{-4} and 12×10^{-4}. Also, to produce more than 10% energy savings from the correction process the intercept of the correction equation should be high, such as 1.7 and not exceed 2. Higher energy savings and a more efficient correction process occur in State College than Phoenix because it has a higher variability in S/E, showing a greater possibility for correction.

Orienting the office model to the North, two shade configurations are assumed to provide more realistic results according to human behavior. The first North shade setting allows the shades to be up all hours of the day. In this organization, a single sensor centered on a window and wall centered sensor show similar results in State College as well as in Phoenix. This means setting either a window-centered sensor or a wall-centered sensor in a North facing office with only shades up doesn't change the performance since these sensors are exposed to the same level of daylight at all hours. The two-sensor setup in both cities does not show obvious improvement in RMSE and energy savings compared to the single sensor performance as these sensors received similar daylight levels. Correcting the two-sensor system's signals resulted in a 15.68 reduction in the RMSE and increased savings by 34.19% in State College. Phoenix has similar achievements with a 13.5 percent reduction in the RMSE and 28.5 percent more savings compared to a single sensor. The line for this correction has a slope of 9×10^{-4} in State College and 17.1×10^{-4}in

Phoenix. Examining other slopes to find a reasonable line fitting the North façade cases in both sites, a suitable correction line for a North orientation with only shades up can be set with a slope range between 10×10^{-4} and 12×10^{-4} producing improvement in savings by more than 20%. To achieve very a high increase in savings for the correction process, the intercept of the correction equation should be low and around a value of one.

The second North-facing shading condition consists of a mix of shades up and halfway shades. Applying a single sensor with this condition results in approximately a 50 percent reduction in the RMSE and a little increase in the savings compared to the shades up setup in both cities, and it did not record intrinsically different performance between the sensor centered on a window and the wall-centered sensor. The two-sensor approach did not show obvious improvements in the photocontrol performance in both sites. However, the performance changed significantly when it came to the correction process. Including a halfway shade setting in the two-sensor corrected system results in a 38.07% RMSE reduction and 26.83% savings increase in State College, and a 62.77% RMSE decrease and 31.11% increase in the savings in Phoenix. This clear reduction in the RMSE for the corrected two-sensor system compared to the North-oriented shades up configuration results in more agreement between the signals and the workplane illuminance in the second shading arrangement compared to the condition with shades up at all hours. Indeed, the halfway shades condition caused more variable S/E ratios compared to a two-sensor corrected system with shades up at all hours, leading to more possibility for correction and better agreement. The proposed slope for the correction line that gives reasonable RMSE and savings values can be standardized between 10×10^{-4} to 12×10^{-4} for a North orientation including both shades up and halfway shade setups at the two sites. To achieve a very high increase in savings for the correction process, the intercept of the correction equation should be low, around a value of one.

The East and West orientations require locating the sensor on the more shaded South side of the space since there is no symmetry in the daylight values over a single day. This leads to either placing the photosensor on the South side or center of the office in the single sensor approach for both East and West orientations. For the East orientation, the South side sensor control provides a reduced RMSE and better energy savings than the center sensor at both sites for a single sensor system. In the two-sensor approach, adding another sensor at the North side of the space did not improve the control performance in State College, although the RMSE value decreased by 7.5% and the savings increased by 12.9% in Phoenix. This improvement in the photocontrol performance in the two-sensor system in Phoenix results from some sky factors, such higher profile angles than State College and clarity of the sky that results in higher levels of daylight. These factors cause shorter unsymmetrical shadowing of the building on the East ground in Phoenix than State

College along with more reflected light from the ground, increasing the signal received by the South sensor and allowing the North sensor to receive a lower signal after noon which led to a possible benefit from the lower signal values of the North sensor. The correcting sensor approach improves the RMSE and savings in State College by a 24.5% reduction and 11.9% increase respectively, whereas the RMSE decreases by 12.1% and the saving increases by 15% compared to a single sensor system. To generate the correction equation, the correction line is set with a slope of 15.4×10^{-4} in State College and 12.2×10^{-4} in Phoenix. Rotating this line with different slopes leads to a range of slopes between 10×10^{-4} and 16×10^{-4} that produce a reasonable improvement in RMSE and savings. Based on different values of intercepts in both sites, the intercept value should be high, with values of more than 1.9 to 2 in order to achieve more than 10 percent energy savings.

When the office is oriented to the West, a single sensor was located on the South side and along the centerline of the space. For the single sensor approach, the wall-centered sensor produces slightly better control performance than a South one in both State College and Phoenix. The similarity in the performance of the South window and wall-centered sensors in Phoenix occurs because they are almost at the same level of effect from sunlight patches and shadows that are caused by sunlight penetration. Selecting the lower signal of a two-sensor system does not obviously improve the control performance in both State College and Phoenix, although the savings increased by 8.64% in State College and 8.11% in Phoenix. The corrected two-sensor approach causes a 5% decrease in RMSE and 14.1% increase in savings in State College, and a 5.3% reduction in RMSE with an increase in savings of 10.38% is achieved in Phoenix compared to a single sensor system. To produce the improvement in the correction approach a correction line is set with a slope of 16.2×10^{-4} in State College and 9.4×10^{-4} in Phoenix. A range of slope between 10×10^{-4} to 16×10^{-4} is valid to obtain good improvement from applying the correction approach in the West orientation office. Also, according to the results from examining different intercepts, the correction equation intercepts should range from 1.4 up to 2 in order to keep the savings of more than 10 percent.

6.8 Correction line setup over several months for the both sites

Under automated shades, five primary month groups were defined since the months within each group behave similarly in terms of data distribution (See Table 5). Each of these month groups was combined with every main orientation of this study and associated with the best possible conditions for setting a proper correction line. These possibilities were defined with five categories: high risk, medium risk, low risk, good potential, and high potential. High and medium risk potential are shaded to show they are risky cases for setting correction lines that would approximate the equation that is stated in Table 3.

Table 5. Calibration appraisals for month and orientation combinations

Month	South	North	East	West
Nov/Dec/Jan/Feb	High risk	High risk	Medium risk	Medium risk
Mar/Oct	Medium risk	Low risk	Low risk	Good potential
Apr/Sep	Low risk	Good potential	Good potential	Good potential
May/Aug	Good potential	Good potential	High potential	High potential
Jun/Jul	High potential	Good potential	High potential	High potential

High risk: a condition when the coupling data has a very short range of signals and the coupling points are scattered without a recognizable pattern.

Medium risk: a condition when the distribution of coupling data has a medium possibility of resulting in no benefit from correction process. This either comes from a small range of signals or highly scattered data points making the setting of a correction line that follows the equation parameters listed in Table 3 and Table 4 somewhat difficult.

Low risk: a condition when a short range of correcting signals or scattered data points results in a good probability of setting a correction line conforming to the recommended slopes and intercepts of the correction line.

Good potential: a condition when there is a sufficient range of correcting signals but the data points are slightly scattered.

High potential: A condition when there is a sufficient range of correcting signals and the data points are very linearly arranged.

Table 6. Preferred calibration conditions for different months and orientation under automated shades (all times are local stander time in correspond to the center of TMI hourly data window)

			Orientations				
			South	North	East		West
Months	Nov Dec Jan Feb	H-Sh			Halfway		Halfway
		H-S			Clear		Clear
		H-T			10:30		13:30 to 14:30
		L-Sh			Halfway	Down	Halfway
		L-S			Mostly cloudy or reduced solar illuminance	Clear sky with low sun altitude	Mostly cloudy
		L-T			10:30	8:30 to 9:30	13:30 to 14:30
	Mar Oct	H-Sh	Up	Up	Halfway		Halfway
		H-S	Clear	Clear	Clear		Clear
		H-T	11:30 to 13:30	11:30 to 13:30	9:30		14:30 to 15:30
		L-Sh	Up	Up	Halfway	Down	Halfway
		L-S	Overcast	Mostly cloudy or overcast	Mostly cloudy	Reduced solar illuminance or clear sky with low sun altitude	Mostly cloudy or reduced solar illuminance
		L-T	8:30 to 10:30 or 14:30 to16:30	7:30 to 8:30 or 16:30 to 17:30	9:30 to 10:30	8:30	14:30 to 15:30
	Apr Sep	H-Sh	Up	Up	Halfway		Halfway
		H-S	Clear	Clear	Clear		Clear
		H-T	11:30 to 13:30	10:30 to 14:30	9:30		14:30
		L-Sh	Up	Up	Halfway	Down	Halfway
		L-S	Most diffused hour	Most diffused hour	Mostly cloudy	Reduced solar illuminance or clear sky with low sun altitude	Mostly cloudy
		L-T	8:30 to 9:30 or 15:30 to 16:30	7:30 to 8:30 or 16:30 to 17:30	9:30	8:30	14:30
	May Aug	H-Sh	Up	Up	Halfway		Halfway
		H-S	Clear	Clear	Clear		Clear
		H-T	11:30 to 13:30	11:30 to 13:30	9:30		15:30
		L-Sh	Up	Up	Halfway	Down	Halfway
		L-S	Most diffused hour	Mostly cloudy or overcast	Mostly cloudy	Reduced solar illuminance	Mostly cloudy
		L-T	8:30 or 16:30	6:30 to 7:30 or 17:30 to 18:30	9:30	8:30	15:30
	Jun Jul	H-Sh	Up	Up	Halfway		Halfway
		H-S	Clear	Clear	Clear		Clear
		H-T	11:30 to 13:30	11:30 to 13:30	9:30		15:30
		L-Sh	UP	Up	Halfway	Down	Halfway
		L-S	Overcast	Mostly cloudy or overcast	Mostly cloudy	Reduced solar illuminance	Mostly cloudy
		L-T	8:30 to 9:30 or 15:30 to 16:30	7:30 or 18:30	9:30	8:30	15:30

H: High point L: Low point Sh: Shades condition S: Sky condition T: Period of measurement time

Table 7. Alternate calibration conditions for high and medium risk orientations and times from Tables 5 and 6.

	Orientations and months				
	South	South	North	East	West
	Nov-Dec-Jan-Feb	Mar-Oct	Nov-Dec-Jan-Feb	Nov-Dec-Jan-Feb	Nov-Dec-Jan-Feb
H-Sh	UP	Halfway	Up	Up	Up
H-S	Overcast at noon	Clearest noon sky	Mostly cloudy or overcast at noon	Clear sky around solar noon within ±5 degrees	Clear sky around solar noon within ±5 degrees
H-T	11:30 to 13:30	11:30 to 13:30	11:30 to 13:30	11:30 to 12:30	12:30 to 13:30
L-Sh	UP	Halfway	Up	Up	Up
L-S	Overcast with low sun altitudes	Reduced solar illuminance to clear with low sun altitude (20 to 30 degrees)	Clear sky with low sun altitudes	Overcast sky or a clear sky after noon with a low altitude 20 to 30 degrees above the horizon	Most cloudy sky or a clear sky before noon with a low altitude 20 to 30 degrees above the horizon
L-T	9:30 to 10:30 or 14:30 to15:30	8:30 to 9:30 or 15:30 to 16:30	8:30 to 9:30 or 15:30 to 16:30	14:30 to 15:30	9:30 to 10:30

6.9 Discussion on Table 5, Table 6 and Table 7

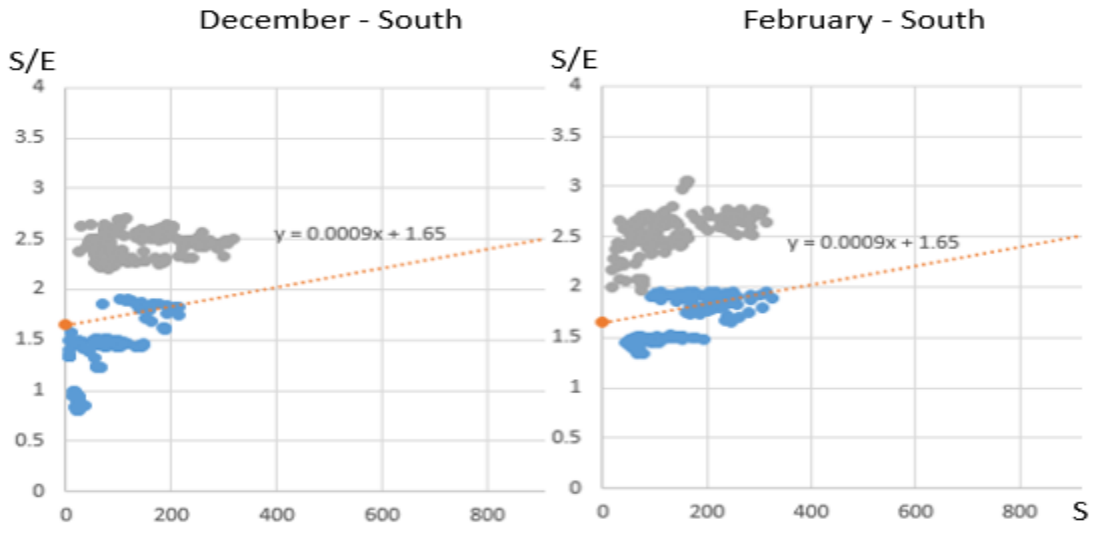

Figure 35. The distribution of scattered data points for a South orientation in State College in both December and February with an automated shades setting showing the correction line from the equation derived from whole year data.

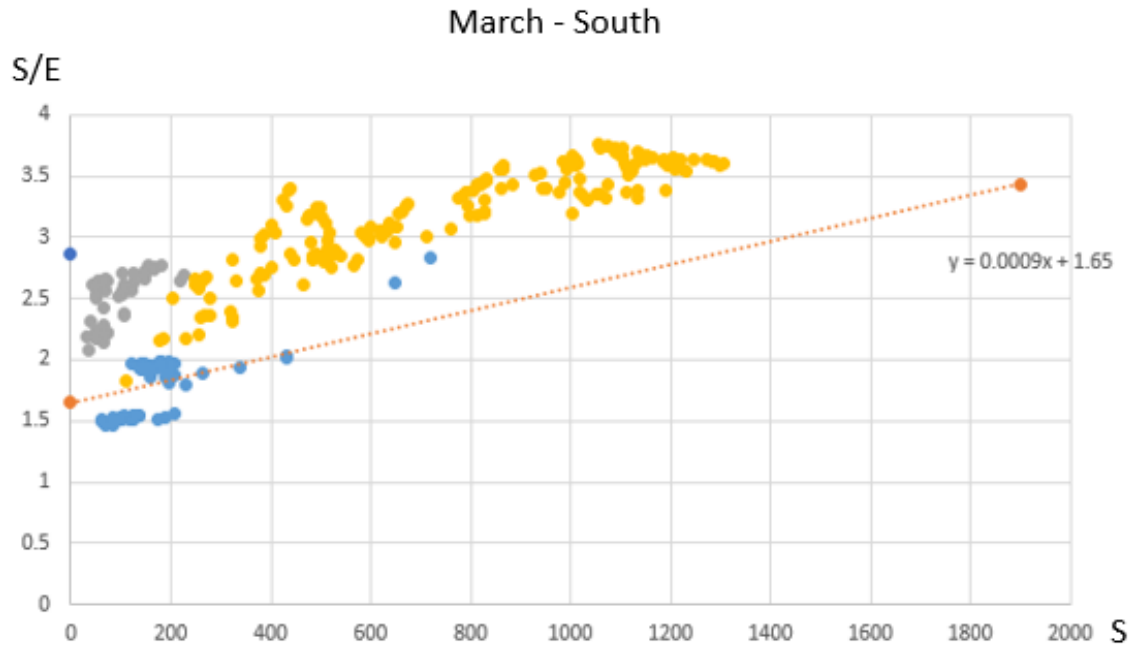

Figure 36. The distribution of scattered data points for a South orientation in State College in March with an automated shades setting showing the correction line from the equation derived from whole year data.

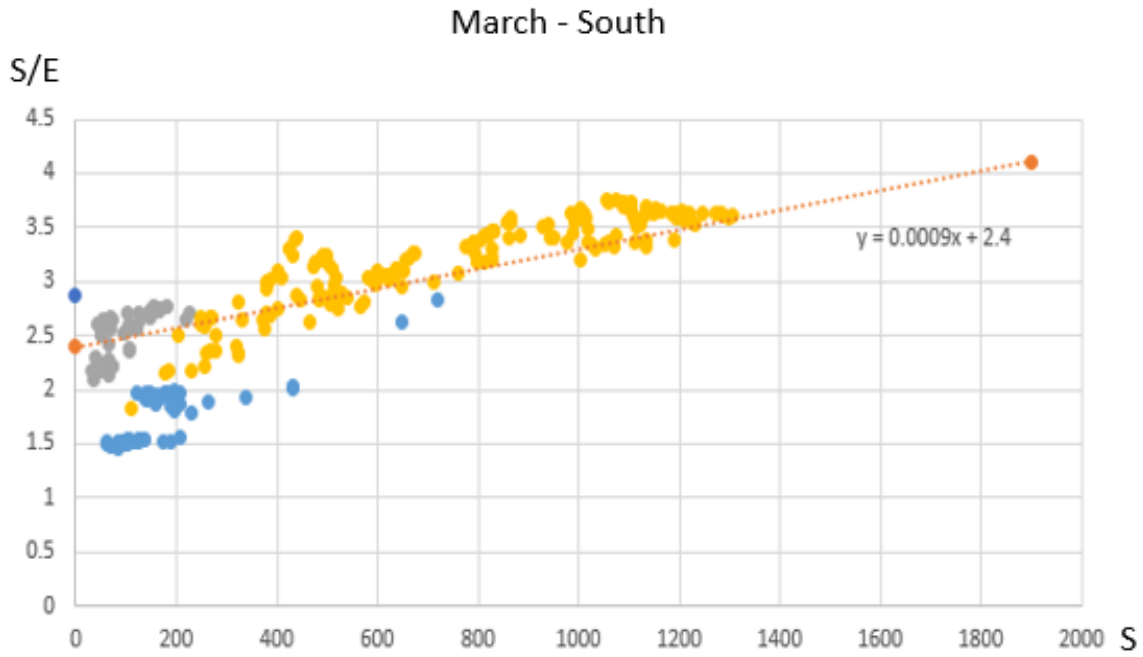

Figure 37. The distribution of scattered data points for a South orientation in State College in March with an automated shades setting showing the main correction line shifted up and crossing the halfway shades condition data points.

In Table 6, specific shade and sky conditions were investigated to set the correction line for each combination of month and orientation according to the main correction equation in Table 3. The accompanying measurement times are selected according to both State College and Phoenix. These shade and sky conditions were investigated to set the high and low points of proper correction lines for the different sites and orientations.

The months November, December, January and February in both South and North orientations are shaded in gray since there is no possibility to set a correction line in these combinations at the automated shade settings. This results from both a short correcting signal range and scattered data points without a linear pattern, as shown in Fig. 35, for the South oriented office in State College. Hence, correction lines for South and North orientation were investigated based on implementing each shading setup individually in these four months as another option (See Fig. 38, Fig. 39, Fig. 48 and Fig. 49). For these month and orientation combinations, this implementation presents that a proper correction line can be set through applying a shades up condition and specified sky conditions as shown in Table 7. However, the North orientation has a ~~possible~~ medium risk for setting a correction line since the produced signal ranges are short and the distribution of data points depends on the variety of sky conditions in these cities in these four months. State College shows more scattered data points than Phoenix in November, December, January, and February as displayed in Fig. 48 and Fig. 49.

The cells with yellow shading in Table 6 displays a possible shortage of data points that help to set the proposed correction line in some particular months and orientation. This is illustrated in Fig. 36 where there are not enough data points to properly identify the high point of the correction line in the month of March for the South oriented office in State College. To overcome this issue, the intercept value of the proposed correction equation was increased to fit the halfway shades condition (yellow) points as shown in Fig. 37. These halfway shades points are investigated to build a slope recovery table as shown in Table 7. Table 7 presents a chance to get only the slope of the proposed correction line for the shaded cells in Table 6. These slopes are combined with the recommended intercepts as presented in the discussion of Table 3 and Table 4.

7. Conclusions

Producing a relatively constant signal to workplane illuminance ratio to more effectively deliver a target workplane illuminance has been addressed in some previous research works. Researchers explored the possible guidelines for various photocontrol configurations. Some of them studied the optimum location for different closed- and open-loop photocontrol algorithms, while others focused on developing a daylight

delivery system, such as automated shades to minimize the effect of direct sunlight component on photosensor readings. This study worked to improve closed-loop photocontrol performance starting from the latest research recommendations. The office space of this study was modeled with automated shade operation (shades up, halfway shades and shades down) and photocontrol performance analysis that was based on the two most frequent workplane critical point locations in this office. Three photosensor system configurations were then analyzed: a single photosensor was investigated for best configuration performance, a two-sensor system applied the most objective signal at each hour, and a third system applied correction to the two-sensor data based on a narrow band sensor directed partially toward the window. For evaluation, RMSE and energy savings tools were evaluated.

For a single sensor application, a wideband (cosine) sensor provides the highest signal to illuminance agreement at one-fourth of the space depth on the ceiling for a window-centered sensor implementation. A cosine sensor in the middle of the office at the same depth provides approximately the same performance except for the East orientation where a window-centered sensor on the South side of the space outperforms a room-center sensor. Also, including halfway shades in a North oriented office reduces the RMSE to half for a single sensor system compared to North orientation with a shades up condition only. In term of hypotheses, the results from this study verified that including more than one sensor in a photocontrol system achieves better control performance and higher energy savings, and these achievements vary with space orientation. A two-sensor system outperforms a single sensor system for a South-oriented office and doesn't show obvious improvements for a North-oriented one. Applying a two-sensor system at an East or West orientation shows improvement ~~with~~ when the site of application has a high level of daylight and clear sky. This system shows improvement of performance in Phoenix and doesn't show any improvement in State College compared to a single-sensor application. Correcting daylight signals of a two-sensor configuration improves control performance for any orientation compared to a single-sensor application. Orienting the space to the South shows similarities in the resulting correcting system performance for both State College and Phoenix as well as North orientation. However, the North orientation with both shads up and halfway shades produces better control performance for the corrected system performance in the site that has higher daylight levels and clearer skies.

The best conditions for calibrating the applied photocontrol system vary based on space orientation. A South, East or West-oriented office requires a correction line with higher intercepts than a North orientation. For the majority of months, a shades up condition is appropriate for correction line commissioning for the South and North orientations. However, correction lines are best commissioned with halfway shade

conditions for East and West exposures. For calibration, a correction equation could be set either with a fixed slope or setting the sky and shade conditions of the correction line as recommended in Table 6.

Even though this study establishes an intrinsic development in the configuration of a photocontrol system and proves the effectiveness of its implementation, it requires a broader investigation. The results of this study are limited to the fixed space variables utilized in this work. The RMSE and energy savings results may change and draw more detailed findings according to different space dimensions and shapes as well as the gross area and dimensions of the windows. This study focused on only one type of blinds, and if the openness or transmittance characteristics are different, the preferred calibration conditions may vary from those stated in this study.

8. Recommendations and contributions

8.1 Photosensor system

For all orientations, the single sensor and two-sensor systems consisted of photosensors with a cosine sensitivity, and these sensors were directed vertically to the floor. However, the two-sensor corrected approach included two cosine sensors and a third photosensor with a cosine 30 sensitivity viewing the window. Fig. 38 shows the photosensor locations, while Table 8 summarizes the recommended configurations for each control system and orientation, according to the findings of this study.

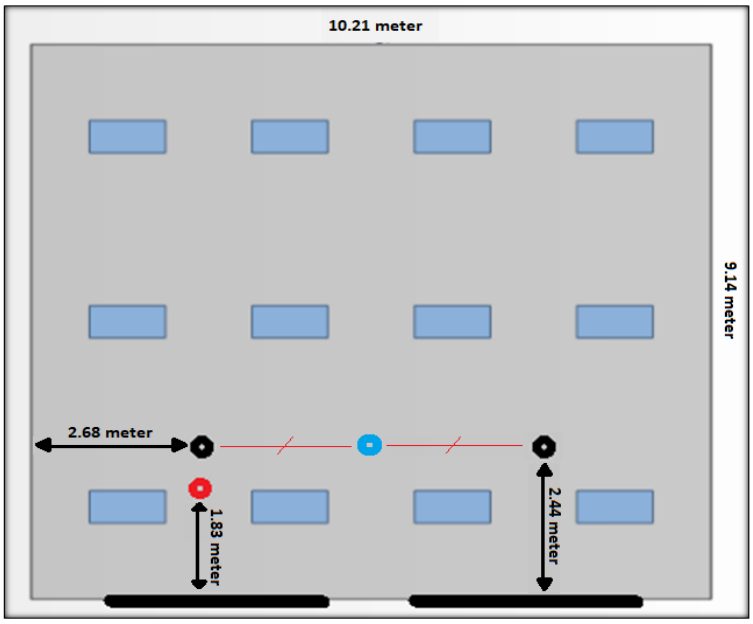

Figure 38. Space dimensions and photosensor locations

Table 8. Photosensor system recommendations. Locations (i.e., the referenced circles) refer to locations shown in Fig. 38.

		Control system				
		Single sensor	Two-sensor		Two-sensor corrected	
		Location	Location	Note	Location	Note
Orientation	South	Any black or blue circle	Both black circles	Highly recommended	Black and red circles	Highly recommended in any site
	North-shades up	Any black or blue circle	Not recommended (does not show any improvement or change)			recommended
	North- shades up & halfway	Any black or blue circle				Highly recommended
	East	Southern black circle	Both black circles	Recommended in high daylight level sites		Recommended
	West	Southern black or blue circle	Both black circles	Recommended in high daylight level sites		Recommended

8.2 Two-sensor corrected system calibration

For this photosensor system configuration, two options are available to calibrate the signal correction system for the main four window orientations. The first option is fixed slopes and intercepts for correction equations, which were developed based on the window orientation. The application of shade and sky conditions is the other option, established based on the orientation and the month of the application. Furthermore, each one of these options can be used to readjust the other applied calibration option.

8.2.1 Correction equation option

Table 9 present the latest calibration details for the fixed correction lines according to each orientation at both study sites. These recommendations are immediate calibration applications and can be readjusted based on a specific time, shade and sky for a more reliable correction.

Table 9. Correction equation recommendations

		orientation			
		South	North	East	West
Equation variables	Slope	10×10^{-4} to 12×10^{-4}	10×10^{-4} to 12×10^{-4}	10×10^{-4} to 16×10^{-4}	10×10^{-4} to 16×10^{-4}
	Intercept	1.7 to 2	1	1.9 to 2	1.4 up to 2
	Note	This slope range maintains more than a 10% savings increase. The intercept should be high and not exceed 2 for more than 10% savings increase	This slope range maintains more than a 20% savings increase. The intercept should be low and closer to 1 to achieve high savings	This slope range maintains more than a 10% savings increase. The intercept should be very high and closer to 2 to achieve high savings	This slope range maintains more than a 10% savings increase. The intercept should be high for more than 10% savings increase

8.2.2 Shade and sky conditions option

Referring to Table 6 and Table 7, these tables provide a summary of the specific shade and sky conditions to set the high and low points of a correction line for each month of the year for this study space, except the North orientation has a serious calibration risk in the months of November, December, January, and February.

8.3 Study contributions

This study explored the possibility of achieving improvements in a photocontrol system in applying the three control approaches of this study (single, two-sensor and two-sensor corrected systems). Investigating the results from applying these three approaches for all orientations shows improvements in energy savings as the number of sensors is increased except for the two-sensor system in the North-oriented spaces where it does not show any increase in the savings.

This study also shows that applying a halfway shades condition in a North-oriented space increases the potential savings from implementing both the single sensor and two-sensor corrected systems. The level of daylight has a high impact on the achieved improvement of these control systems, where the two-sensor system displays improvements in East and West-oriented spaces when the site provides high daylight levels and clear skies. On the other hand, a site with a clearer sky and higher daylight level produces less savings achievement when changing a single sensor system to a two-sensor corrected system for a South-oriented space.

In terms of further investigation and exploration, this study initiates a solid baseline to apply the studied three approaches to spaces with different dimensions, window conditions and blind specifications in order to obtain more information about calibration boundaries. Additionally, further studies of these control systems at different sites provides an opportunity for more detailed installation and implementation guidelines.

Appendix A. Optimum energy savings based on critical points

Table 10 shows the optimum energy savings that may be obtained based on the first and second workplane illuminance critical points. In other words, these optimum savings were calculated according to the optimum diming levels based on two critical points and the automated shades implementation.

Table 10. Optimum energy savings for different orientations

	Orientation				
	South	North-shades up	North-shades up & halfway shades	East	West
State College	51.21%	53.31%	49.03%	52.14%	46.12%
Phoenix	62.05%	57.65%	51.44%	55.70%	42.32%

Appendix B. Data showing different shade implementations throughout a year

South orientation

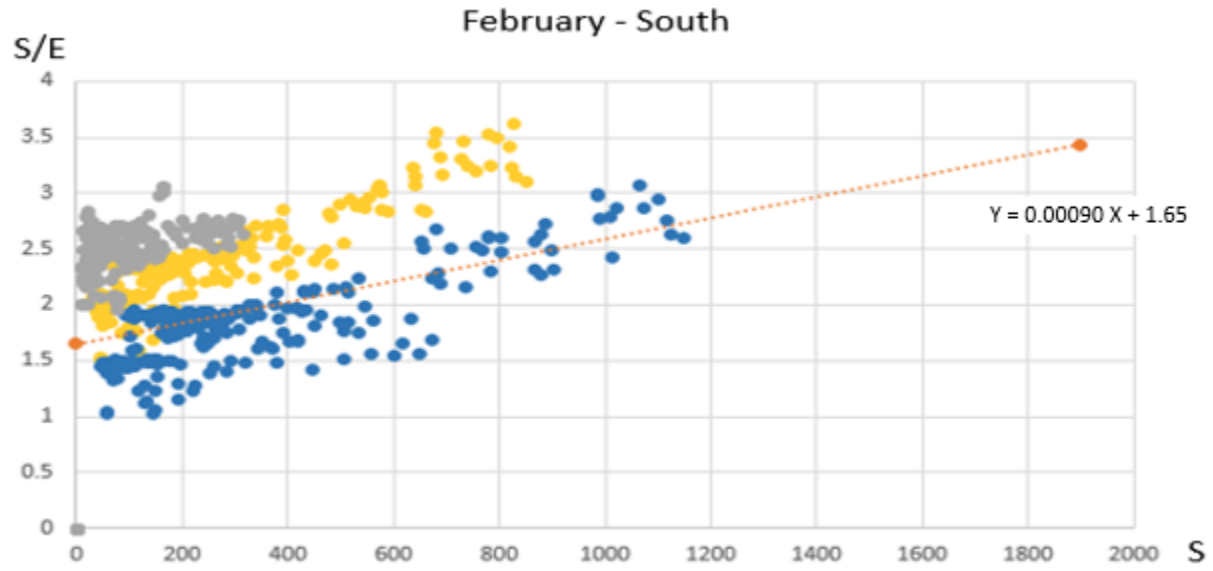

Figure 39. Daylight signal to daylight illuminance ratios of the two-sensor system and the correcting signals for the South orientation in the month of February in State College. (Blue points are shades up, yellow points are halfway shades and gray points are shades down)

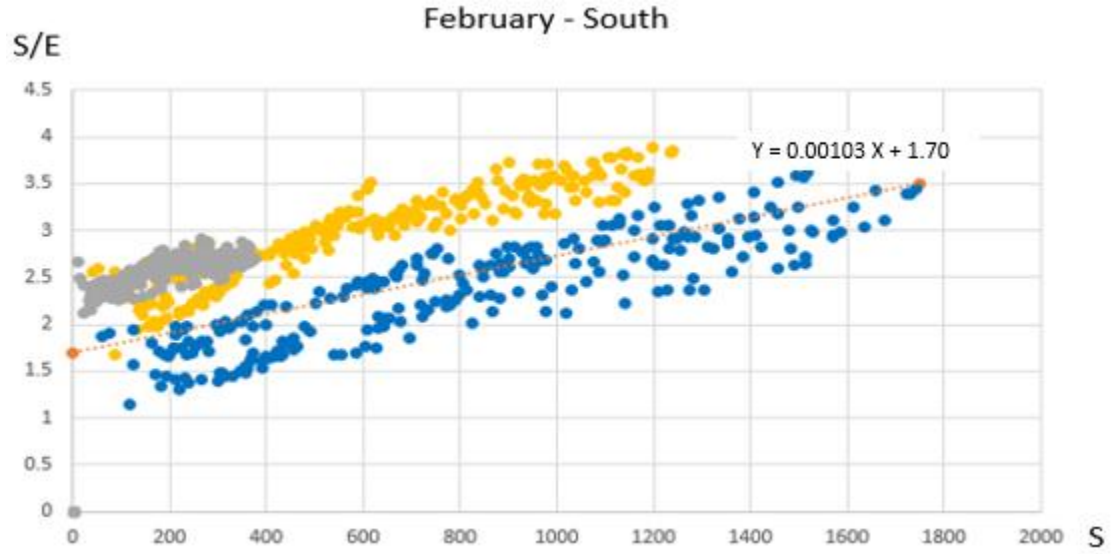

Figure 40. Daylight signal to daylight illuminance ratios of the two-sensor system and the correcting signals for the South orientation in the month of February in Phoenix. (Blue points are shades up, yellow points are halfway shades and gray points are shades down)

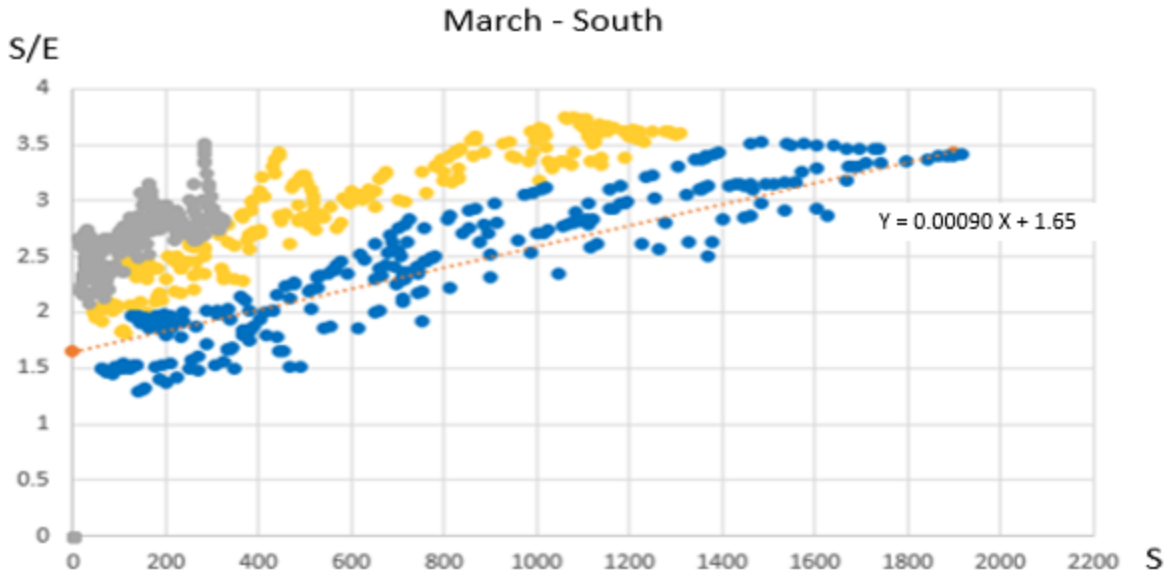

Figure 41. Daylight signal to daylight illuminance ratios of the two-sensor system and the correcting signals for the South orientation in the month of March in State College. (Blue points are shades up, yellow points are halfway shades and gray points are shades down)

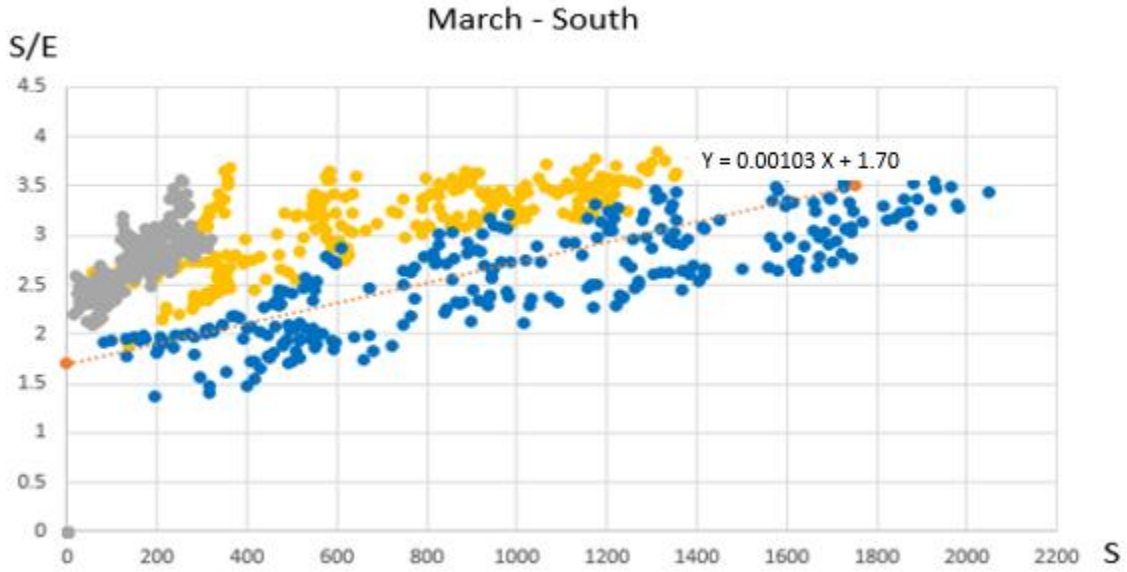

Figure 42. Daylight signal to daylight illuminance ratios of the two-sensor system and the correcting signals for the South orientation in the month of March in Phoenix. (Blue points are shades up, yellow points are halfway shades and gray points are shades down)

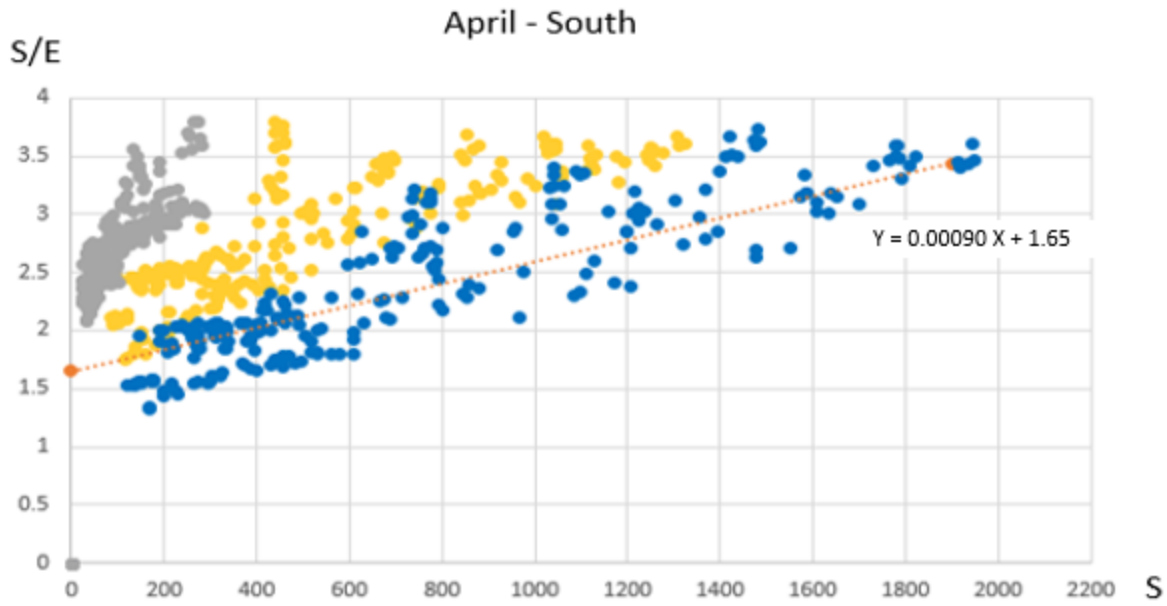

Figure 43. Daylight signal to daylight illuminance ratios of the two-sensor system and the correcting signals for the South orientation in the month of April in State College. (Blue points are shades up, yellow points are halfway shades and gray points are shades down)

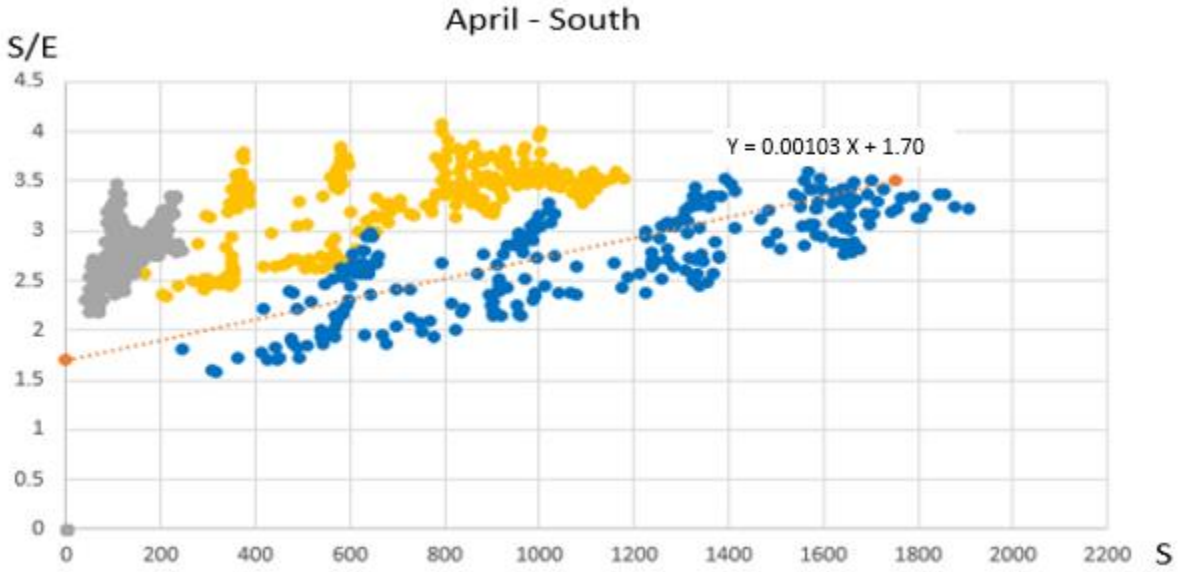

Figure 44. Daylight signal to daylight illuminance ratios of the two-sensor system and the correcting signals for the South orientation in the month of April in Phoenix. (Blue points are shades up, yellow points are halfway shades and gray points are shades down)

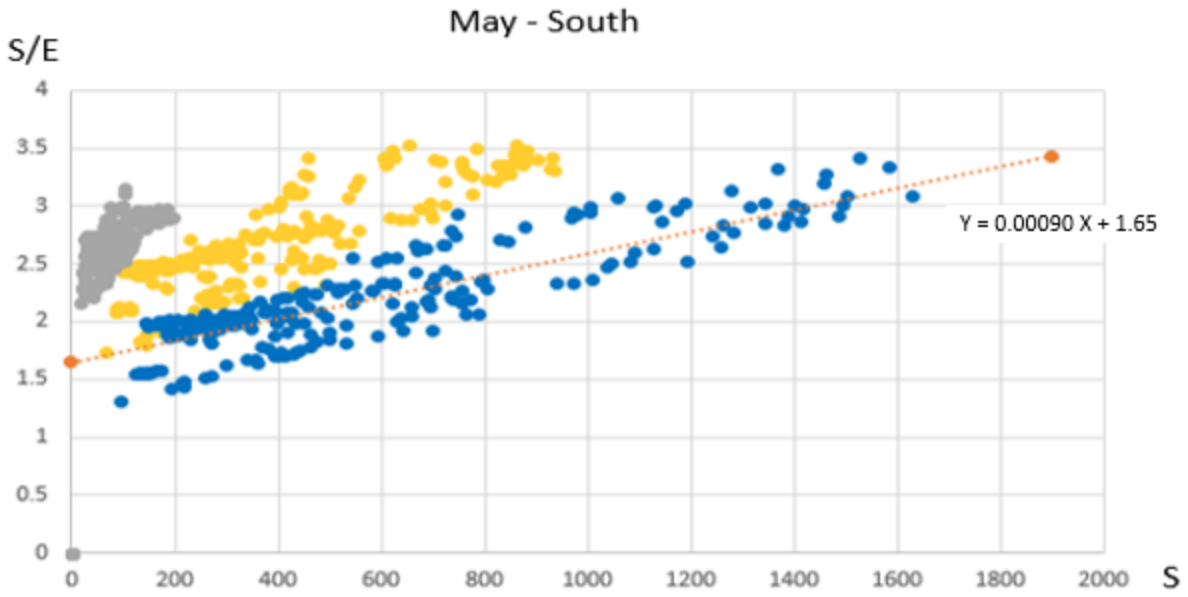

Figure 45. Daylight signal to daylight illuminance ratios of the two-sensor system and the correcting signals for the South orientation in the month of May in State College. (Blue points are shades up, yellow points are halfway shades and gray points are shades down)

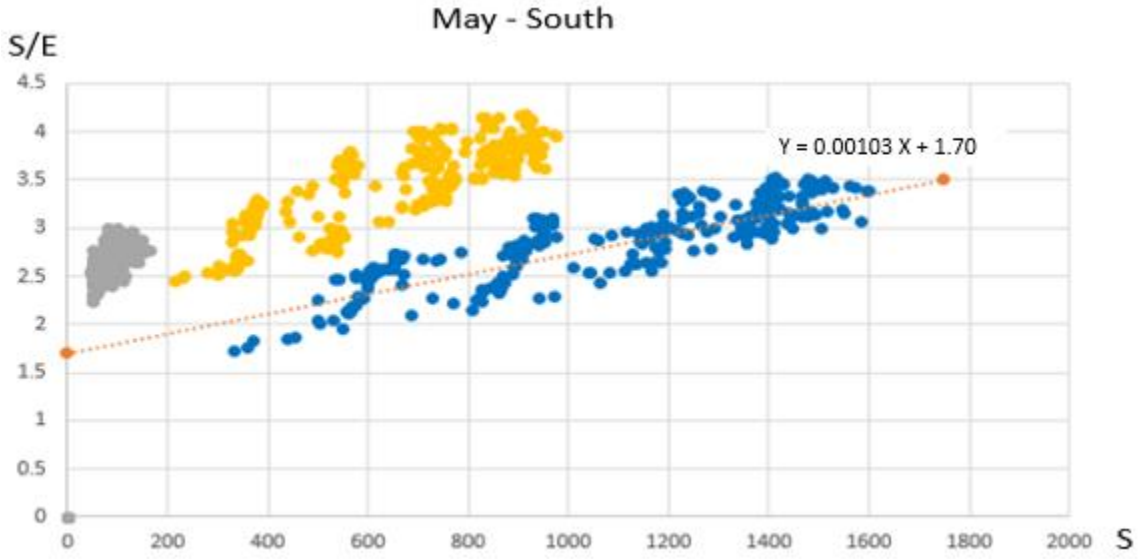

Figure 46. Daylight signal to daylight illuminance ratios of the two-sensor system and the correcting signals for the South orientation in the month of May in Phoenix. (Blue points are shades up, yellow points are halfway shades and gray points are shades down)

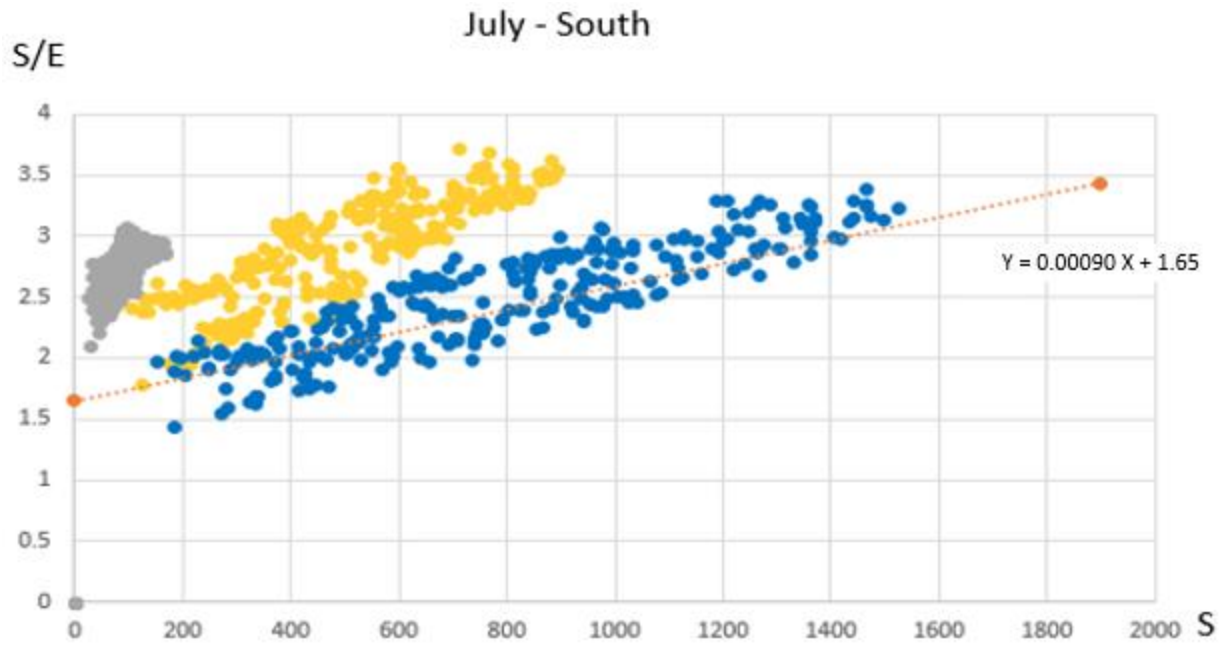

Figure 47. Daylight signal to daylight illuminance ratios of the two-sensor system and the correcting signals for the South orientation in the month of July in State College. (Blue points are shades up, yellow points are halfway shades and gray points are shades down)

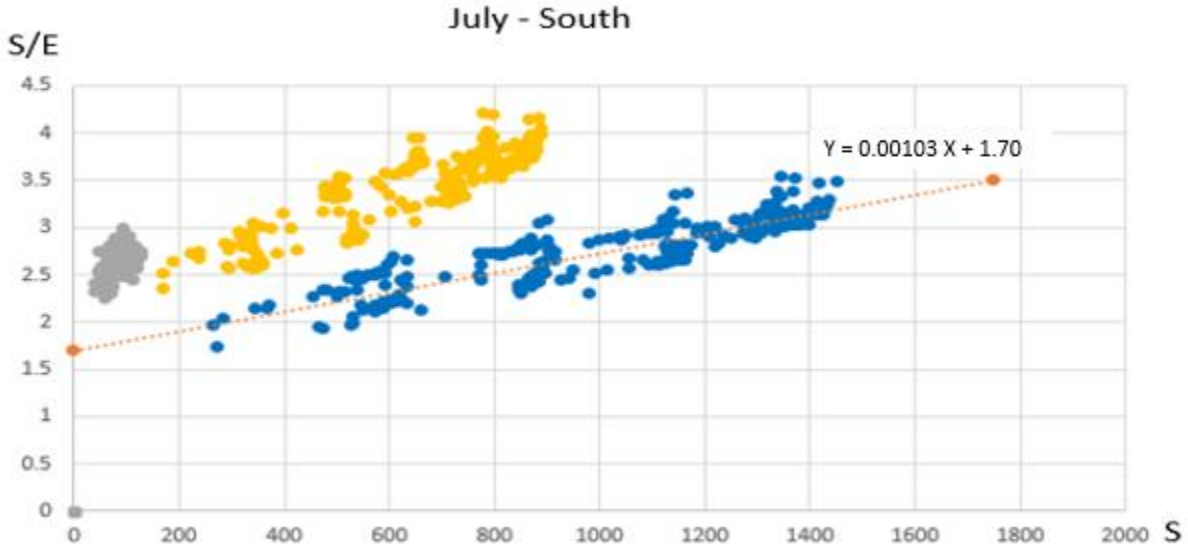

Figure 48. Daylight signal to daylight illuminance ratios of the two-sensor system and the correcting signals for the South orientation in the month of July in Phoenix. (Blue points are shades up, yellow points are halfway shades and gray points are shades down)

North orientation

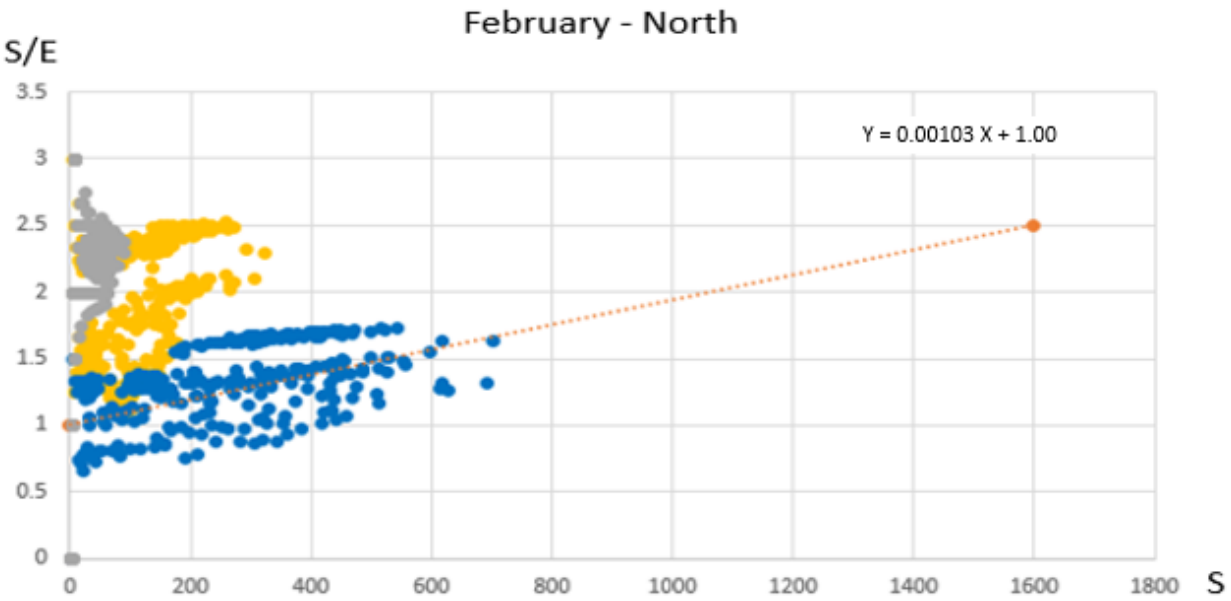

Figure 49. Daylight signal to daylight illuminance ratios of the two-sensor system and the correcting signals for the North orientation in the month of February in State College. (Blue points are shades up, yellow points are halfway shades and gray points are shades down)

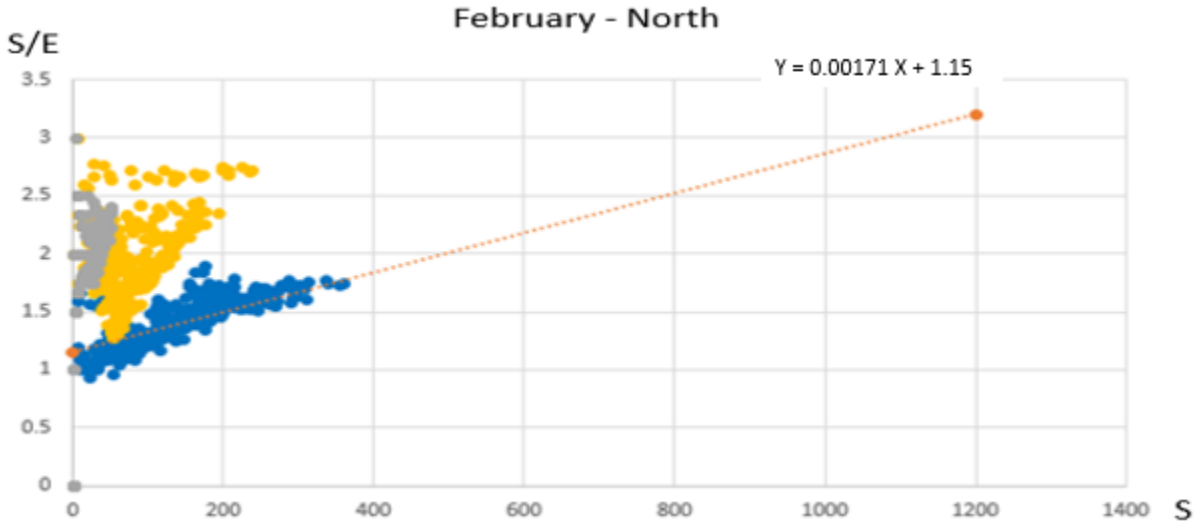

Figure 50. Daylight signal to daylight illuminance ratios of the two-sensor system and the correcting signals for the North orientation in the month of February in Phoenix. (Blue points are shades up, yellow points are halfway shades and gray points are shades down)

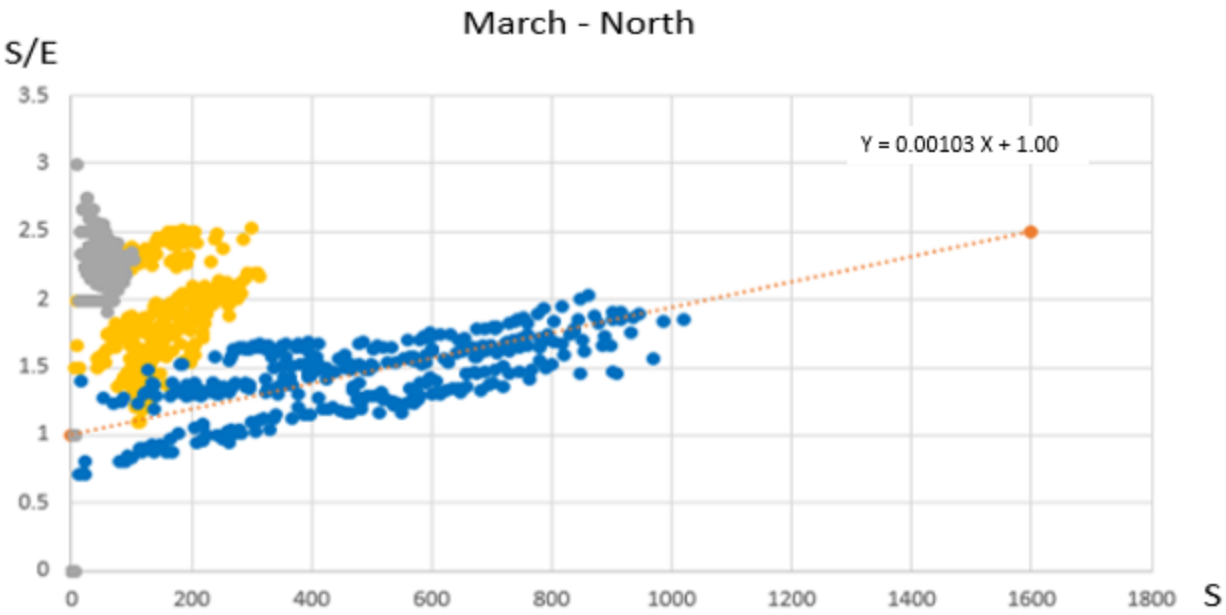

Figure 51. Daylight signal to daylight illuminance ratios of the two-sensor system and the correcting signals for the North orientation in the month of March in State College. (Blue points are shades up, yellow points are halfway shades and gray points are shades down)

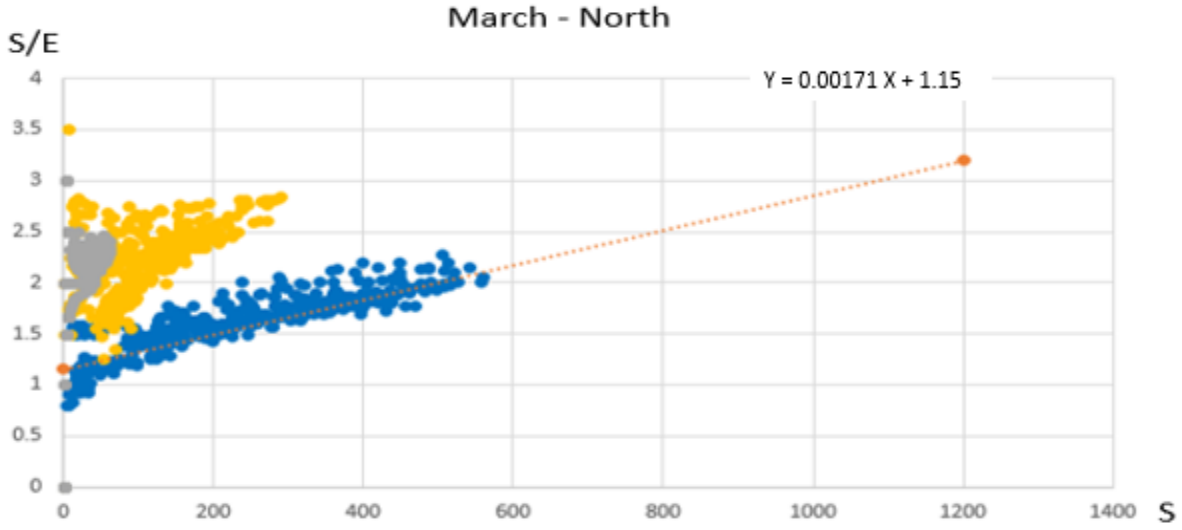

Figure 52. Daylight signal to daylight illuminance ratios of the two-sensor system and the correcting signals for the North orientation in the month of March in Phoenix. (Blue points are shades up, yellow points are halfway shades and gray points are shades down)

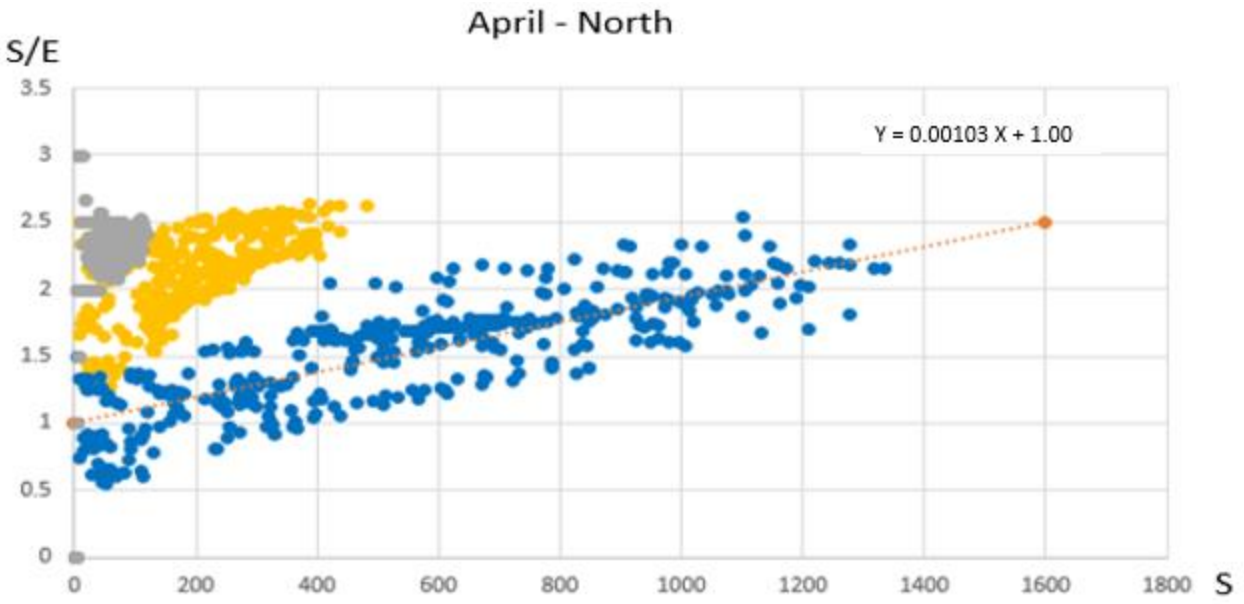

Figure 53. Daylight signal to daylight illuminance ratios of the two-sensor system and the correcting signals for the North orientation in the month of April in State College. (Blue points are shades up, yellow points are halfway shades and gray points are shades down)

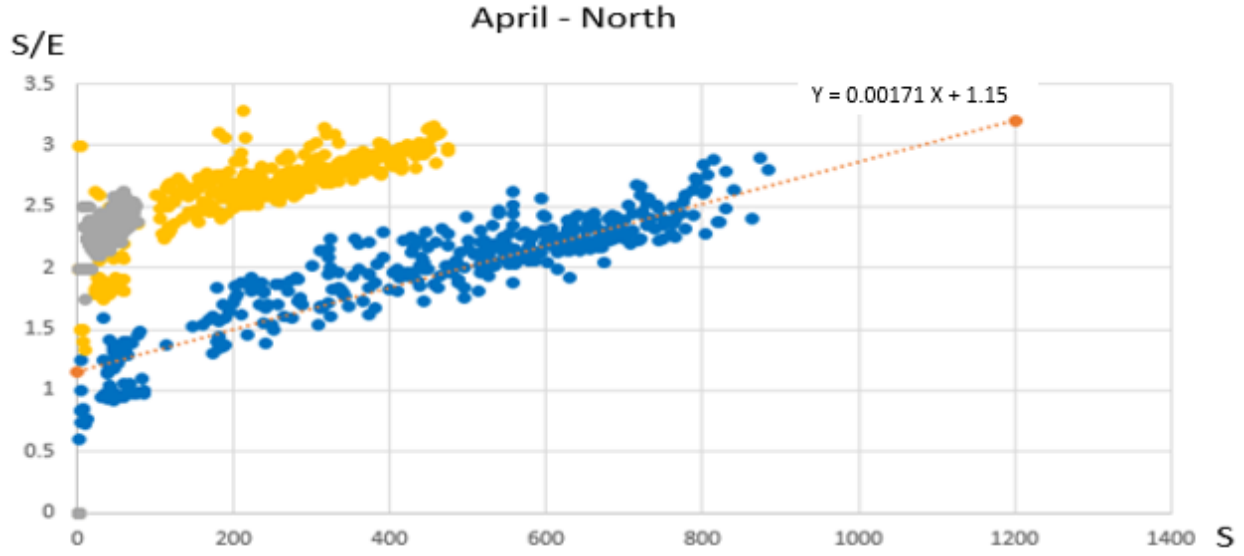

Figure 54. Daylight signal to daylight illuminance ratios of the two-sensor system and the correcting signals for the North orientation in the month of April in Phoenix. (Blue points are shades up, yellow points are halfway shades and gray points are shades down)

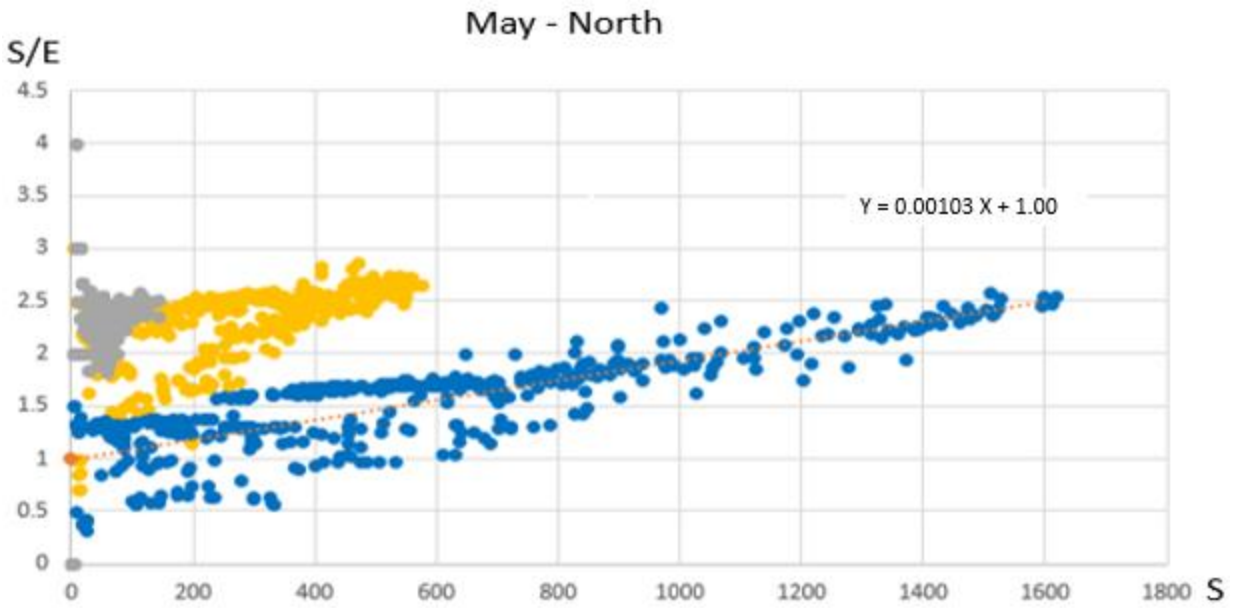

Figure 55. Daylight signal to daylight illuminance ratios of the two-sensor system and the correcting signals for the North orientation in the month of May in State College. (Blue points are shades up, yellow points are halfway shades and gray points are shades down)

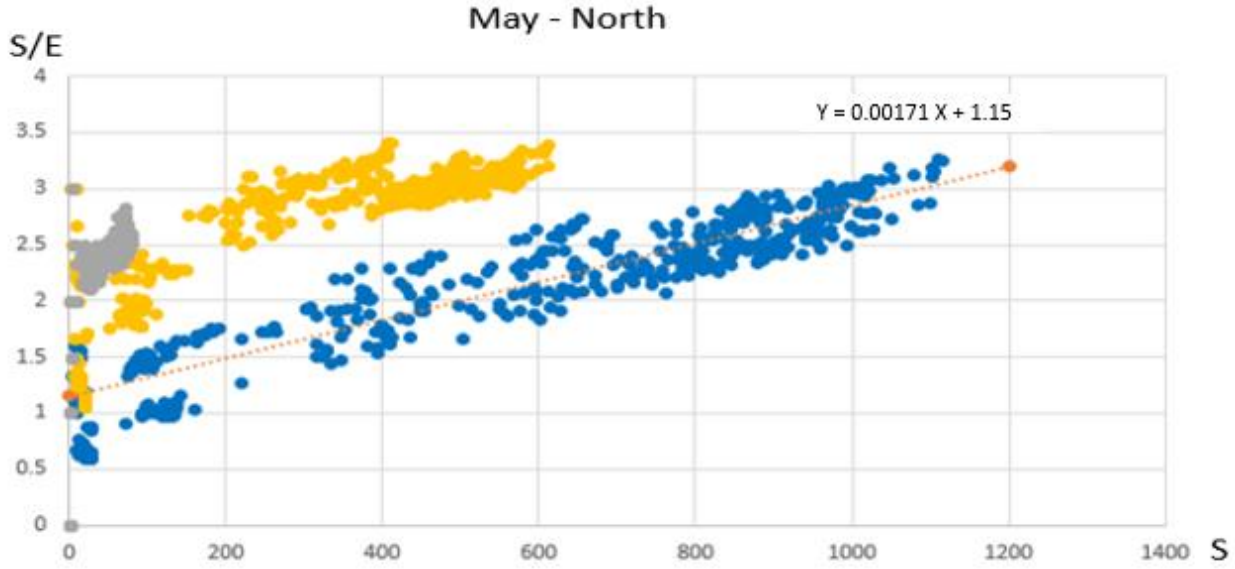

Figure 56. Daylight signal to daylight illuminance ratios of the two-sensor system and the correcting signals for the North orientation in the month of May in Phoenix. (Blue points are shades up, yellow points are halfway shades and gray points are shades down)

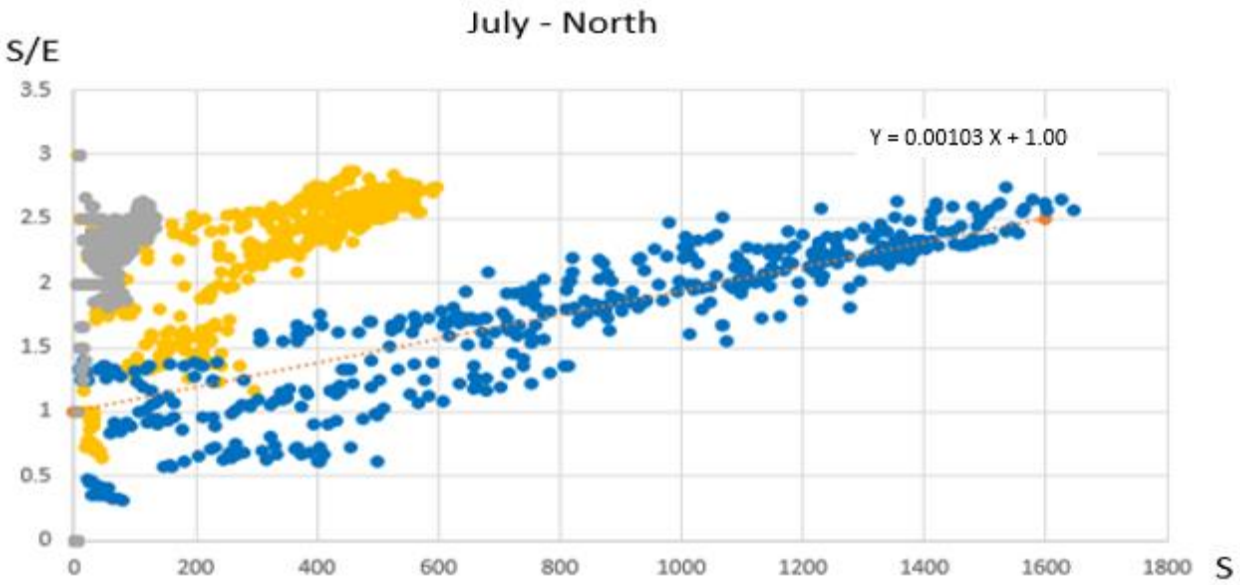

Figure 57. Daylight signal to daylight illuminance ratios of the two-sensor system and the correcting signals for the North orientation in the month of July in State College. (Blue points are shades up, yellow points are halfway shades and gray points are shades down)

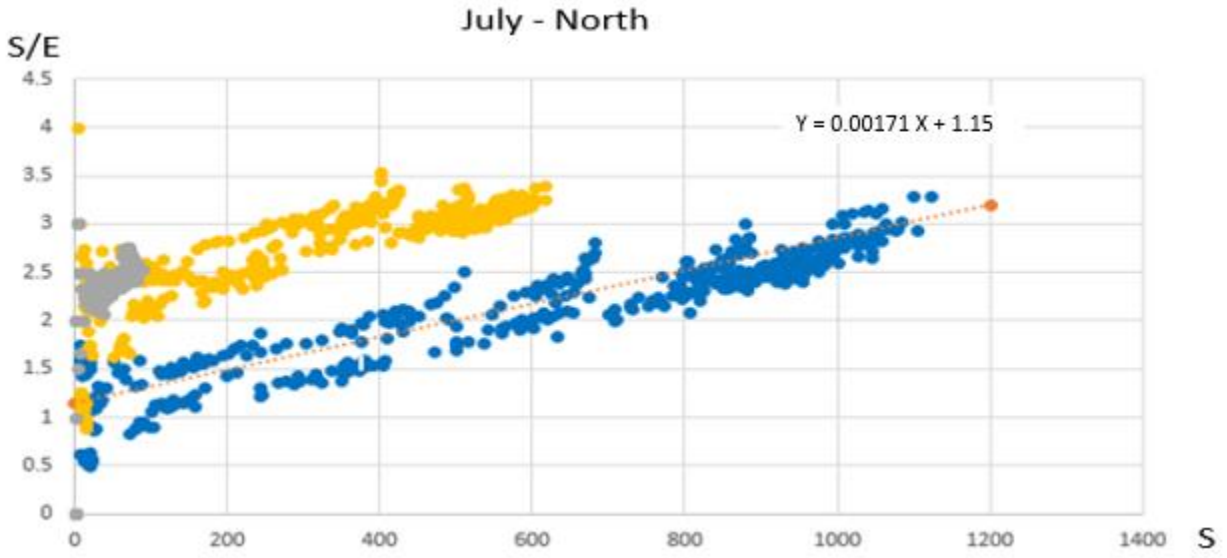

Figure 58. Daylight signal to daylight illuminance ratios of the two-sensor system and the correcting signals for the North orientation in the month of July in Phoenix. (Blue points are shades up, yellow points are halfway shades and gray points are shades down)

East orientation

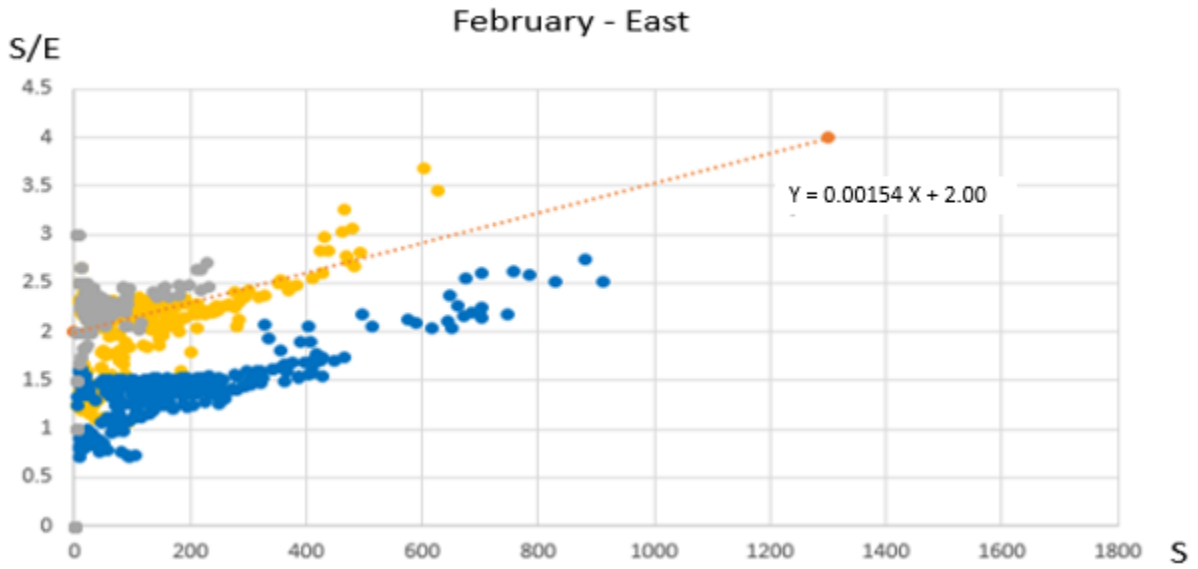

Figure 59. Daylight signal to daylight illuminance ratios of the two-sensor system and the correcting signals for the East orientation in the month of February in State College. (Blue points are shades up, yellow points are halfway shades and gray points are shades down)

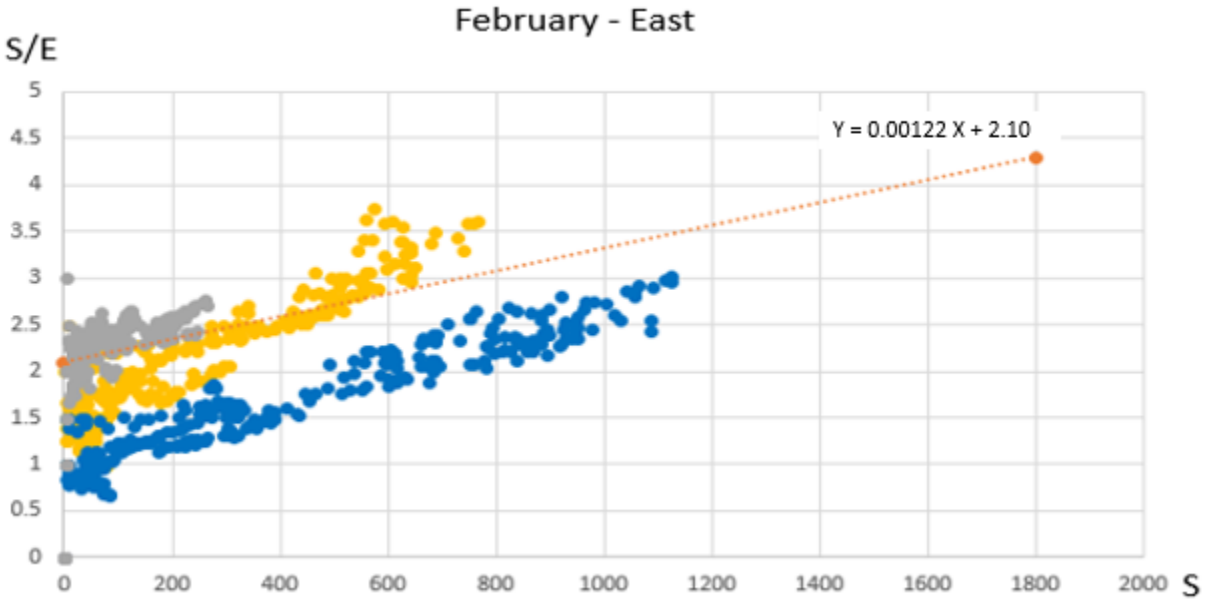

Figure 60. Daylight signal to daylight illuminance ratios of the two-sensor system and the correcting signals for the East orientation in the month of February in Phoenix. (Blue points are shades up, yellow points are halfway shades and gray points are shades down)

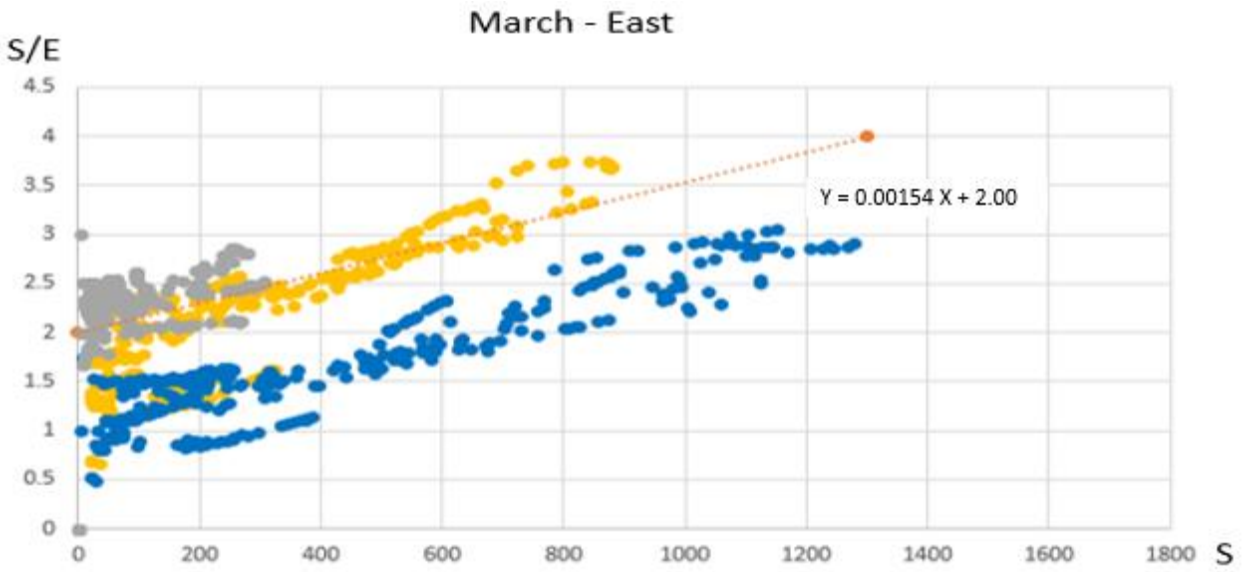

Figure 61. Daylight signal to daylight illuminance ratios of the two-sensor system and the correcting signals for the East orientation in the month of March in State College. (Blue points are shades up, yellow points are halfway shades and gray points are shades down)

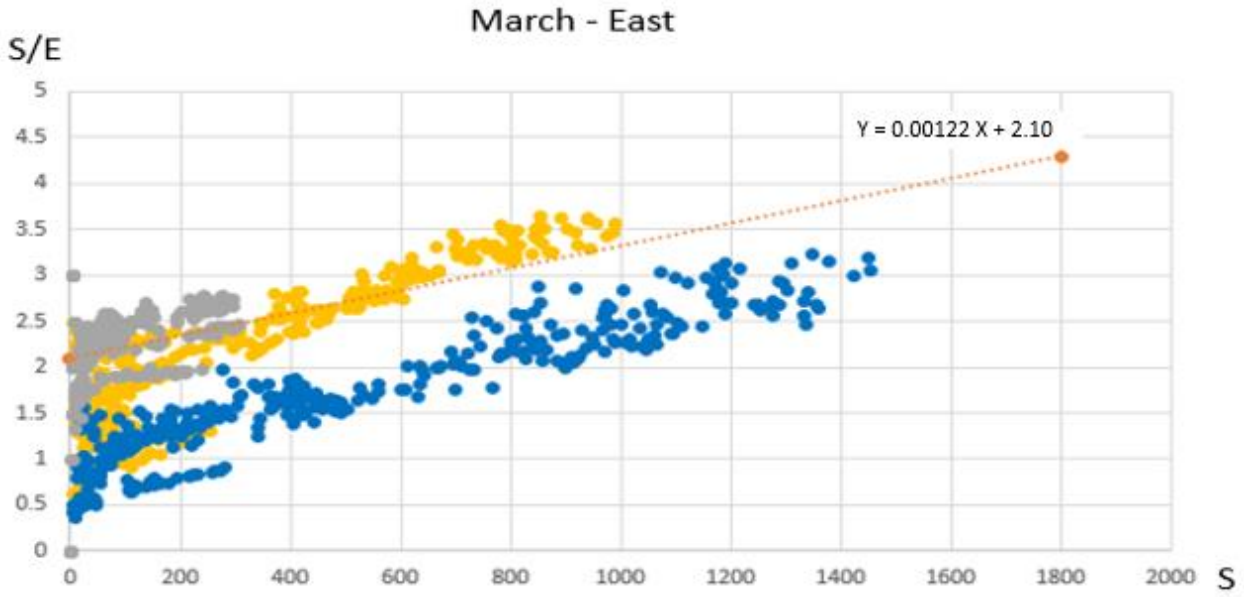

Figure 62. Daylight signal to daylight illuminance ratios of the two-sensor system and the correcting signals for the East orientation in the month of March in Phoenix(Blue points are shades up, yellow points are halfway shades and gray points are shades down)

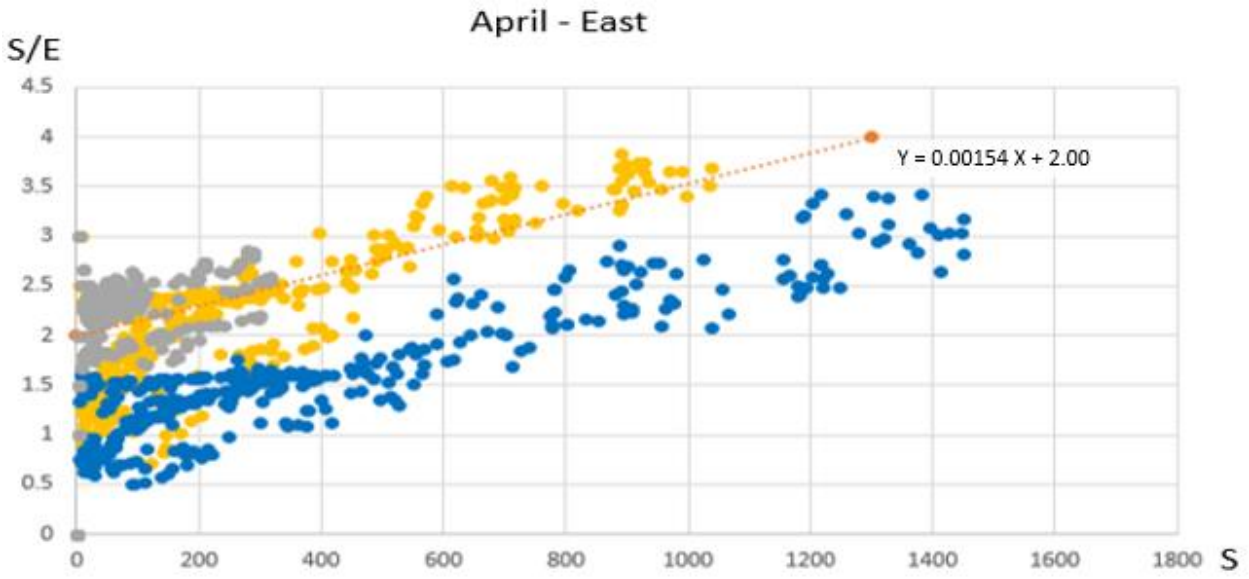

Figure 63. Daylight signal to daylight illuminance ratios of the two-sensor system and the correcting signals for the East orientation in the month of April in State College. (Blue points are shades up, yellow points are halfway shades and gray points are shades down)

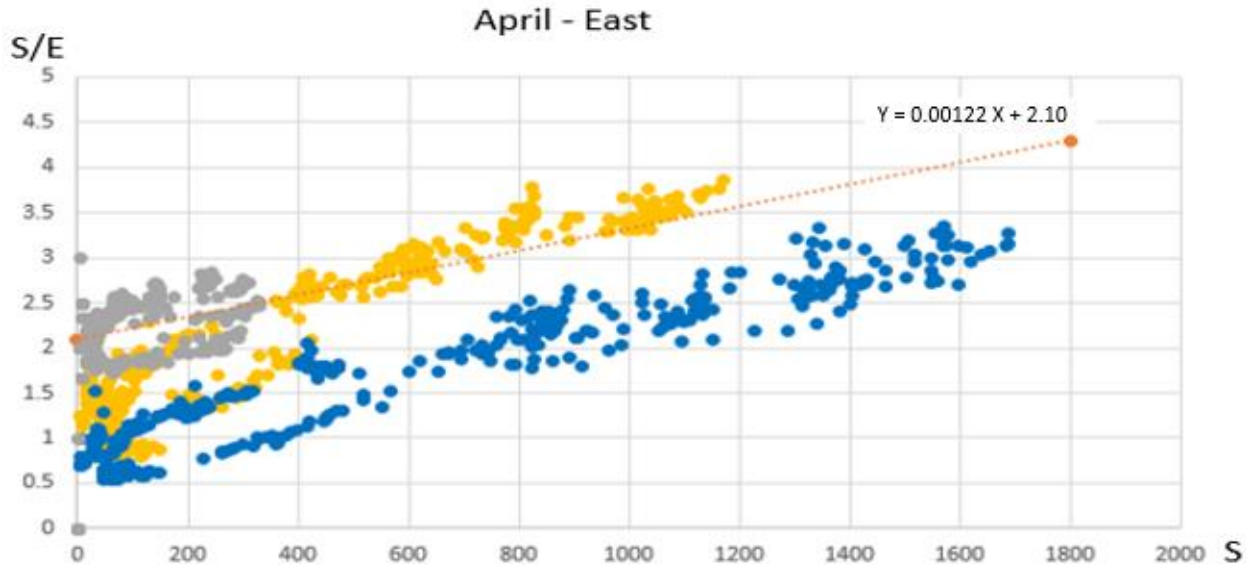

Figure 64. Daylight signal to daylight illuminance ratios of the two-sensor system and the correcting signals for the East orientation in the month of April in Phoenix. (Blue points are shades up, yellow points are halfway shades and gray points are shades down)

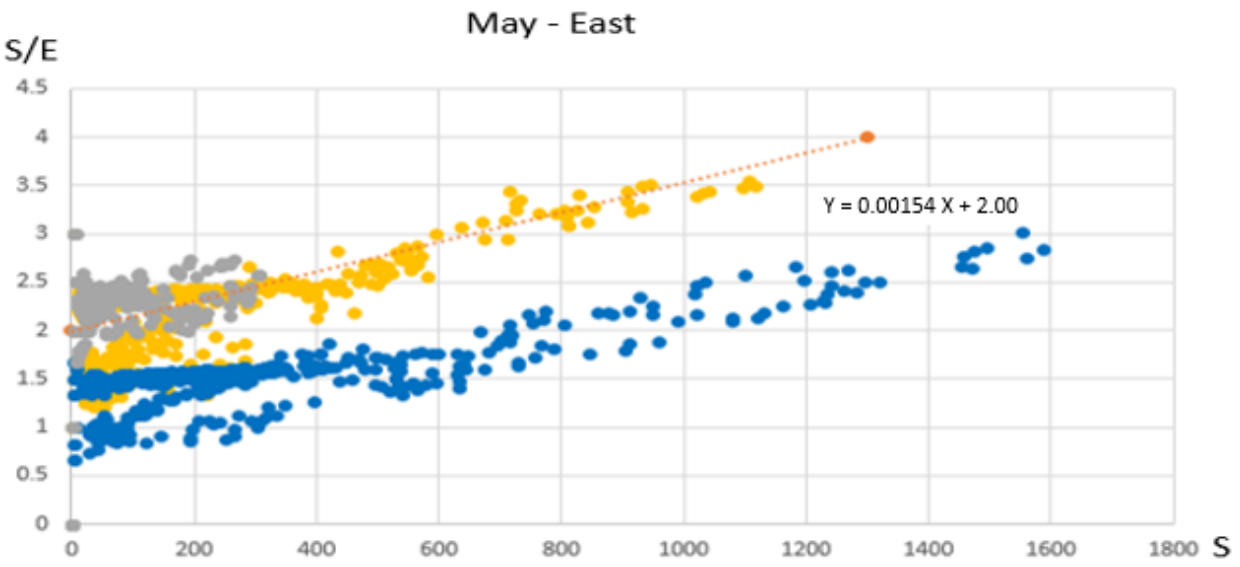

Figure 65. Daylight signal to daylight illuminance ratios of the two-sensor system and the correcting signals for the East orientation in the month of May in State College. (Blue points are shades up, yellow points are halfway shades and gray points are shades down)

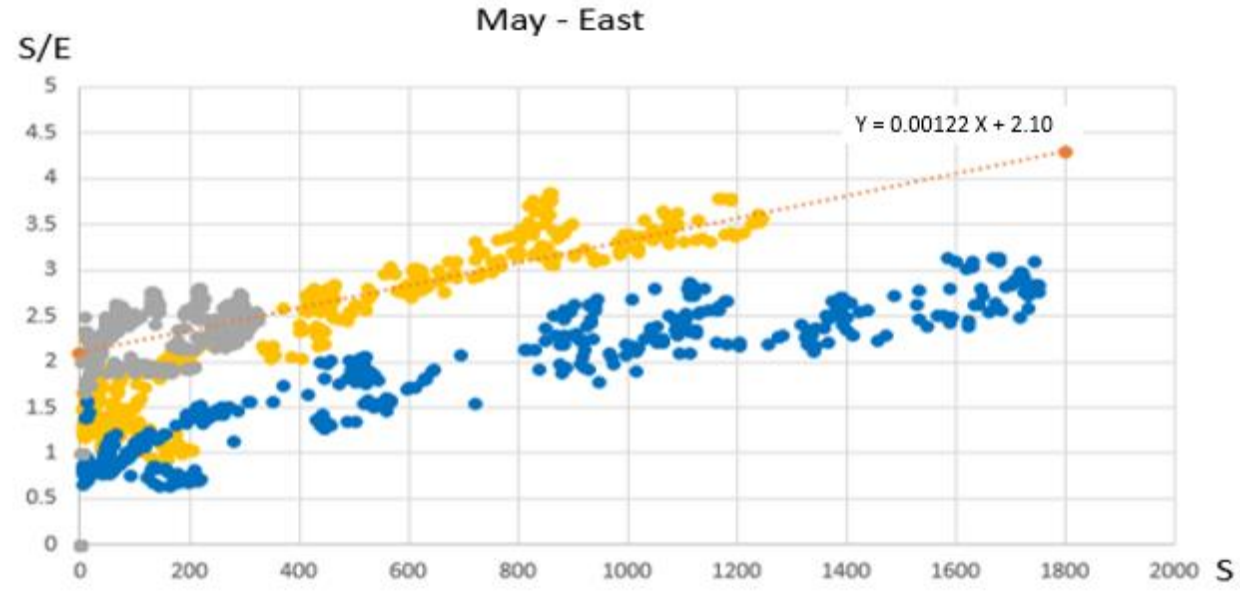

Figure 66. Daylight signal to daylight illuminance ratios of the two-sensor system and the correcting signals for the East orientation in the month of May in Phoenix. (Blue points are shades up, yellow points are halfway shades and gray points are shades down)

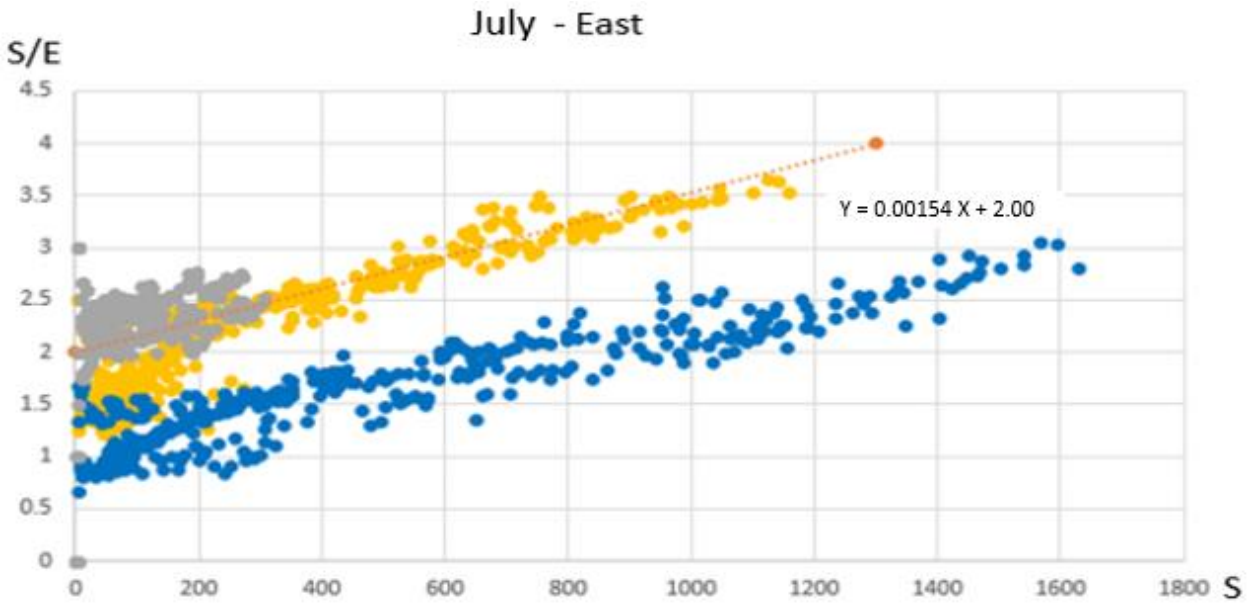

Figure 67. Daylight signal to daylight illuminance ratios of the two-sensor system and the correcting signals for the East orientation in the month of July in State College. (Blue points are shades up, yellow points are halfway shades and gray points are shades down)

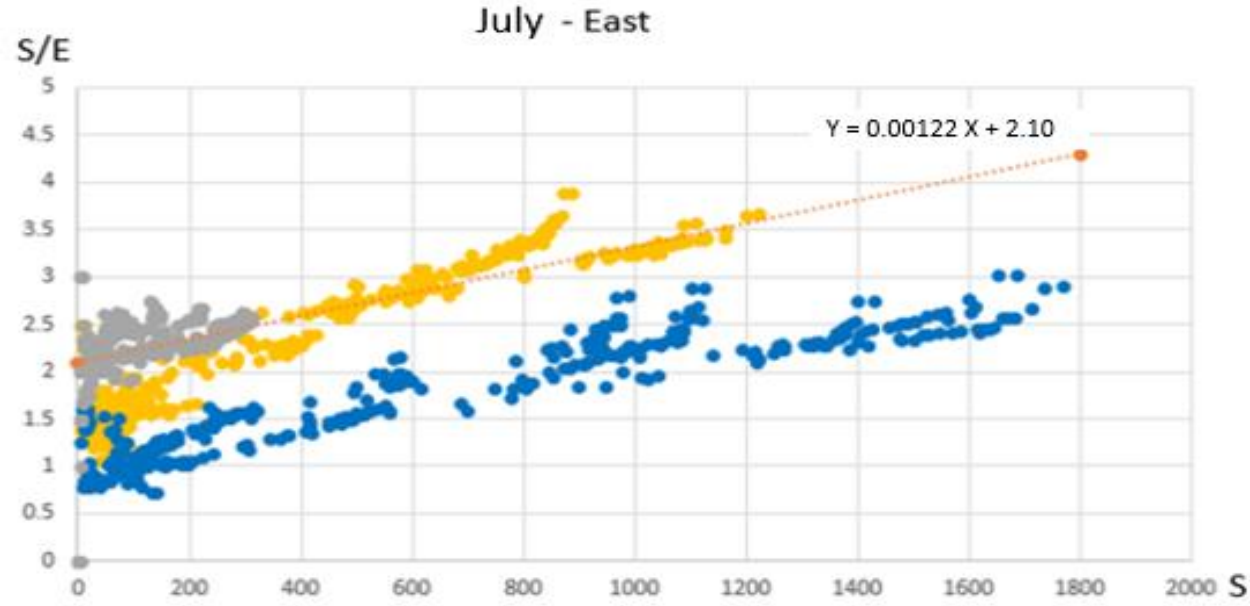

Figure 68. Daylight signal to daylight illuminance ratios of the two-sensor system and the correcting signals for the East orientation in the month of July in Phoenix. (Blue points are shades up, yellow points are halfway shades and gray points are shades down)

West orientation

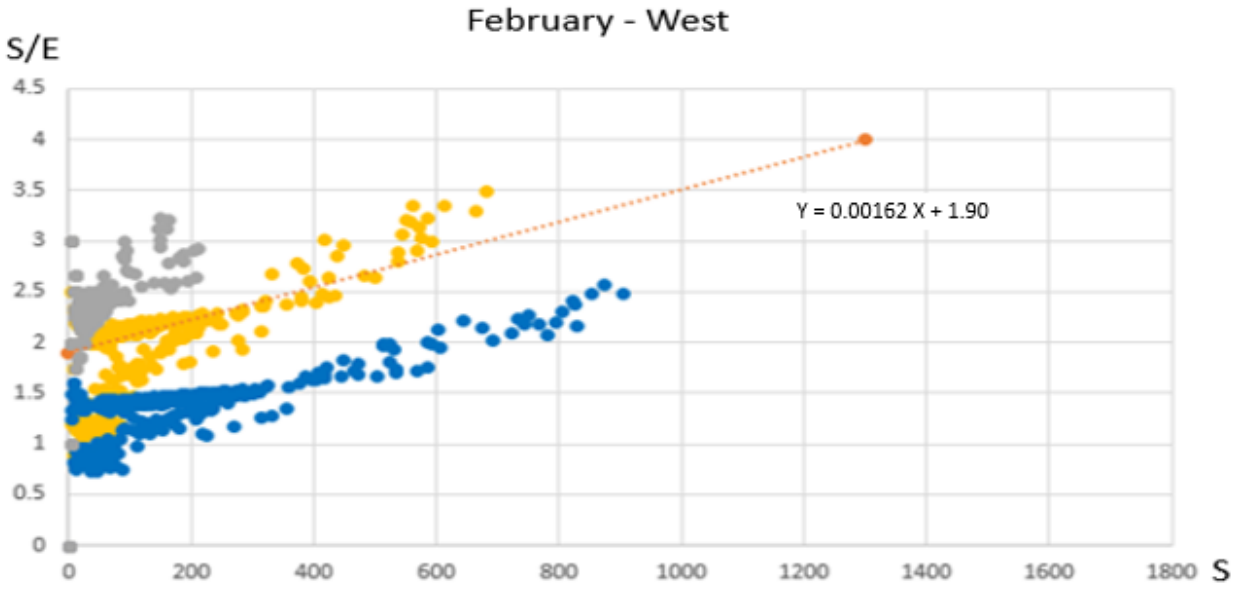

Figure 69. Daylight signal to daylight illuminance ratios of the two-sensor system and the correcting signals for the West orientation in the month of February in State College. (Blue points are shades up, yellow points are halfway shades and gray points are shades down)

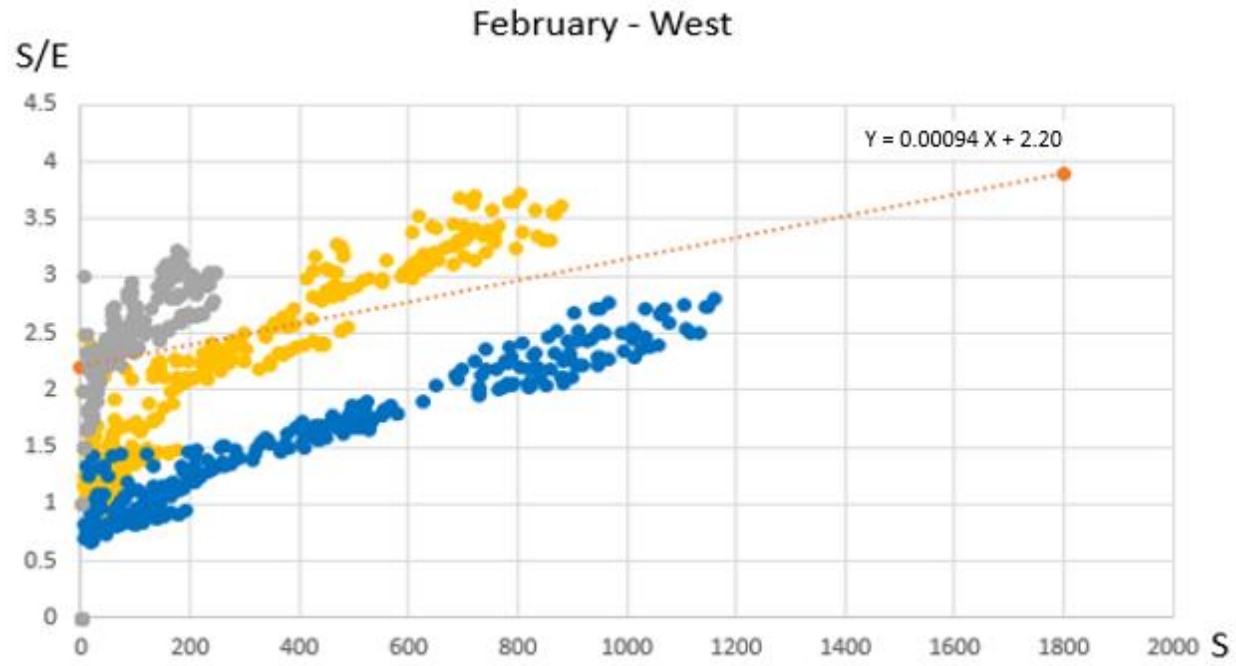

Figure 70. Daylight signal to daylight illuminance ratios of the two-sensor system and the correcting signals for the West orientation in the month of February in Phoenix. (Blue points are shades up, yellow points are halfway shades and gray points are shades down)

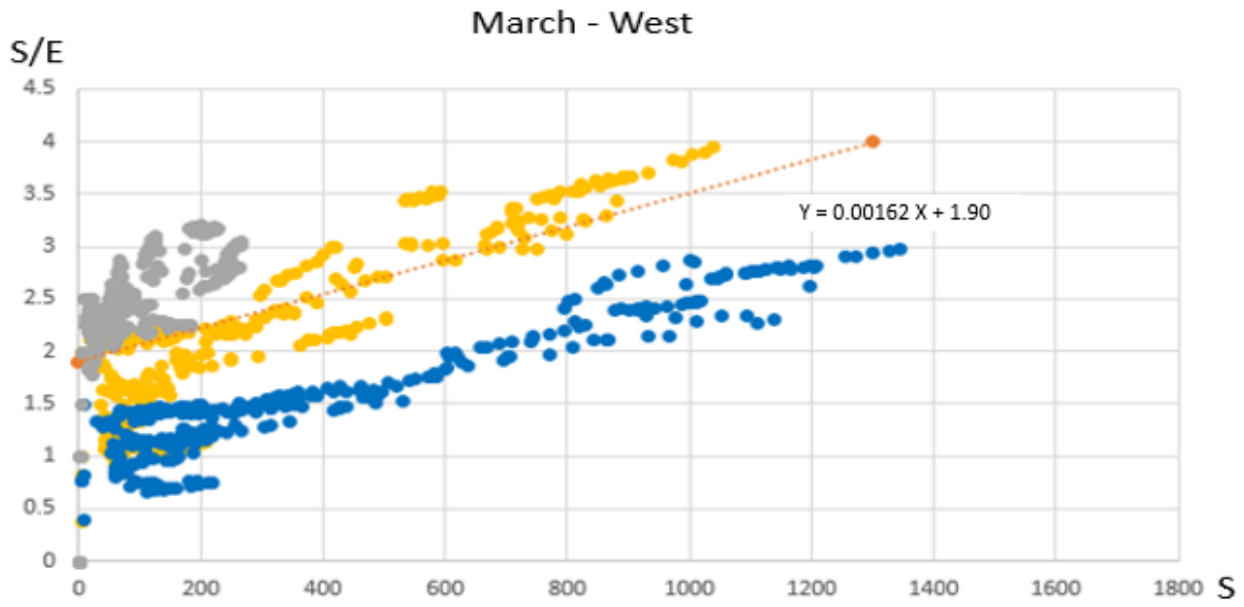

Figure 71. Daylight signal to daylight illuminance ratios of the two-sensor system and the correcting signals for the West orientation in the month of March in State College. (Blue points are shades up, yellow points are halfway shades and gray points are shades down)

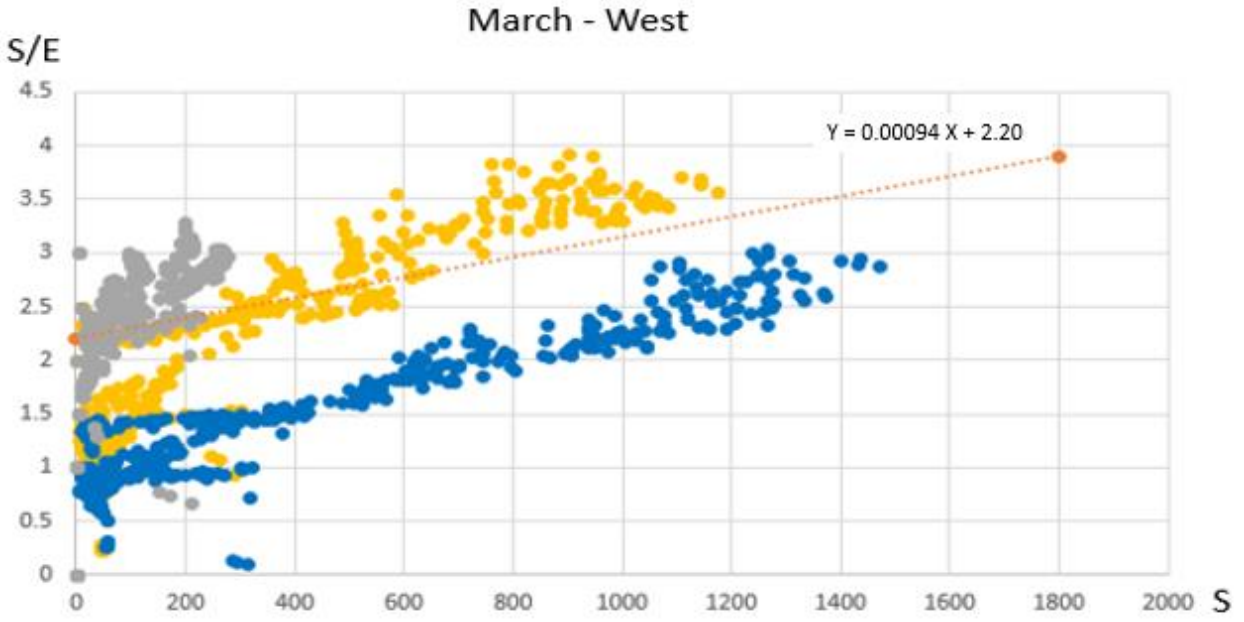

Figure 72. Daylight signal to daylight illuminance ratios of the two-sensor system and the correcting signals for the West orientation in the month of March in Phoenix. (Blue points are shades up, yellow points are halfway shades and gray points are shades down)

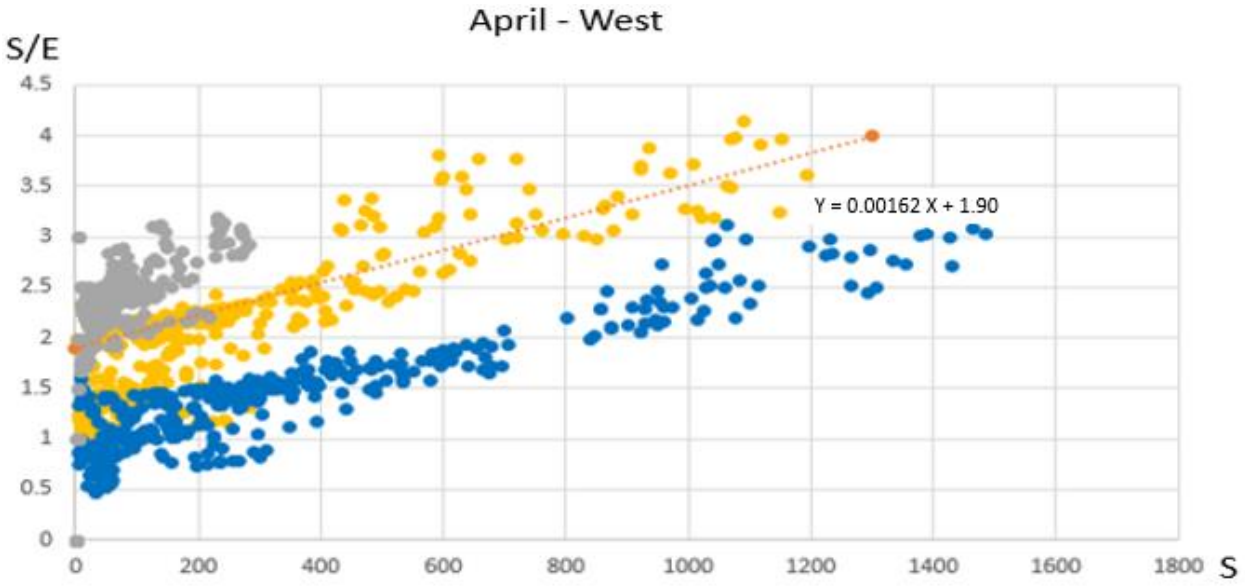

Figure 73. Daylight signal to daylight illuminance ratios of the two-sensor system and the correcting signals for the West orientation in the month of April in State College. (Blue points are shades up, yellow points are halfway shades and gray points are shades down)

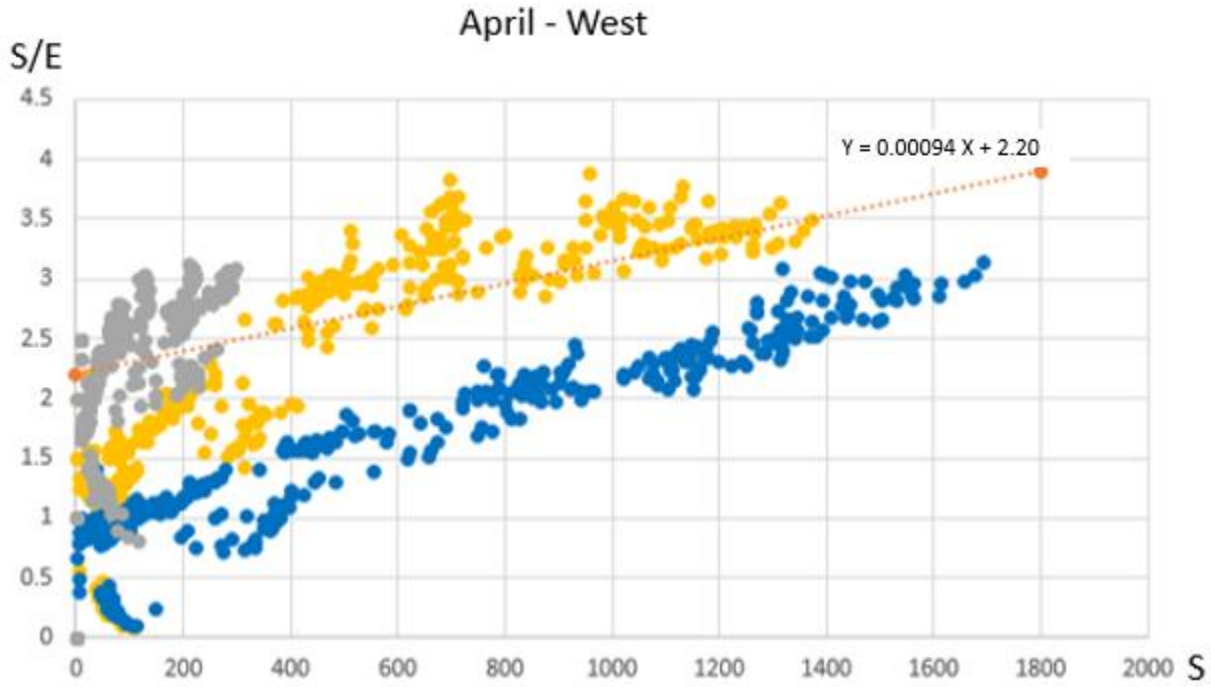

Figure 74. Daylight signal to daylight illuminance ratios of the two-sensor system and the correcting signals for the West orientation in the month of April in Phoenix. (Blue points are shades up, yellow points are halfway shades and gray points are shades down)

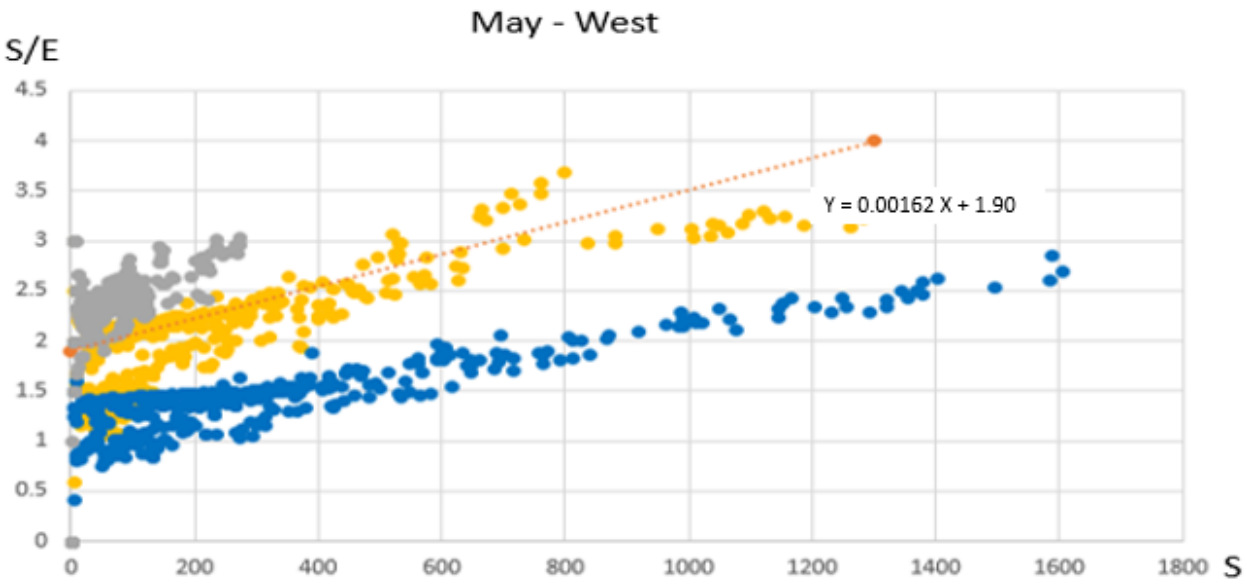

Figure 75. Daylight signal to daylight illuminance ratios of the two-sensor system and the correcting signals for the West orientation in the month of May in State College. (Blue points are shades up, yellow points are halfway shades and gray points are shades down)

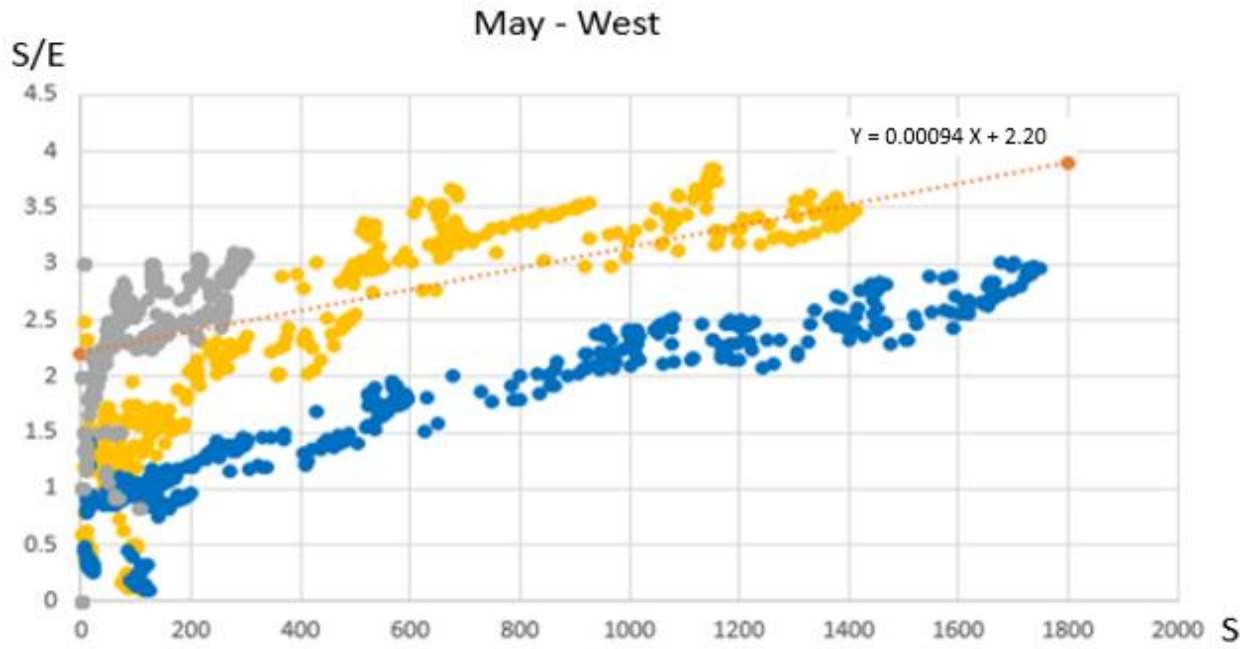

Figure 76. Daylight signal to daylight illuminance ratios of the two-sensor system and the correcting signals for the West orientation in the month of May in Phoenix. (Blue points are shades up, yellow points are halfway shades and gray points are shades down)

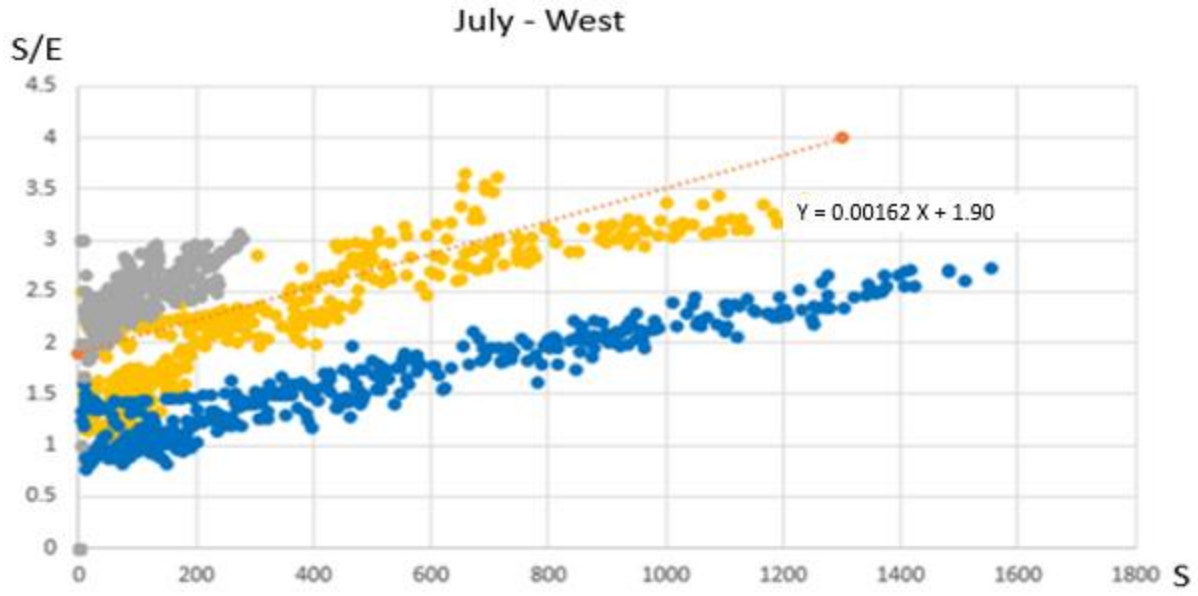

Figure 77. Daylight signal to daylight illuminance ratios of the two-sensor system and the correcting signals for the West orientation in the month of July in State College. (Blue points are shades up, yellow points are halfway shades and gray points are shades down)

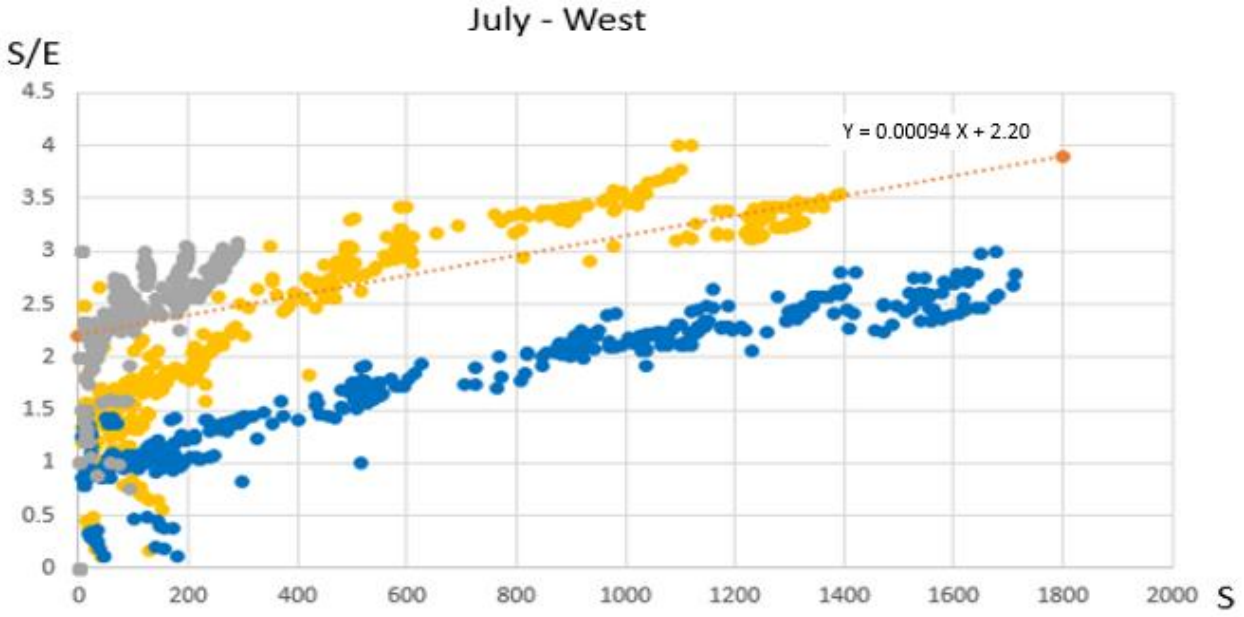

Figure 78. Daylight signal to daylight illuminance ratios of the two-sensor system and the correcting signals for the West orientation in the month of July in Phoenix. (Blue points are shades up, yellow points are halfway shades and gray points are shades down)

References

Caicedo, D., Pandharipande, A., & Willems, F. M. (2014). Daylight-adaptive lighting control using light sensor calibration prior-information. *Energy and Buildings*, *73*, 105-114.

Casares, F. J., Ramírez-Faz, J., & López-Luque, R. (2014). Development of synthetic hemispheric projections suitable for assessing the sky view factor on horizontal planes. *Energy and Buildings*, *82*, 696-702.

Casey, C., & Mistrick, R. (2012, November). Determining the critical point for design, analysis, and commissioning of a photocontrolled dimming system. In *Proceedings of the 2012 IES Annual Conference, Minneapolis, MN, USA* (Vol. 1113).

Casey, C. and R. Mistrick (2015). Simulation tools for architectural daylighting and integrated controls (stadic) - utilities. 14th International Radiance Workshop. Philadelphia, U.S.

Chen, L. (2013). *Sensor Performance of Advanced Photocontrol Systems*. The Pennsylvania State University.

Chen, L. (2017). *Performance Analysis of Photocontrol Systems Across Shade Settings* (Doctoral dissertation, Pennsylvania State University).

Choi, A. S., & Sung, M. K. (2000). Development of a daylight responsive dimming system and preliminary evaluation of system performance. *Building and Environment*, *35*(7), 663-676.

DiLaura, D. L., Houser, K. W., Mistrick, R. G., & Steffy, G. R. (2011). *The lighting handbook: Reference and application* (pp. 1328-p). New York (NY): Illuminating Engineering Society of North America.

Doulos, L., Tsangrassoulis, A., & Topalis, F. V. (2014). Multi-criteria decision analysis to select the optimum position and proper field of view of a photosensor. *Energy Conversion and Management*, *86*, 1069-1077.

Ehrlich, C., Papamichael, K., Lai, J., & Revzan, K. (2002). A method for simulating the performance of photosensor-based lighting controls. *Energy and buildings*, *34*(9), 883-889.

Galasiu, A. D., & Reinhart, C. F. (2008). Current daylighting design practice: a survey. *Building Research & Information*, *36*(2), 159-174.

Gibson, T., & Krarti, M. (2015). Comparative analysis of prediction accuracy from daylighting simulation tools. *Leukos*, *11*(2), 49-60.

Heschong, L., Howlett, O., McHugh, J., & Pande, A. (2005). Sidelighting photocontrols field study. *NEEA and PG&E and SCE*.

Kim, S. Y., & Mistrick, R. (2001). Recommended daylight conditions for photosensor system calibration in a small office. *Journal of the Illuminating Engineering Society*, *30*(2), 176-188.

Kim, S. Y., & Song, K. D. (2007). Determining photosensor conditions of a daylight dimming control system using different double-skin envelope configurations. *Indoor and Built Environment*, *16*(5), 411-425.

Kim, S. Y., Alzoubi, H. H., & Ihm, P. (2009). Determining photosensor settings for optimum energy saving of suspended lighting systems in a small double-skinned office. *International Journal of Energy Research*, *33*(6), 618-630.

Klusmann, D. L., & Murphy, M. S. (2015). *U.S. Patent No. 9,049,756*. Washington, DC: U.S. Patent and Trademark Office.

Krarti, M., Erickson, P. M., & Hillman, T. C. (2005). A simplified method to estimate energy savings of artificial lighting use from daylighting. *Building and Environment*, *40*(6), 747-754.

Lebedev, L. P., & Cloud, M. J. (2003). *Tensor analysis*. World Scientific.

Leslie, R. P., Raghavan, R., Howlett, O., & Eaton, C. (2005). The potential of simplified concepts for daylight harvesting. *Lighting Research & Technology*, *37*(1), 21-38.

Littlefair, P. J., & Motin, A. (2001). Lighting controls in areas with innovative daylighting systems: a study of sensor type. *Transactions of the Illuminating Engineering Society*, *33*(1), 59-73.

Mistrick, R. G., & Thongtipaya, J. (1997). Analysis of daylight photocell placement and view in a small office. *Journal of the Illuminating Engineering Society*, *26*(2), 150-160.

Mistrick, R. G. (1998). Analysis of daylight responsive dimming system performance. *Building and Environment*, *34*(3), 231-243.

Mistrick, R., Chen, C. H., Bierman, A., & Felts, D. (2000). A comparison of photosensor-controlled electronic dimming systems in a small office. *Journal of the Illuminating Engineering Society*, *29*(1), 66-80.

Mistrick, R., & Sarkar, A. (2005). A study of daylight-responsive photosensor control in five daylighted classrooms. *Leukos*, *1*(3), 51-74.

Mistrick, R. G., & Casey, C. A. (2011, December). Performance modeling of daylight integrated photosensor-controlled lighting systems. In *Proceedings of the Winter Simulation Conference* (pp. 903-914). Winter Simulation Conference.

Mistrick, R., Casey, C., Chen, L., & Subramaniam, S. (2015). Computer modeling of daylight-integrated photocontrol of electric lighting systems. *Buildings*, *5*(2), 449-466.

O'Connor, J., Lee, E., Rubinstein, F., & Selkowitz, S. (1997). Tips for daylighting with windows: the integrated approach. *LBNL Publication*, *790*.

Park, B. C., Choi, A. S., Jeong, J. W., & Lee, E. S. (2011). A Preliminary Study on the Performance of Daylight Responsive Dimming Systems with Improved Closed-Loop Control Algorithm. *Leukos*, *8*(1), 41-59.

Park, B. C., Choi, A. S., Jeong, J. W., & Lee, E. S. (2011). Performance of integrated systems of automated roller shade systems and daylight responsive dimming systems. *Building and Environment*, *46*(3), 747-757.

Ranasinghe, S., & Mistrick, R. (2003). A study of photosensor configuration and performance in a daylighted classroom space. *Journal of the Illuminating Engineering Society*, *32*(2), 3-20.

Reinhart, C. F., & Herkel, S. (2000). The simulation of annual daylight illuminance distributions—a state-of-the-art comparison of six RADIANCE-based methods. *Energy and Buildings*, *32*(2), 167-187.

Reinhart, C. F., & Walkenhorst, O. (2001). Validation of dynamic RADIANCE-based daylight simulations for a test office with external blinds. *Energy and buildings*, *33*(7), 683-697.

Reinhart, C. F., Mardaljevic, J., & Rogers, Z. (2006). Dynamic daylight performance metrics for sustainable building design. *Leukos*, *3*(1), 7-31.

Reinhart, C., & Breton, P. F. (2009). Experimental validation of Autodesk® 3ds Max® Design 2009 and DAYSIM 3.0. *Leukos*, *6*(1), 7-35.

Rubinstein, F. (1984). Photoelectric control of equi-illumination lighting systems. *Energy and Buildings*, *6*(2), 141-150.

Subramaniam, S., Chen, L., & Mistrick, R. (2013, October). Annual Performance Metrics for Photosensor-Controlled Daylight-Responsive Lighting Control Systems. In *Proceedings of the 2013 IES Annual Conference, Huntington Beach, CA, USA* (Vol. 2729).

Ward, G., Mistrick, R., Lee, E. S., McNeil, A., & Jonsson, J. (2011). Simulating the daylight performance of complex fenestration systems using bidirectional scattering distribution functions within radiance. *Leukos*, *7*(4), 241-261.

Williams, A., Atkinson, B., Garbesi, K., Page, E., & Rubinstein, F. (2012). Lighting controls in commercial buildings. *Leukos*, *8*(3), 161-180.

Yoon, Y., Lee, J. H., & Kim, S. (2015). Development of computational algorithm for prediction of photosensor signals in daylight conditions. *Building and Environment*, *89*, 229-243.

Yoon, Y., Moon, J. W., & Kim, S. (2016). Development of annual daylight simulation algorithms for prediction of indoor daylight illuminance. *Energy and Buildings*, *118*, 1-17.